RICE UNIVERSITY

Toward Fullerene Immunotherapy with Water-Soluble Paclitaxel-Fullerene Conjugates

by

Christopher Scott Berger

A THESIS SUBMITTED
IN PARTIAL FULFILLMENT OF THE
REQUIREMENTS FOR THE DEGREE

Doctor of Philosophy

Approved, Thesis Committee:

Prof. Lon J. Wilson, Ph.D., Chair
Professor of Chemistry

Prof. W. Edward Billups, Ph.D.
Professor of Chemistry

Prof. James A. McNew, Ph.D.
Associate Professor of Biochemistry
& Cell Biology

Prof. Michael G. Rosenblum, Ph.D.
Professor of Experimental Therapeutics
The University of Texas M.D. Anderson
Cancer Center

Houston, Texas
SEPTEMBER 2012

Abstract

Toward Fullerene Immunotherapy with Water-Soluble Paclitaxel-Fullerene Conjugates

by

Christopher Scott Berger

For the first time, two distinct, well-characterized water-soluble chemotherapeutic-C_{60} conjugates have been constructed for targeted drug delivery of paclitaxel to cancer cells.

In vitro work was carried out in two stages to determine IC_{50} values of the conjugates. Primarily, work was performed on A375m melanoma, T-24 bladder carcinoma, and Hep 3B hepatocellular carcinoma cell lines. In these studies, it was revealed that although the first compound, a paclitaxel-2'-succinate-C_{60} derivative, experienced a dramatic loss of cytotoxicity in comparison to paclitaxel, the second derivative, utilizing a poly(ethylene glycol) linker, demonstrated over 10× better cytotoxicity than paclitaxel itself.

Additional *in vitro* studies were conducted to create a chemotherapeutic-fullerene-monoclonal antibody immunoconjugate for targeted drug delivery. Endohedral $Gd@C_{60}(OH)_x$ was associated to antibodies via supramolecular forces instead of covalent chemical bonding. ELISA assays showed that $Gd@C_{60}(OH)_x$-mAb immunoconjugates retain binding specificity, and inductively coupled plasma mass spectrometry (ICP-MS) demonstrated selective internalization of the immunoconjugate into targeted cells. Subsequent studies utilized a similar strategy of fullerene-antibody association to construct a immunoconjugate for targeted chemotherapy with a water-soluble

paclitaxel-2'-succinate-C_{60} derivative. While cytotoxicity was measurable, no discernible advantage was seen by the targeted C_{60}-(ZME-018) immunoconjugate over a MuIgG control, thus leaving room for further refinement of the approach for targeted cancer therapy.

In vivo work, using the potent paclitaxel-poly(ethylene glycol)-C_{60} derivative in a murine model, demonstrated success by producing a similar capacity for tumor-reduction compared to the FDA-approved drug Abraxane®, without associated weight-loss in animals seen for Abraxane.

A major contribution of this work is the progress made toward development of Fullerene Immunotherapy (FIT) and the potential translation of FIT into the clinic. Having demonstrated the potent, improved cytotoxicity of a paclitaxel-C_{60} conjugate, the next step in the development of FIT is the successful construction of a therapeutic fullerene-antibody immunoconjugate. The results documented in this work have now shifted the onus of FIT from a theoretical concept to a realistic goal awaiting final developmental refinement.

Acknowledgements

John Donne was correct when he meditated, “No man is an island.” While the work in this thesis is my own, it also represents the accumulation of a lifetime of professional and personal contributions from friends, family and collaborators.

On a general level, I must acknowledge the friendship and mentorships of Messrs. Ashe Jones, Bill Munro, Fred White, Carter Kittrell, Mrs. Connie Wells, Drs. Bruce Johnson and Daniel Heller, Profs. Bob Curl and Bob Willcott. Each of them has provided an enormous amount of mentorship and support for me over the years, without which, I can’t even imagine where I would be today. I am truly fortunate.

Additionally, I would like to thank the friends I have made through the University of Saint Thomas and the Catholic Chaplain Corps. These especially include John & Molly Hittinger, Steve Toomey, Bill Henri, Peter Dorairaj and Page Polk. Mere words fail to describe the deep esteem and affection that I hold for each of them.

Also, to my family and friends, whose support has always been there, especially Ron, Christy, Matt and Dani Berger, Klaus and Eugenia Weissenberger, Brian Webster and Katy Bosworth, Eric Libby, Michael Chiang, Matt Barnett, Tony Kellems, Douglas Mitchell, Shahin Salehoun and Adam Adams.

Thanks to the National Institutes of Health (NIH-SBIR Grant R43CA128277) and the Welch Foundation (Grant C-0627) for their continued support of research and for sponsoring my own graduate studies.

Special thanks go to my fellow scientists in the Wilson lab, the University of Houston, and to our collaborators at TDA, Inc. and The University of Texas M. D.

Anderson Cancer Center. In particular, research in this thesis would have proven difficult, if not impossible, without the assistance of Drs. Yuri Mackeyev (Rice), Yongjun Gao (UH), Stephen Curley (MDACC) and Michael Rosenblum (MDACC). Additionally, the research support of Messrs. Matthew Cheney (Rice), Brandon Cisneros (MDACC) and Bill Marks (MDACC) proved vital for my research, and it was a pleasure working with them all.

Thank you to the members of my committee, Professor Edward Billups, Professor James McNew and Professor Michael Rosenblum for taking time out of their busy schedules to serve on my thesis committee.

Finally, I want to most of all thank my advisor, Professor Lon Wilson. It has been quite a journey since I took his CHEM 351 class in the fall of 1998, but the destination was well worth it.

Table of Contents

List of Figures

Page

Page

Page

List of Tables

Chapter 1

Introduction

1.1 Background

Since the initial discovery of buckminsterfullerenes (C_{60}) in 1985[1] and carbon nanotubes in 1991,[2] the unique chemical and physical properties of carbon nanostructures have ignited the field of nanotechnology and attracted the attention of researchers focusing on applications ranging from superconductivity to chemical sensors,[3] with medical applications being one of the most prominent areas of study.[4]

Although their toxicity is still under debate, carbon nanostructures appear to be ideal scaffolds for medical applications. Initially, their low solubility in aqueous solution limited their use for biomedical purposes, but extensive derivatization methods have resulted in the facile availability of aqueous fullerene derivatives.[5,6,7] Properly derivatized carbon nanostructures appear not to be intrinsically immunogenic (although more study is needed), stable, and are eventually excreted from mammals,[8,9] making them an ideal biological scaffold for medical materials. Attaching hydrophilic substituents to a fullerene core not only provides water solubility, but also controls and modifies the biological activity of fullerene derivatives.[10] Additionally, carbon nanomaterials can be internally loaded, either during initial synthesis (fullerenes) or in post-production steps (carbon nanotubes), with materials possessing useful properties for therapy or diagnosis, such as radionuclides for α-radiotherapy[11] or Gd^{3+} ions for MRI.[12] New potential pharmaceuticals derived from C_{60} show promising biological profiles and efficacies as HIV-1 protease inhibitors,[13] antioxidants,[14] bone-vectoring agents,[15] sensitizers for photodynamic

therapy,[16] MRI contrast agents,[17] transfection agents,[18] x-ray contrast agents,[19] and slow-release systems for liposome aerosol delivery.[20]

1.2 Fullerene HIV-1 Protease Inhibitors

The hydrophobicity of C_{60}, while a problem for many biological applications, also makes it a potential inhibitor of enzymes with hydrophobic active sites, such as HIV-1 protease. Molecular modeling and calculations show C_{60} to fit into the catalytic cavity of HIV-1 protease,[21] while experimental studies show many C_{60} derivatives to demonstrate anti-HIV activity with EC_{50} values within the range of 0.9-2.9 μM.[22] Due to the hydrophobic amino acids lining the HIV-1 protease active site, presumably hydrophobic interactions are the main force behind C_{60}/HIV-1 protease association. Additional cycloaddition functionalization of fullerenes with positively charged quaternary amines further increased inhibition binding and reduced EC_{50} to values in the high nanomolar range, possibly by strengthening electrostatic interactions with negatively-charged catalytic aspartic acids (Asp 25 and Asp 125) lining the active site.[23]

1.3 Fullerene Antioxidant Properties

Due to its electron-accepting nature, C_{60} is highly reactive towards free radicals.[24] This reactivity assigns C_{60} compounds a prominent role in the possible prevention and treatment of various neurological diseases such as Parkinson's disease, Alzheimer's disease, senility, and schizophrenia, in which the role of free radical production has only recently come into focus.[25,26,27] In particular, the production of superoxides and hydroxyl

free radicals plays a key role in aging, raising the potential for fullerenes as important inhibitors for aging. Recently, Baati *et al.* administered oral solutions of C_{60} in olive oil (0.8 mg/mL) at reiterated doses (1.7 mg/kg) to rats.[14] The control group (water) had a median lifespan of 22 months, while the group receiving olive oil had a slightly longer median lifespan of 26 months. However, the group receiving C_{60}/olive oil suspension survived for 42 months, a 90.9% increase in lifespan over the control group. Additionally, oxidative stress was studied in the rats by intraperitoneal injection of CCl_4, a potent hepatotoxin activated by mitochondria metabolism to form trichloromethyl free radical (CCl_3•). After administration, the rats treated with the C_{60}/olive oil suspension showed significantly improved recovery rates over the water and olive oil controls, demonstrating the potent antioxidant activity of C_{60} *in vivo*.

1.4 Singlet Oxygen Applications of Fullerenes

Paradoxically, while C_{60} shows promising activity as a quencher of reactive radical species, its long absorption wavelength, long-lived triplet excited state and high quantum yield also make it an ideal substrate for generating reactive oxygen species such as singlet oxygen ($^1O_2$) and superoxide (O_2^-). Supercoiled, covalently closed, helical pBR322 plasmid DNA (Form I), in the presence of C_{60} and visible-light irradiation became open circular, nicked DNA (Form II), conclusively indicating biological damage, while C_{60}-incubation without irradiation showed no cleavage whatsoever.[28] Additionally, HeLa S3 cells incubated with a series of C_{60}-carboxylic acid derivatives showed significant growth inhibition after two one hour visible light irradiations. No activity in

HeLa cells was observed from any C_{60} derivatives in the dark.[29] More recently, C_{60} was covalently conjugated with polyethylene glycol (PEG) for water solubility, whereupon the terminal PEG hydroxyl was esterified to the commercially-used octadentate ligand diethylene triamine pentaacetic acid (DTPA). With introduction of Gd^{3+} into the DTPA ligand and intravenous administration into tumor-bearing mice, the C_{60}-PEG-Gd complex formed a theranostic treatment demonstrating comparable relaxivity with the clinical standard MRI contrast agent Magnevist® and significant anti-tumor activity with visible light irradiation for 10 minutes.[30] This ability of irradiated C_{60} derivatives to induce DNA cleavage *in vitro* and *in vivo* results in a relatively high cytotoxicity for a material normally considered to be biologically inert, which suggests possibilities for new applications.

On a different note, a new direction of C_{60} free radical generation is being taken toward industrial purification of drinking water, where singlet oxygen and other free radical species are generated *in situ* to eliminate both organic molecules and microorganisms.[31,32] By immobilizing polyadduct amine-functionalized fullerene (amino-C_{60}) on silica, $^1O_2$ generation actually became more efficient, an effect hypothesized by the investigators to be most likely attributable to better dispersion in solution and decreased C_{60} aggregation/agglomeration. Hexakis-adduct, amino-C_{60} silica demonstrated the most $^1O_2$ activity, rapidly photodegrading both ranitidine and cimetidine in visible light at concentrations of 0.1 mmol/gram silica. In addition to organic compound degradation, micromolar concentrations of photoirradiated amino-C_{60} on silica inhibited growth of *E. Coli,* clearly showing the potential of C_{60} for antiseptic applications.

1.5 Fullerene Contrast Agents for Magnetic Resonance Imaging

Shortly after the first evidence of buckminsterfullerenes appeared, following on its heels was the idea of encapsulating metal ions within its carbon cage to form endohedral metallofullerenes.[33] By sequestering metal ions with beneficial physical properties, but deleterious chemical properties, inside a biologically impenetrable carbon cage, these fullerenes poses a major advantage over traditional metal chelates and show significant potential as medical agents. Gadolinium(III) ion, the clinical standard for T_1-weighted MRI contrast enhancement, possesses seven unpaired f electrons, making it highly paramagnetic and effective at reducing T1 (longitudinal) and T2 (transverse) relaxation times in surrounding protons. $Gd@C_{60}[C(COOH)_2]_{10}$, a water-soluble carboxyl malonate $Gd@C_{60}$ derivative, demonstrated proton relaxivity comparable to that of the Gd^{3+} chelate MRI contrast agents,[34] while $Gd@C_{82}(OH)_n$ fullerenols displayed proton relaxivities 20 times higher than clinically used contrast agents.[35,36]

Finally, posing perhaps the most important advance in fullerene MRI contrast agents are trimetallic nitride templated (TNT) endohedral gadolinium fullerenes ($Gd_3N@C_{80}$). Recently, a water-soluble TNT derivative ($Gd_3N@C_{80}(OH)_{\sim 26}(CH_2CH_2COOH)_{\sim 16}$) was reported with T1 and T2 relaxivities almost 50 times those of clinical contrast agents.[37] With the added advantage of three gadolinium ions per fullerene, these compounds are produced in relatively high yields and pose what could be a promising step toward the production of a fullerene-based clinical agent.

1.6 Fullerene Liposomes

Liposomes are artificially-prepared vesicles composed of a hydrophobic-hydrophilic bilayer, used as a vehicle to administer pharmaceuticals. Pharmaceutical liposomes utilize the membranes to encapsulate a hydrophobic region containing therapeutic molecules; upon contact with other bilayers, such as those found in the cell membrane, a liposome's lipid bilayer can fuse, thus delivering its contents to its sites of action.

The versatile chemistry and natural hydrophobicity of C_{60} make it an excellent candidate for liposomal study. In one study, Partha *et al.*[38] built on the previous research of Hirsch and co-workers,[39] to construct amphiphilic fullerenes, with a single hydrophilic malonate dendrimer unit, while five other octahedral positions on the fullerene occupied by hydrophobic aliphatic malonates. By sonicating these fullerenes with paclitaxel in 10 mM citrate buffer (pH: 7.4) for 1 minute, paclitaxel-containing spherical structures (referred to as "buckysomes") of 100-200 nm were formed. *In vitro* testing with MCF-7 breast cancer cells showed the buckysomes to have chemotherapeutic potency on the same order of Abraxane®, a clinically-used protein-bound paclitaxel formulation, in which paclitaxel is bound to albumin for use as a water-soluble delivery vehicle.[40]

Another avenue toward fullerene-liposome delivery of paclitaxel was taken by Zakharian *et al.* through direct covalent conjugation of paclitaxel with C_{60}.[20] By synthesizing and characterizing a discrete, homogeneous, fullerene-paclitaxel compound, these researchers were able to construct stable dilauroylphosphatidylcholine (DLPC) liposomes, with a mean diameter of 2.77 μm, for potential aerosol delivery to lung

carcinomas. IC_{50} values of the fullerene-paclitaxel-DLPC and fullerene-DLPC liposomes were respectively 410 and 253 nM, demonstrating a marked decrease in potency upon conjugation of the paclitaxel. However, with the promise of lung-directed delivery, the potential of fullerenes for use as a drug delivery vector appears promising.

1.7 Water-Soluble Fullerenes for Chemotherapy

By conjugating the anthracycline chemotherapeutic, doxorubicin, to water-soluble fullerenols ($C_{60}(OH)_x$), via a carbamate linker, Chaudhuri *et al*. constructed a material that, *in vivo*, was successful at significantly reducing the tumor volume of B16/F10 melanomas.[41] Additionally, measured stress on the murine subjects showed little loss in heart or spleen mass, compared to the control PBS solution, and a significant improvement over the naked doxorubicin, which causes significant weight loss in subjects.

Chapter 2

Design of a Water-Soluble C_{60}- Paclitaxel Conjugate

2.1 Targeted Therapeutics

The goal of targeted therapeutics has been one of the holy grails of modern medicine for over 100 years. At the dawn of immunology, modern passive immunization began in two stages. In 1888, Émile Roux, Emil von Behring and Kitasato Shibasaburo, of the Pasteur Institute immunized lab animals with heat-attenuated forms of diptheria and tetanus, which contained the bacterial toxins, but no live specimens. Collected sera from these animals was injected into infected animals with manifested symptoms, only to result in sera antitoxins relieving patient symptoms and eventually leading to recovery from infections that would previously have been fatal.

Behring's "serum therapy" eventually reached mass-production in horses and first saw treatment in humans in 1896, becoming the first immunity-based treatment for infectious disease since Jenner's smallpox vaccine developed over a century before. In the wake of this revolutionary therapy, Paul Ehrlich, who had assisted von Behring, noted that prokaryotic cell walls of certain infection bacterial strains were susceptible to staining from dyes (a precursor to Gram staining). This led Ehrlich to then infer that if dyes could target and bind to cell walls, it must be possible to find toxic materials that would target foreign bacteria in an infected patient over native tissue. This theoretical "magic bullet" would target problematic cells in a patient with no peripheral damage,

producing little or no side effects. Ehrlich, thus, had made a prediction that became the goal for medical treatment over the next century.

Ehrlich's concept of a magic bullet persists to this day. Current estimates are that only 1 in 10^4 to 1 in 10^5 of an administered pharmaceutical reaches its intended destination,[42] so even a small increase in the gradient of therapy delivered to target could produce significant improvements in patient outcome. The simple goal of targeted therapies is to produce high concentrations of the therapeutic agent in the appropriate biological area, thus reducing patient side effects while allowing higher pharmaceutical doses to be administered. The development of cell-targeted agents for imaging and therapeutic applications in medicine is accelerating.

As the search continues to develop new therapies to treat cancer, research progresses to find a modality selective enough to chaperone pharmaceuticals to targeted cells, yet versatile enough to incorporate many different classes of molecules for delivery. To accomplish this goal, cytokines, growth factors, kinase inhibitors and monoclonal antibodies (mAbs) all show promise for their ability to deliver payloads to the cell surface and into the cytoplasm of targeted cancer cells.[43] Using a patient's own cellular identification system to target cancer with immunoconjugates is evolving into a potent anticancer therapy in personalized medicine.[44,45,46] To date, numerous attempts have already been made at attempting to provide cellular targeting by attachment of paclitaxel to mAbs,[47,48] tumor-recognizing peptides[49] and hyaluronic acid (a linear polysaccharide overexpressed at sites of tumor attachment)[50] in order to select rapidly growing cancer cells over an organism's normal, healthy cells. Currently, however, the most versatile and

successful class of agents to show targeting capabilities for specific cancers are mAbs.

Three immunoconjugates are currently FDA-approved for clinical use. Two murine mAbs immunoconjugates, ibritumomab tiuxetan and tositumomab, act as direct therapy to target the B-cell glycoprotein CD20 to treat non-Hodgkin's lymphomas. Once they have targeted lymphoma cells, radionuclides chelated to the antibody release β^- particles to directly kill cancer cells.[51,52,53,54] A third covalently conjugated therapy, brentuximab vedotin, received approval in August 2011 for treatment of anaplastic large cell lymphoma (ALCL) and Hodgkin's lymphoma. Brentuximab vedotin targets the tumor cell marker CD30, and once internalized into tumor cells, releases monomethyl auristatin E, an antineoplastic and antimitotic agent that blocks tubulin polymerization.[55] Interestingly, gemtuzumab ozogamicin, an immunoconjugate used in the treatment of acute myelogenous leukemia, was withdrawn from clinical use in June 2010 when human trials showed the drug actually increased patient death and proved no benefit over conventional cancer therapies.[56] If anything, the withdrawl of gemtuzumab ozogamicin highlights both the challenge of development and increasing demand for targeted therapies, with over a dozen other antibody-drug conjugate (ADC) therapies already in clinical trials. For optimal efficacy, these immunoconjugates must internalize effectively within target cells after binding to the cell-surface antigen.

By using fullerenes as a novel delivery vehicle for paclitaxel, the potential for a new modality of targeted therapy is introduced. Fullerene immunotherapy (FIT) should provide a versatile tool capable of combining different potent pharmaceuticals in high ratios with different antibodies to custom make potent cocktails to attack cancer. A new

strategy is being capitalized on by combining two current drug delivery methods: fullerenes as a delivery vector and ester conjugations. As new technologies have increased the diversity and reduced the cost of clinical antibodies, research is heavily underway to use antibodies as delivery vectors.

By using an ester bond to attach paclitaxel to water-soluble C_{60} and then non-covalently "associating" the functionalized fullerene with an antibody, we are seeking to create an entirely new, multifunctional moiety for drug delivery with a higher therapy:mAb ratio than is currently available. The eventual goal is that upon clinical administration of a paclitaxel-C_{60}-mAb immunoconjugate, antibody internalization will occur into the cell, resulting in cellular digestion of the antibody and releasing paclitaxel-C_{60} into the cytosol. Ubiquitous cellular esterases, on which many cell labeling and drug delivery techniques already rely, will release the paclitaxel freeing it for therapeutic activity.

2.2 Paclitaxel Structure and Activity

Paclitaxel (Bristol-Myers Squibb Brand Name: Taxol®) is a potent cytotoxic and antimitotic natural diterpenoid first discovered and isolated from the Pacific yew, *Taxus brevifolia*, in 1967 by Drs. Monroe E. Wall and Mansukh Wani of the Research Triangle Institute during a systematic screening of materials for their pharmacological properties.[57] Although initial anticancer properties in clinical trials were promising, early studies were limited by the low natural abundance of paclitaxel (1.2×10^3 kg of yew bark yielding only 10 g of actual paclitaxel)[58] and further development languished. In 1989, the National

Cancer Institute announced a competition for further development of paclitaxel, and by 1992, Bristol-Myers Squibb had been selected as the developer and paclitaxel was approved and commercialized under the brand name Taxol. With the first total synthesis of paclitaxel in 1994, developed by Professor Robert A. Holton at Florida State University,[59] paclitaxel soon became one of the pharmaceuticals of choice in the chemotherapeutic arsenal against cancer.

Paclitaxel and its FDA-approved analog, docetaxel (Sanofi-Aventis Brand Name: Taxotere®), comprise taxanes, one of the most active anticancer agents in clinical use. Paclitaxel has FDA-approved indications for use in treatment of metastatic breast cancer, HIV-related Kaposi's sarcoma, and ovarian and non-small cell lung carcinomas. Total annual sales for both paclitaxel and docetaxel are approximately $4 billion *per annum*, though with the recent patent expiration of docetaxel in 2010, this number is expected to drop rapidly as it becomes available generically. By binding to β-tubulin subunits in cellular microtubules, paclitaxel promotes assembly and permanent hyperstabilization of microtubules, preventing disassembly of the polymeric protein structures composing the eukaryotic cellular cytoskeleton.[60] As microtubules are essential for mitosis and microtubule disassembly is an important process in cell division, this hyperstabilization leads to arrested cell division and the cell remains in the G2/M phase of the cell cycle, eventually triggering apoptosis.[61]

In addition to its own inherent cytotoxicity, paclitaxel is able to potently increase the susceptibility of cancer cells to concurrent attacks by DNA-damaging radiation or chemotherapeutics, such as cisplatin.[62] Although the precise mechanism of action for this

effect is not clear, current research indicates that a cell's G2/M phase is its period of most sensitivity to DNA-attack (possibly related to elevated growth as the cell prepares for mitosis), and paclitaxel's arrest of the cell in this phase may be linked to its radio- and chemosensitization properties.[63] Despite its impressive therapeutic activities, paclitaxel still suffers from significant limitations including multidrug resistance (MDR),[64] extremely low aqueous solubility and high systemic toxicities (especially hematologic and neurologic). Clinically, paclitaxel is currently administered in the nonionic surfactant Cremophor EL®, a polyethoxylated castor oil that is linked to allergic reactions and can lead to medium to severe paclitaxel hypersensitivity.[65] Paclitaxel's low solubility profile and high systemic toxicity are related, in that poorly soluble therapeutics experience high plasma protein binding, generally binding to human serum albumin rather than being available to efficiently traverse cell membranes for their intended goal. As bound therapeutics slowly reenter the bloodstream, before they can assume their intended therapeutic role, hepatic metabolism digests them into metabolites that can cause serious side effects. Therefore, a water-soluble prodrug of paclitaxel should be effective in providing greater bioavailability and circumventing the drawbacks of Cremophor EL, enhancing therapeutic effectiveness.[66,67] For this reason, this thesis is predominantly concerned with the development and study, both *in vitro* and *in vivo*, of a water-soluble fullerene-paclitaxel conjugate and its antibody-targeted drug delivery by fullerene immunotherapy (FIT). The general practicality of FIT has been previously demonstrated by our earlier work.[68,69]

For our study, $Gd@C_{60}$ is conjugated to both a melanoma antibody (ZME-018) and a control, non-targeting murine IgG antibody (MuIgG). ZME-018 targets the gp240 antigen, found on the surface of >80% of human melanoma cell lines[70] and functionalized conjugates of ZME-018 have been utilized extensively, with studies ranging from *in vitro* fluorescent studies of surface antigens,[71] to ^{111}In-ZME-018 conjugate targeting as both a laboratory and clinical *in vivo* tumor imaging agent.[72,73] ZME-018 already has shown great promise in clinical imaging trials[74] for the delivery of toxins, cytokines and other therapeutic agents to melanoma cells both *in vitro* and *in vivo*.[75] Immunoconjugates containing ZME-018 are known to rapidly internalize into melanoma cells[76] and effectively localize *in vivo* into melanoma xenografts after systemic administration and demonstrate impressive cytotoxic effects against established tumors in orthotopic models.[77,78] The reliable targeting properties of ZME-018 conjugates and thorough characterization in varied immunoconjugate systems make ZME-018 an ideal antibody for studying fullerene conjugate delivery.

Methods and Materials

2.3 $Gd@C_{60}(OH)_x$ and C_{60}-Paclitaxel Syntheses

2.3.1 $Gd@C_{60}(OH)_x$ Synthesis

Synthesis and characterization of the fullerenes was accomplished using a previously established procedure.[12] Since the $Gd@C_{60}(OH)_x$ sample used for antibody conjugation contained both $Gd@C_{60}(OH)_x$ and $C_{60}(OH)_x$ species,[79] inductively coupled plasma optical emission spectrometry (ICP-OES) from PerkinElmer (Waltham, Massachusetts) was used to determine the amount of Gd^{3+} contained in the product used for conjugation, and thus the overall percentage of $Gd@C_{60}(OH)_x$ (41.9%).

2.3.2 C_{60}-Paclitaxel Derivative Syntheses

Chemical synthesis of the target C_{60}-Succinate-Paclitaxel (Compound **7**) and conjugate C_{60}-Poly(ethylene glycol)-Paclitaxel (Compound **9**) conjugates each occurred in four distinct steps as shown in Schemes 1-4: (1) preparation of the BOC-protected amino linker malonate (Compound **1**) and reaction with C_{60} (Compound **2**); (2) preparation of the acetate-protected, water-solubilizing, serinol malonate (Compound **3**), reaction with BOC-amino-C_{60} (Compound **4**) and subsequent deprotection of the BOC-amine and serinol malonate groups (Compound **5**); (3) synthesis of paclitaxel-2'-succinate (Compound **6**) and conjugation of the succinate carboxylic acid with the fullerene amine (Compound **7**); and (4) synthesis of water-soluble paclitaxel-2'-poly(ethylene glycol) (Compound **8**) and conjugation of the terminal carboxylic acid with the fullerene amine (Compound **9**). Proton nuclear magnetic resonance spectra were

measured on a Bruker (Fremont, California, USA) 500 MHz NMR Spectrometer with 0.05% (by volume) tetramethylsilane as an internal standard, and processed with Nucleomatica iNMR software (Molfetta, Bari, Italia). Fourier-transformed infrared spectra were obtained using a Nexus 670 FTIR Thermo-Nicolet (Waltham, Massachusetts, USA) spectrometer with a Smart Golden Gate horizontal, single-reflection ATR in the range of 500–4000 cm^{-1}. Analysis of infrared spectra was provided by Advanced Chemistry Development Spectrus Processor (Toronto, Ontario, Canada). Mass spectrometry data for water-insoluble compounds were collected using an Autoflex MALDI TOF-TOF mass spectrometer (MS Autoflex). Mass spectrometry data for water-soluble fullerene derivatives were obtained utilizing electrospray ionization time-of-flight mass spectrometry (MS micrOTOF ESI). Both mass spectrometers are Bruker Daltonics, Inc. (Billerica, Massachusetts) instruments. Purity and commercial sources of the compounds used are shown in Table **A1** of the Supplemental Information. Mass spectrometry, infrared (IR) spectroscopy and nuclear magnetic resonance (NMR) spectroscopy data are given, respectively, in Appendices **A2**, **A3** and **A4.**

Figure 2.1: Synthesis scheme of 3'-ethoxycarbonyl-3'-((2-((*tert*-butoxycarbonyl)amino)ethoxy)carbonyl)-[1,2](C_{60}-I_h)[5,6]fullerene (**2**).

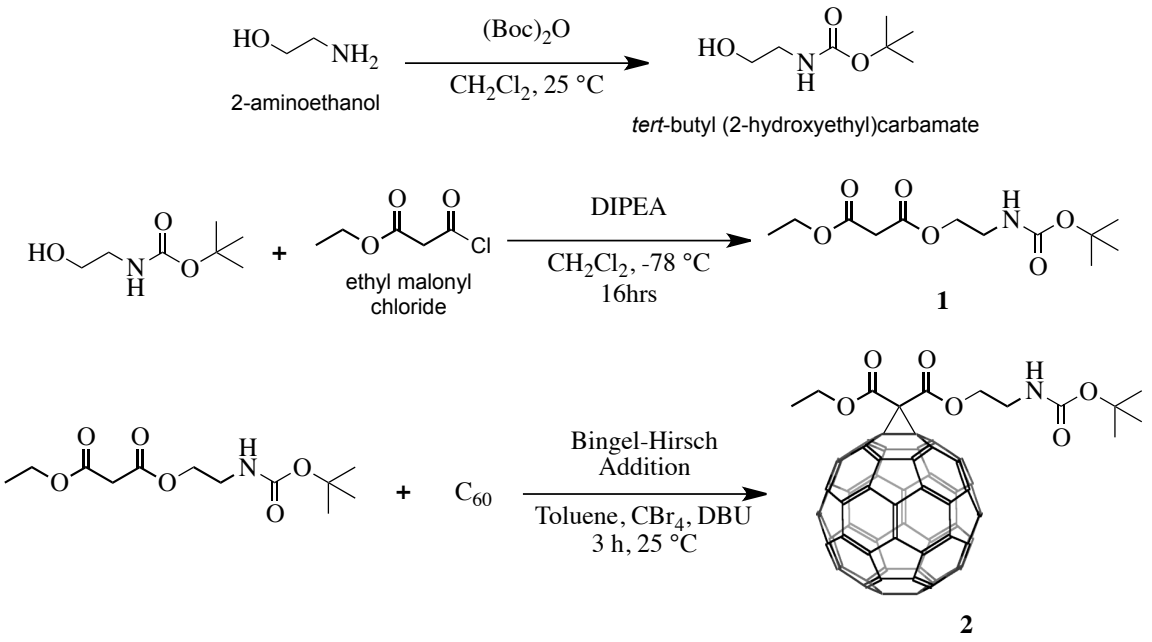

Figure 2.2: Synthesis scheme of 3'-ethoxycarbonyl-3'-((2-ammoniumethoxy)carbonyl)-3'', 3'', 3''', 3''', 3'''', 3'''', 3''''', 3''''', 3'''''', 3''''''-deca-(2-hydroxy-1-(hydroxymethyl)ethylcarbamoyl)-3'H, 3''H, 3'''H, 3''''H, 3'''''H, 3''''''H-hexacyclopropa[1,2:18,36:22,23:27,45:31,32:55,60](C_{60}-I_h)[5,6]fullerene monohydrochloride (**5**).

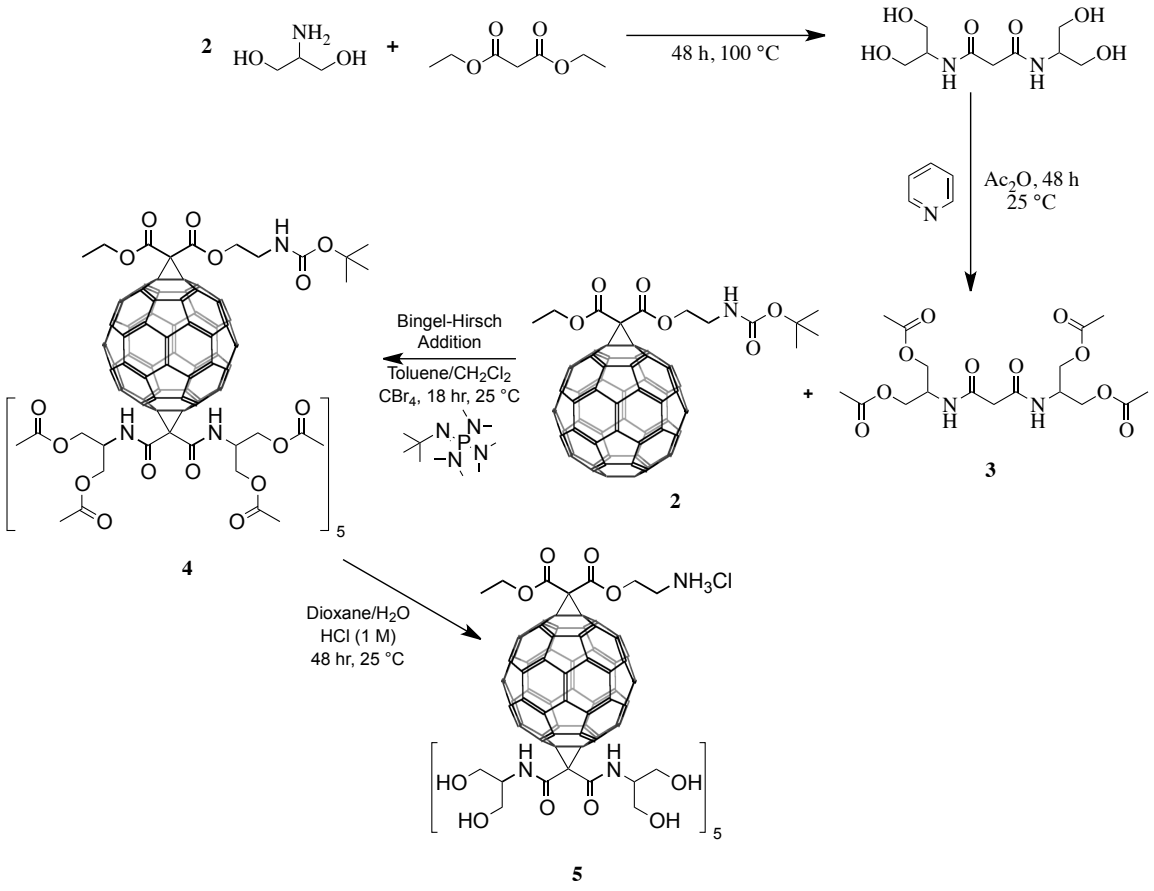

Figure 2.3: Synthesis scheme of the serinol-C_{60}-paclitaxel-2'-succinate derivative (**7**).

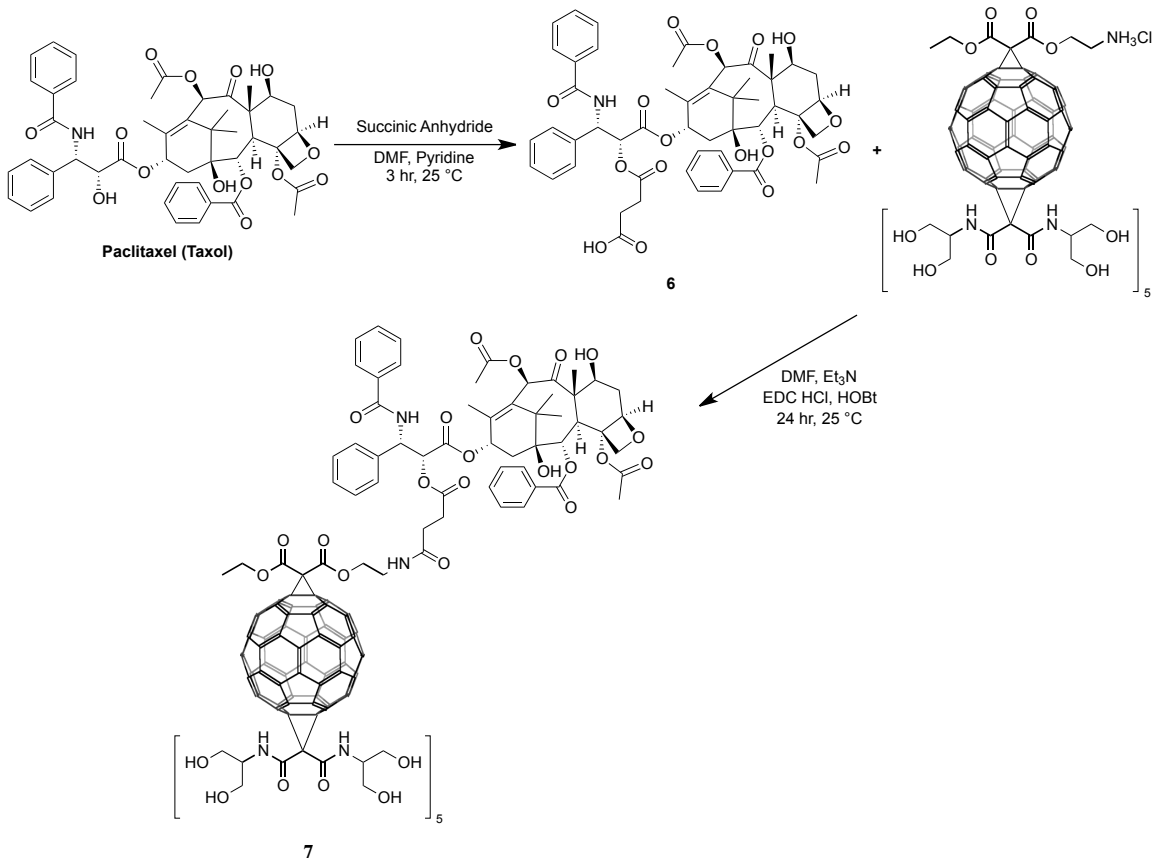

Figure 2.4: Synthesis scheme of the serinol-C_{60}-paclitaxel-2′-poly(ethylene glycol) ester derivative (**9**).

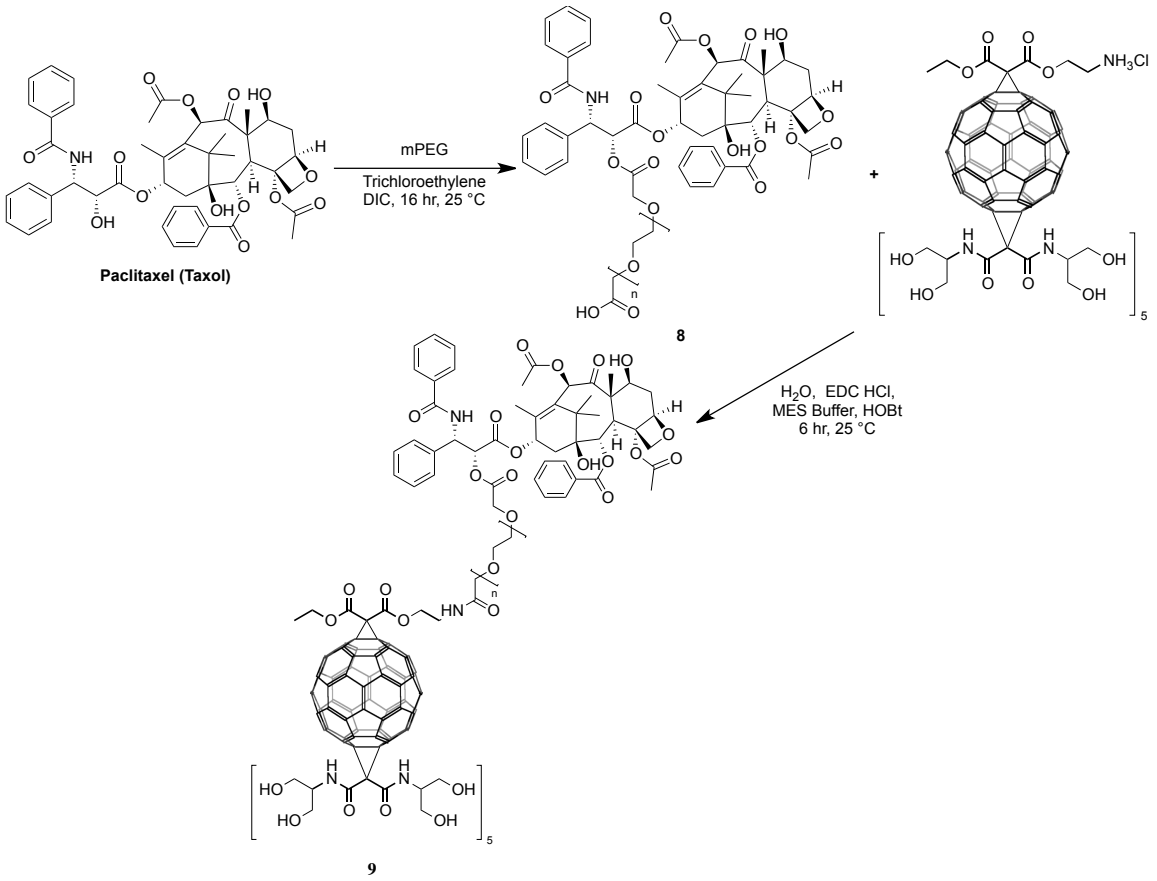

2.3.2.1 2-((*Tert*-butoxycarbonyl)amino)ethyl ethyl malonate (1)

Tert-butyl (2-hydroxyethyl)carbamate was prepared according to a previously published method.[80] 2-Aminoethanol was suspended in CH_2Cl_2 and reacted with di-*tert*-butyl pyrocarbonate (3% excess) at 25 °C for 16 hours. The product was isolated *in vacuo* and purified using flash chromatography ($CHCl_3$:CH_3OH, 2:1; silica: Mallinckrodt, 60-200 μm particles, 150 Å pore size). Yield: 99%. 2-((*Tert*-butoxycarbonyl)amino)ethyl ethyl malonate was then prepared by slow addition of ethyl malonyl chloride (25 g, 0.16 mols) to a dry-ice-cooled solution (-78 °C) of *tert*-butyl (2-hydroxyethyl)carbamate

(25 g, 0.16 mols) and *N,N*-diisopropylethylamine (DIPEA, 20 g, 0.15 mol) in dry methylene chloride (450 mL) under argon. The reaction mixture reached 25 °C and was then allowed to react for 16 hours. The solution was washed twice with water, once with NaCl brine, and then dried with Na_2SO_4. Flash chromatography (hexane:ethyl acetate, 9:1; silica: Mallinckrodt, 75-250 μm particles, 150 Å pore size) purified the solution producing a pale, yellow oil. Yield: 37 g (0.13 mol, 87%). MS Autoflex (positive-ion mode): calculated mass = 275.14 Da; observed masses = 293.367 Da [M^++H_2O], 316.703 Da [$M+K^+$]. NMR (500 MHz, $CDCl_3$, 0.05% (v/v) TMS reference): ^{1}H δ (ppm) = 1.290 (t, 3H, CH_3), 1.439 (s, 9H, $C(CH_3)_3$), 3.409 (s, 2H, CH_2), 4.209 (q, 2H, CH_2CH_3), 5.322 (t, 2H, CH_2NH); ^{13}C δ (ppm) = 14.069, 28.357, 39.418, 41.422, 48.963, 61.587, 64.537, 79.302, 155.939, 166.554. The mass spectrometry, IR and NMR spectral data are all respectively provided in Appendix Figures **A2.1**, **A3.1** and **A4.1**.

2.3.2.2 3'-Ethoxycarbonyl-3'-((2-((*tert*-butoxycarbonyl)amino)ethoxy)carbonyl)-[1,2](C$_{60}$-I$_h$)[5,6]fullerene (2)

C_{60} (727 mg, 1.00 mmol) was dissolved in freshly distilled toluene (500 mL) with CBr_4 (500 mg, 1.49 mmol), and **1** (413 mg, 1.50 mmol). At 25 °C, 1,8-diazabicyclo[5.4.0]undec-7-ene (DBU, 230 mg, 1.48 mmol) in toluene was added to the solution over 1 hour, and the reaction was allowed to proceed for 18 additional hours. Flash chromatography (toluene:ethyl acetate, 9:1; silica: Mallinckrodt, 75-250 μm particles, 150 Å pore size) isolated the product. Yield: 331.6 mg (33.4 mmol, 33.4%). MS Autoflex (positive-ion mode): calculated mass = 993.12 Da; observed mass =

993.197 Da [M^+]. NMR (500 MHz, $CDCl_3$, 0.05% (v/v) TMS reference): ^1H δ (ppm) = 1.296 (t, 3H, CH_3), 1.447 (s, 9H, $C(CH_3)_3$), 4.221 (q, 2H, CH_2CH_3), 4.903 (t, 2H, CH_2NH); ^{13}C δ (ppm) = 14.068, 28.345, 39.439, 41.477, 51.949, 61.701, 64.670, 79.602, 138.649, 139.339, 140.948, 140.989, 141.836, 141.892, 142.180, 142.927, 143.016, 143.071, 143.842, 143.881, 144.571, 144.630, 144.646, 144.674, 144.892, 144.919, 145.036, 145.111, 145.170, 145.193, 145.256, 145.168, 163.535, 166.439, 166.549. The mass spectrometry, IR and NMR spectral data are all respectively provided in Appendix Figures **A2.2**, **A3.2** and **A4.2**.

2.3.2.3 Bis(2-acetoxy-1-acetoxymethylethylcarbamoyl)methane (3)

2-amino-1,3-propanediol (25.0 g, 269 mmol) and diethyl malonate (17.5 mL, 112 mmol) were combined neat and heated with vigorous stirring at 100 °C under argon for 48 hrs. The resulting mixture was dissolved in boiling isopropyl alcohol and allowed to cool slowly, giving small needles of white, unprotected serinol malonate. After recrystallization was performed twice in isopropyl alcohol, the white solid (T_m: 132 °C) was obtained. The compound is highly soluble in water, DMF, *N*-Methyl-2-pyrrolidone (NMP), methoxyethanol and poorly soluble in alcohols.

Serinol malonate (25.0 g, 99.9 mmol) was dried under lyophilization, and then suspended in pyridine (100 mL, 1240 mmol) at 0 °C, to which acetic anhydride (150 mL, 1590 mmol) was added dropwise over the course of an hour. After reaching 25 °C, dissolution occurred and the solution was stirred continuously for 48 hours. At 0 °C, methanol (50 mL, 1225 mmol) was added to quench remaining acetic anhydride and the

solution was stirred for 1 hour, whereupon the solvents were removed *in vacuo* and the residue (yellow oil) was dissolved in isopropyl ether and recrystallized over 48 hours in hexane (hexane:isopropyl ether 9:1). The precipitate was collected by filtration, washed with hexanes and dried *in vacuo*. Yield: 33 g (79 mmol, 79%). T_m: 91.5–92.5 °C. MS Autoflex MALDI-TOF (positive-ion mode): calculated mass = 418.16 Da; observed masses = 420.006 Da [$M+H^+$], 450.230 Da [$M+Na^+$]. NMR (500 MHz, $CDCl_3$, 0.05% (v/v) TMS reference): ^1H δ (ppm) = 2.082 (s, 12H, CH_3), 3.255 (s, 2H, CH_2), 4.181 (d, 8H, CH_2), 4.405 (octet, 2H, CH), 7.889 (d, 2H, NH); ^{13}C δ (ppm) = 20.129 (4C, CH3), 41.966 (1C, CH2), 46.855 (2C, CH), 62.002 (4C, CH_2), 166.987 (2C, C1⁄4O, amide), 170.159 (4C, C1⁄4O, ester). The mass spectrometry, IR and NMR spectral data are all respectively provided in Appendix Figures **A2.3**, **A3.3** and **A4.3**.

2.3.2.4 3'-ethoxycarbonyl -3'-((2-((*tert*-butoxycarbonyl)amino)ethoxy)carbonyl)- 3'', 3'', 3''', 3''', 3'''', 3'''', 3''''', 3''''', 3'''''', 3''''''-deca-(2-acetoxy-1-acetoxymethylethylcarbamoyl)-3'H, 3''H, 3'''H, 3''''H, 3'''''H, 3''''''H-hexacyclopropa[1,2:18,36:22,23:27,45:31,32:55,60](C_{60}-I_h)[5,6]fullerene (4)

At 25 °C, **2** (99.5 mg, 0.100 mmol) was dissolved in a solution of 300 mL of freshly distilled toluene:CH_2Cl_2 (2:1), with CBr_4 (332 mg, 0.991 mmol) and **3** (837 mg, 2 mmol) to which a solution of *tert*-butylimino-tris(dimethylamino)phosphorane (141 mg, 0.584 mmol) in dry methylene chloride (100 mL) was added over 6 hours. After 18 hours, at 25 °C, the product was isolated using flash chromatography (chloroform:ethanol, 19:1). Yield: 107.8 mg (35.0 mmol, 35.0%). MS Autoflex MALDI-

TOF (positive-ion mode): calculated mass = 3073.84 Da; observed masses = 3074.8 Da [M+H^+], 3097.5 Da [M+Na^+], 3113.4 Da [M+K^+]. The mass spectrometry and IR spectral data are respectively provided in Appendix Figures **A2.4** and **A3.4**.

2.3.2.5 3'-ethoxycarbonyl-3'-((2-ammoniumethoxy)carbonyl)- 3'', 3'', 3''', 3''', 3'''', 3'''', 3''''', 3''''', 3'''''', 3''''''-deca-(2-hydroxy-1-(hydroxymethyl)ethylcarbamoyl)-3'H, 3''H, 3'''H, 3''''H, 3'''''H, 3''''''H-hexacyclopropa[1,2:18,36:22,23:27,45:31,32:55,60](C_{60}-I_h)[5,6]fullerene monohydrochloride (5)

Product **4** (154 mg, 50.1 mmol) was dissolved in 10 mL of 1,4-dioxane:water (99:1) and saturated with HCl gas at 25 °C up to 1 M concentration. The reaction flask was kept closed for 48 hours at 25 °C, to which solvents were removed *in vacuo* and the product was purified using a cellulose ester dialysis membrane (Thermo Scientific, 2000 MWCO) over 7 days using DI water, with trace amounts of HCl, to remove acetate and isopropyl alcohol. Yield: 111 mg (49.6 mmol, 99%). MS MicroTOF ESI (positive-ion mode): calculated mass = 2134.58 Da; observed masses = 2135.5 Da [M+H^+], 2177.5 Da [M+Na^+]. The mass spectrometry and IR spectral data are respectively provided in Appendix Figures **A2.5** and **A3.5**.

2.3.2.6 Paclitaxel-2′-Succinate (6)

Paclitaxel-2′-succinate was prepared by a modified literature procedure.[81] Paclitaxel (1.00 g, 1.15 mmol) and succinic anhydride (1.80 g, 17.81 mmol) were combined and dissolved in dry pyridine (24 mL, 296.4 mmol). The solution was stirred under argon at 25 °C for 3 h and then concentrated *in vacuo*. The residue was treated with DI H_2O (40 mL), stirred for 20 min, and filtered. The precipitate was dissolved to saturation in acetone, after which water was slowly added dropwise to precipitate white crystals of **6**. The product was then filtered and lyophilized. Yield: 1.03 g (1.08 mmol, 93.8%). MS Autoflex MALDI-TOF (positive-ion mode): calculated mass = 953.35 Da; observed masses = 954.471 Da [$M+H^+$], 976.466 Da [$M+Na^+$], 992.495 Da [$M+K^+$]. NMR (500 MHz, $CDCl_3$, 0.05% (v/v) TMS reference): ^1H δ (ppm) = 1.125 (s, 3H), 1.216 (s, 3H), 1.666 (s, 3H), 1.856 (dd, 1H), 1.908 (s, 3H), 2.200 (s, 4H), 2.329-2.672 (m, 3H), 2.430 (s, 3H), 3.798 (d, 1H), 4.241 (dd, 2H), 4.426 (ddd, 1H), 4.965 (dd, 1H), 5.504 (d, 1H), 5.685 (d, 1H), 5.985 (dd, 1H), 6.244 (q, 1H), 6.288 (s, 1H), 7.196 (d, 1H), 7.309-7.831 (m, 14H), 8.125 (dd, 1H). ^{13}C δ (ppm) = 8.611, 14.766, 20.825, 22.126, 22.644, 26.771, 28.561, 28.703, 35.510, 35.538, 43.146, 45.572, 52. 774, 58.415, 71.854, 72.072, 74.159, 75.095, 75.606, 76.415, 78.893, 81.016, 84.438, 126.597, 127.205, 128.524, 128.690, 128.743, 129.081, 129.181, 130.216, 132.076, 132.794, 133.439, 133.682, 136.719, 142.608, 166.831, 167.735, 167.932, 169.831, 171.189, 171.270,175.697, 203.780. The mass spectrometry, IR and NMR spectral data are all respectively provided in Appendix Figures **A2.6**, **A3.6** and **A4.5**.

2.3.2.7 Serinol-C_{60}-Paclitaxel-2'-Succinate Derivative (7)

Compound **6** (9.54 mg, 0.010 mmol) was dissolved in DMF (200 μL), to which triethylamine (2.3 mg, 0.023 mmol), 1-ethyl-3-(3-dimethylaminopropyl)carbodiimide hydrochloride (EDC, 2.11 mg, 0.011 mmol) and 1-hydroxybenzotriazole hydrate (0.5 mg, ~0.004 mmol, catalytic amount) were added. Over 5 minutes, to the solution was added **5** (32.6 mg, 0.015 mmol) in DMF (300 μL), while stirring. The reaction was allowed to run for 24 hours, after which the solvent was removed and the water-soluble fraction was collected for further purification. The product was isolated using a cellulose ester dialysis membrane (Thermo Scientific, 2000 MWCO) for 7 days using DI water to remove water soluble byproducts, in the dark to prevent fullerene oxidation. Sample was dried *in vacuo*. Yield: 2.75 mg (0.9 μmol). MS MicroTOF ESI-TOF (positive-ion mode): calculated mass = 3071.9 Da; observed masses = 3071.6 Da [M^+]. The mass spectrometry and IR spectral data are respectively provided in Appendix Figures **A2.7** and **A3.7**.

Unfortunately, the coupling of paclitaxel-2'-succinate to the fullerene derivative was plagued with a poor yield and extreme difficulty in preparative separation of compound **7** from compound **5**, although HPLC was used to analytically determine a ratio of (Compound **7**):(Compound **5**). For these reasons, it was decided to take a complimentary synthetic approach to paclitaxel coupling with the hopes of increasing both yield and purity of the final conjugate. By utilizing conjugation of paclitaxel to polyethylene glycol (PEG), although the yield of the initial synthesis step was less, taking advantage of this water-soluble paclitaxel derivative whose synthesis is well-documented also produced a higher fullerene-paclitaxel conjugate yield (Compound **9**) that was easily

purified by HPLC. This higher-yield conjugate permitted synthesis of a fullerene-paclitaxel conjugate (Compound **9**) in sufficient quantity (>100 mg) to conduct the animal studies described below.

In vitro studies of compound **7** were performed using A375m melanoma cells, by Mr. John W. Marks, in the laboratory of Dr. Michael Rosenblum, Ph.D., at The University of Texas M.D. Anderson Cancer Center (MDACC). However, as we progress to performing *in vivo* studies, we transitioned to the laboratory of Dr. Steven Curley, M.D., a laboratory equipped for animal model testing. To better suit his specialty of hepatic cancer, *in vitro* and *in vivo* work was performed using the hepatocellular carcinoma Hep 3B cell line.

2.3.2.8 Paclitaxel-2′-Poly(ethylene glycol) Ester Derivative (8)

Paclitaxel-2′-Poly(ethylene glycol) ester was prepared by a modified literature procedure.[82] Poly(ethylene glycol) bis(carboxymethyl) ether (mPEG acid, Avg. M_n: 600 Da, 540 mg, 0.900 mmol) was dissolved in trichloroethylene (20 mL), and to this solution at 0 °C were added *N,N′*-diisopropylcarbodiimide (DIC, 176 µL, 1.15 mmol), paclitaxel (1.00 g, 1.15 mmol) and 4-dimethylaminopyridine (DMAP, 300 mg, 2.43 mmol). The resulting solution was allowed to achieve room temperature and left for 16 h. The reaction mixture was washed with 0.005 M HCl, dried, and evaporated *in vacuo* to yield a white solid. At 25 °C, the product was isolated using flash chromatography, (chloroform:methanol, 1:1). Yield: 580 mg (64%). MS Autoflex MALDI-TOF (positive-ion mode): calculated masses = 1277.53, 1321.55, 1365.58, 1409.60, 1453.63, 1497.66,

1541.68, 1585.71, 1629.74, 1673.76, 1717.79, 1761.81, 1805.84 Da; observed masses = 1278.708, 1322.736, 1366.754, 1410.789, 1454.808, 1498.844, 1542.902, 1586.920, 1630.972, 1675.000, 1719.051, 1764.033, 1808.182 Da [$M+H^+$], 1300.736, 1344.764, 1388.827, 1432.827, 1476.859, 1520.893, 1564.968, 1608.990, 1653.069, 1697.077, 1741.202 Da [$M+Na^+$]. NMR (500 MHz, $CDCl_3$, 0.05% (v/v) TMS reference): ^1H δ (ppm) = 1.109 (d), 1.177 (s), 1.223 (d), 1.643 (s), 1.671 (d), 1.808 (t), 1.931 (d), 2.043 (dd), 2.213 (d), 2.333 (s), 2.471 (t), 3.489-3.697 (m), 3.721 (dd), 3.746 (s), 4.013 (bs), 4.162 (dd), 4.262 (t), 4.244(s), 4.262 (t), 4.272-4.333 (m), 4.367 (dd), 4.433 (dd), 4.904 (d), 4.934 (d), 5.542 (q), 5.596 (s), 5.610 (s), 5.625 (s), 5.954 (d), 6.085 (t), 6.230 (s), 6.291 (s), 7.155 (t), 7.301-7.556 (m), 7.631 (q), 7.754 (d), 7.903 (d), 8.071 (d), 8.137 (d). ^{13}C δ (ppm) = 203.818, 172.816, 171.238, 171.184, 170.471, 169.861, 167.255, 166.842, 142.787, 134.407, 133.712, 132.540, 130.204, 130.138, 129.210, 129.189, 129.014, 129.001, 128.702, 128.682, 128.627, 128.516., 128.492, 128.454, 128.435, 128. 408, 128.186, 127.711, 127.631, 127.568, 127.313, 127.285, 84.414, 84.343, 80.677, 79.015, 78.942, 76.393, 76.372, 75.612, 75.587, 75.070, 73.455, 72.067, 70.878, 70.867, 70.851, 70.512, 70.466, 70.444, 70.406, 70.391, 70.381, 70.365, 70.344, 70.310, 70.209, 70.143, 69.940, 69.910, 69.811, 69.792, 69.751, 69.720, 69.669, 69.632, 69.598, 69.559, 69.525, 69.511, 58.436, 58.409, 45.594, 45.552, 43.141, 43.130, 43.106, 35.536, 26.777, 26.769, 26.664, 22.642, 22.098, 22.089, 21.844, 20.873, 20.834, 14.808, 14.690, 9.585, 9.544. The mass spectrometry, IR and NMR spectral data are all respectively provided in Appendix Figures **S2.8**, **S3.8** and **S4.6**.

2.3.2.9 Serinol-C_{60}-Paclitaxel-2′-Poly(ethylene glycol) Ester Derivative (9)

Compound **8** (78.97 mg, 0.055 mmol) was dissolved in water (15 mL, 1% MES Buffer, pH: 6.75) to which 1-ethyl-3-(3-dimethylaminopropyl)carbodiimide hydrochloride (EDC, 8.71 mg, 0.055 mmol) and 1-hydroxybenzotriazole hydrate (HOBt, 0.5 mg, 0.004 mmol, catalytic amount) were added. To the solution was added **5** (108.57 mg, 0.050 mmol) in H_2O (10 mL) while stirring. The reaction was allowed to run for 6 hours, after which the solvent was removed *in vacuo* and the product was isolated via HPLC. Yield: 5.5 mg (0.020 mmol, 40%). MicroTOF ESI (positive-ion mode): calculated masses = 3437.11, 3481.14, 3525.17, 3569.19, 3613.22 Da; observed mass = 3440.0, 3483.4, 3528.1, 3572.1 Da [M^+], 3461.6, 3505.5, 3550.3 Da [$M+Na^+$], 3566.9 Da [$M+K^+$]. The mass spectrometry and IR spectral data are respectively provided in Appendix Figures **S2.9** and **S3.9**.

2.3.2.10 3', 3", 3", 3"', 3"', 3"", 3"", 3""", 3""", 3"""", 3""""-dodeca-(2-hydroxy-1-{hydroxymethyl}ethylcarbamoyl)-3'H, 3"H, 3"'H, 3""H, 3"""H, 3"""" H-hexacyclopropa[1,2:18,36:22,23:27,45:31,32:55,60](C_{60}-I_h)[5,6]fullerene (10)

Serinol malonate fullerene was prepared by a modified literature procedure as shown in Scheme 5.[7] At 25 °C, C_{60} (1.00 g, 1.37 mmol), CBr_4 (4.14 g, 12.36 mmol) and **3** (5.17 g, 12.36 mmol) were combined and dissolved in 500 mL of a mixture of freshly distilled solvent (toluene:CH_2Cl_2, 1:1). To the resulting solution was added 1.92 g of DBU (12.36 mmol). After 18 hours, at 25 °C, the fullerene was isolated using flash chromatography, chloroform:methanol mixture (3:1). For removal of the acetate

protecting groups, the fullerene was dissolved in MeOH saturated with K_2CO_3 and sonicated for 1 hour, whereupon the solvent was removed *in vacuo* and the resulting product was purified using a cellulose ester dialysis membrane (Thermo Scientific, 2000 MWCO) for 7 days using DI water. Yield: 819.7 mg (0.371 mmol, 27%). MicroTOF ESI (positive-ion mode): calculated masses = 1960.50 (pentakis), 2208.61 Da (hexakis); observed mass = 1984.2 (pentakis), 2232.3 (hexakis) Da [$M+Na^+$]. The mass spectrometry and IR spectral data are respectively provided in Appendix Figures **S2.10** and **S3.10**.

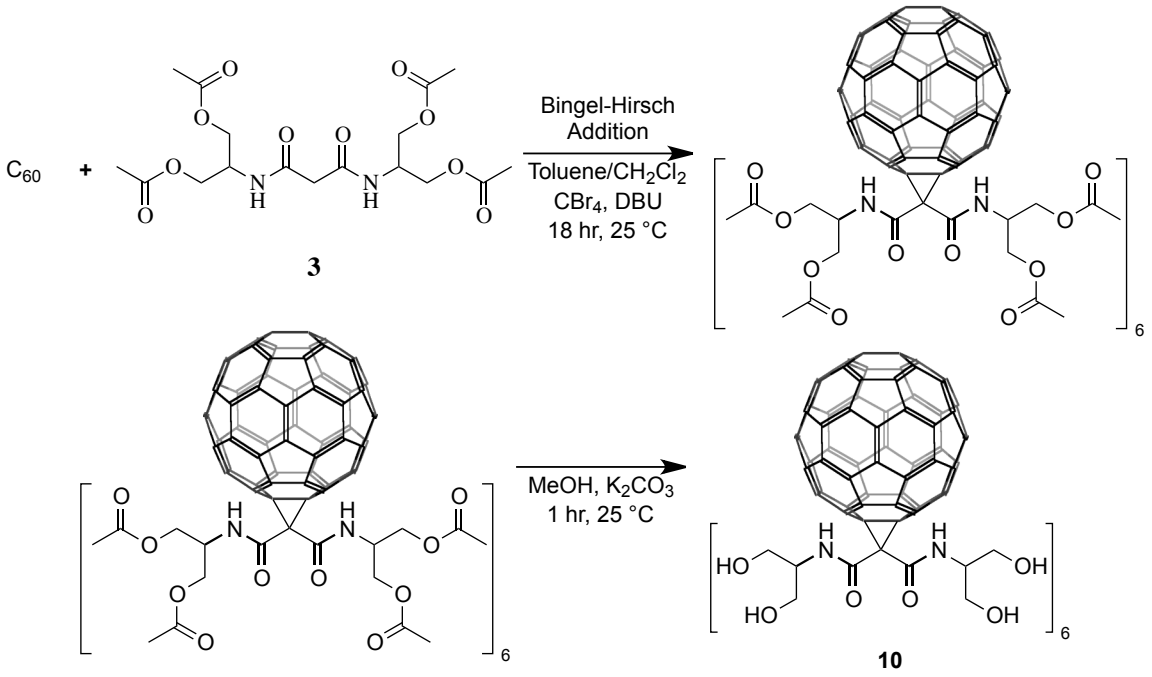

Figure 2.5: Synthesis scheme of 3', 3'', 3'', 3''', 3''', 3'''', 3'''', 3''''', 3''''', 3'''''', 3''''''-dodeca-(2-hydroxy-1-{hydroxymethyl}ethylcarbamoyl)-3'H, 3''H, 3'''H, 3''''H, 3'''''H, 3'''''' H-hexacyclopropa[1,2:18,36:22,23:27,45:31,32:55,60](C_{60}-I_h)[5,6]fullerene (**10**).

2.3.3 Dynamic Light Scattering Measurements

To understand the behavior of the serinol-C_{60}-paclitaxel-2′-poly(ethylene glycol) ester derivative (**9**) in solution, dynamic light scattering (DLS) measurements were performed on a solution of **9** at 100 μg/mL, using a Malvern Zetasizer, Model Zen 3600 (He-Ne laser, 4.0mW, 632.8 nm; Malvern Instruments Ltd, Malvern, Worcestershire, United Kingdom). For comparative purposes, measurements of the unconjugated water-soluble fullerene derivative (**5**) and the water-soluble paclitaxel-2′-poly(ethylene glycol) ester derivative (**8**) were measured at equivalent molar concentrations (61.1 μg/mL and 40.4 μg/mL, respectively). Scans for each solution were performed in triplicate, and for better dispersion in solution, all three samples were filtered upon dissolution using a Whatman Puradisc™ 25 mm, 0.45 μm pore size, polyethersulfone syringe filter (Maidstone, Kent, United Kingdom). Results were graphed using SigmaPlot 9.0 (Systat Software, San Jose, California).

2.4 *In Vitro* Studies of Gd@$C_{60}(OH)_x$ and C_{60}-Paclitaxel Derivatives

2.4.1 *In Vitro* Cytotoxicity of Serinol-C_{60}-Paclitaxel-2'-Succinate Derivative (Compound 7) and Serinol-C_{60}-Paclitaxel-2′-Poly(ethylene glycol) Ester Derivative (Compound 9)

A375m melanoma, Hep 3B hepatic carcinoma cells were passed and diluted to 25,000 cells/mL in medium (DMEM/High Glucose [Life Technologies] with 10% fetal bovine serum, non-essential amino acids (1×), MEM vitamin solution (1×) and sodium pyruvate (1×)). The samples were pipetted onto 96-well flat-bottom sterile plates (100

μL/well), with one row left empty for blanks. For a negative control, T-24 cells were passed and diluted to 20,000 cells/mL in medium, then pipetted as above. The plates were subsequently incubated overnight (37 °C, 5% CO_2, 100% humidity). Samples of paclitaxel, compound **7**, PEG-Paclitaxel (compound **8**), compound **9** and compound **10** were then prepared in medium at 2× intended concentration and then pipetted onto the cell plates (100 μL/well). Over the course of the experiment's 72 hours, when each well reached its assigned time point (4, 8, 24 or 72 hrs.), all media was removed from the well and replaced with fresh medium for the remainder of the experiment. After 72 hours, medium was removed from each well, and the plates were washed twice with phosphate-buffered saline, to which crystal violet stain solution was added (100 μL/well) to stain the samples for 30 minutes. The stain was removed and the plates were thoroughly washed with water and allowed to air-dry. For a more accurate reading, Sorenson's Buffer (150 μL/well, 50% ethanol in 0.1 M Citrate (Na^+), pH=4.2) was used to solubilize the crystal violet stain and the plates were gently shaken for 1 hour. Plates were read at 595 nm on a Bio-Tek ELx300 spectrophotometric plate reader, and the results are plotted as the log(sample concentration) × percent control [A(595) sample/A(595) no-sample control x 100]. GraphPad software was used to determine the IC_{50} points for each sample by non-linear regression.

2.4.2 *In Vitro* Studies of Metallofullerene Immunoconjugates

2.4.2.1 $Gd@C_{60}$ Immunoconjugate Preparation

Immunoconjugates of $Gd@C_{60}(OH)_x$ (hereafter referred to as $Gd@C_{60}$) were prepared using a procedure similar to previous C_{60}-based immunoconjugates, where conjugation is achieved via supramolecular chemistry rather than by conventional covalent attachment.[83] $Gd@C_{60}$ was combined in PBS solution with ZME-018 antibody (5:1 $Gd@C_{60}$:ZME-018) and stirred overnight at 4 °C. The solution was then removed and purified on a G-25 sephadex size-exclusion column, which removed any non-conjugated C_{60} from the sample, using buffer solution (10 mM Na_3PO_4, 140 mM NaCl at pH=7.2). After $Gd@C_{60}$-mAb conjugation and purification, Bio-Rad protein assays were used to determine concentrations of the antibody in the samples.

2.4.2.2 ELISA Testing of the $Gd@C_{60}$-mAb Immunoconjugates

The cell binding affinity of the $Gd@C_{60}$-mAb immunoconjugates was evaluated by calculating IP(50) values from enzyme-linked immunosorbent assay (ELISA) plots. 96-well plates containing adherent A375m (antigen-positive) cell plates were utilized. However, to better understand and characterize binding efficiencies and non-specific binding, T24 (antigen-negative) cells were also used for comparison with antigen positive cells. ELISA plates were prepared by versene-stripping desired A375m cells from tissue culture flasks, washing twice using DPBS, before resuspension in DPBS to a cell concentration of 1 M/mL. 50 μL of the cell suspension were placed into Falcon 3912 96-well μL plates, leaving 2 wells without cells for blanks. The plates were dried overnight

(37 °C), leaving the cell surface proteins intact, and stored (4 °C). At 25 °C, blocking buffer (200 μL) was added to the wells for 1 hour. The blocking buffer was removed via decanting, with immediate addition of control standards and experimental solutions (100 μL/well). The plate was incubated (25 °C) for 3 hours and the solution was removed. Each well was washed 3× with a washing buffer for preparation of IgG component detection. Anti-mouse IgG-HRP was diluted 1:1000 in diluting buffer, making 11 mL/ plate, which was aliquoted (100 μL/well) and incubated 15 minutes at 25 °C. The wells were then washed 3× with washing buffer. H_2O_2 (11 μL) was added to 2,2'-azino-bis(3-ethylbenzothiazoline-6-sulphonic acid (ABTS, 11 mL), aliquoted (100 μL/well) and incubated for 10 minutes (25 °C). The plate was then read at 405 nm to calculate the 50% inflection point of the concentration curve IC_{50} values.

2.4.2.3 Gd@C_{60}-ZME-018 Immunoconjugate Internalization into A375m Melanoma Cells

Cell internalization studies for the Gd@C_{60}-immunoconjugates were performed to determine the efficiency and rate with which the cell-specific Gd@C_{60}-immunoconjugates internalize into melanoma cells. Antigen positive (A375m) and negative (T24) cells were prepared on 100 mm^2 tissue culture plates at 2×106 cells/plate in Dulbecco's modified eagle medium (10% fetal bovine serum, pH=7.4). The cells were incubated overnight at 37 °C, followed by addition of 1×10^{-6} g/mL (6.67 nM), 10 mL/ plate, of the Gd@C_{60}-immunoconjugates over various time frames. The plates were incubated for 1, 2, 4 and 24 hours at 37 °C. At the end of the incubation period, the media

was removed and each cell sample washed with glycine buffer solution (10 mL, 0.05 M, pH 2.5 + 0.1 M NaCl), to remove any remaining cell-surface bound Gd@C_{60}-immunoconjugate. The sample plates were then washed with a neutralizing buffer (0.15 M Tris, pH 7.4), 10 mL. Using a trypsin solution (0.25% Trypsin + EDTA [GIBCO]), the cells were then detached and centrifuged for ICP-MS analysis. Trypsinization has not been previously shown to be a factor in influencing the outcome of internalization studies.

2.4.2.4 Determination of Gd^{3+}-ion concentration for the Gd@C_{60}-(ZME-018) Immunoconjugates in A375m Melanoma Cells

Once the binding efficiency had been determined to have been retained for the immunoconjugates, samples of the conjugates (0.667 nM) were digested with oxidizing HNO_3 (70%), heated to dryness and ICP-MS spectrometry was then used to determine the conjugate Gd@C_{60}:mAb ratio. For each cell internalization study, ICP-MS sampled and measured the [Gd^{3+}] ten times for each of the Gd@C_{60}-(ZME-018) and Gd@C_{60}-(MuIgG) immunoconjugates. An average of ten determinations per time point was used as the final [Gd^{3+}] with its standard deviation. ICP-OES to determine the Gd^{3+} concentration of the Gd@$C_{60}(OH)_x$/$C_{60}(OH)_x$ sample was performed using a Perkin-Elmer Optima 3000 DV ICP-OES system. ICP-MS to determine the Gd^{3+} concentration of the Gd@C_{60}-(ZME-018), Gd@C_{60}-(MuIgG), A375m and T24 samples were performed using a Varian 810 quadruple ICP-MS system.

2.4.3 *In Vitro* Studies of C_{60}-Paclitaxel Immunoconjugates

2.4.3.1 Serinol-C_{60}-Paclitaxel-2'-Succinate Derivative Immunoconjugate Preparation

Immunoconjugates of serinol-C_{60}-paclitaxel-2'-succinate immunoconjugate were prepared using the procedure stated in **2.4.2.1**, combining compound **7** separately with ZME-018 and MuIgG2a mAb samples (5:1) and stirring overnight at 4 °C. The sample solutions were then removed and purified on a G-25 sephadex size-exclusion column, which removed any non-conjugated **7** from the sample, using buffer solution (10 mM Na_3PO_4, 140 mM NaCl at pH=7.2). After **7**-mAb conjugation and purification, Bio-Rad protein assays were used to determine concentrations of the antibody in the samples. Additionally, for determination of the final **7**:mAb ratio, the UV-Vis spectra of the naked antibodies and their compound **7**-immunoconjugates were obtained.

2.4.3.2 *In Vitro* Timed Pulse Experiment for the Serinol-C_{60}-Paclitaxel-2'-Succinate Derivative Immunoconjugates

In vitro cytotoxicity of the Serinol-C_{60}-Paclitaxel-2'-Succinate Derivative Immunoconjugates was determined using the same procedure listed in **2.4.1**, utilizing A375m melanoma and T-24 bladder carinoma (control) cells.

2.5 *In Vivo* Studies of a C_{60}-Paclitaxel Derivative (Compound 9)

The animal experiments were performed by Mr. Brandon H. Cisneros at the M.D. Anderson Cancer Center. Cells from a luciferase, green fluorescent protein-transfected,

Hep 3B cell line were injected underneath the liver capsule of 29 severe combined immunodeficiency (CB17-SCID) mice, giving them orthotopic, hepatocellular carcinomas. Cells for this injection were cultured per American Type Culture Collection (ATCC) recommendations for Hep 3B cells. Four weeks post-injection, tumor growth in the mice was assessed using *in vivo* luminescence imaging by injecting the mice with luciferin (25 mg/kg, single dose). Luminescence was observed in all mice, indicating conversion of luciferin to oxy-luciferin with generation of light. This confirmed the presence of carcinomas. The mice were then randomized into five equal groups of six mice determining the material administered to them: (1) paclitaxel (suspended in Cremophor EL), (2) Abraxane® (a water soluble, clinically-available form of paclitaxel bonded to albumin), (3) compound **9** (C_{60}-paclitaxel), (4) compound **10** (water soluble C_{60}-serinol), and (5) phosphate buffered saline (PBS, control). The group administered **10** consisted of five mice instead of six.

For the paclitaxel group, paclitaxel was administered per intraperitoneal (IP) injection for 5 consecutive days at 12.5 mg/kg per dose per mouse in 100 μL sterile 1× PBS dilution. Abraxane and **9** were administered, each to their respective groups, for 5 consecutive days per IP injection, at 30 mg paclitaxel (equivalent)/kg per dose per mouse, in 100 μL sterile 1× PBS dilution. Concentrations for **9** were calculated with the assumption that the sample was 90% pure. Compound **10** was administered at 78 mg/kg per dose per mouse, in 100 μL sterile 1× PBS dilution. This dosage of water-soluble, non-conjugated fullerene represents the molar equivalent to that of **9** administered to the mice in their group. Prior to injection, each of the mice was weighed.

Hydrolysis of the ester linkage formed with paclitaxel's 2' hydroxyl appeared to be relatively labile and would precipitate in aqueous solutions over time, so careful steps were necessary to preserve its integrity. Dilutions of Abraxane and paclitaxel were prepared freshly each day of administration, while solutions of **9** were prepared in advance and frozen to prevent degradation. Aliquots of **9** were thawed per necessity and administered within an hour.

According to protocol, the study was to be terminated when two mice in any single treatment group (other than controls) required euthanasia. This was required to preserve statistical power for inferential testing while allowing maximum time for treatment effect. This occurred first in the control group, with mice being euthanized on days 5 and 7, and then subsequently in the Abraxane group, on day 9. Primary euthanization of the mice was performed with CO_2 and secondary euthanization was with cervical decapitation. Samples of kidney, liver, and intestine were fixed in formalin, while tumors were excised, trimmed of any healthy or adherent tissues, weighed and then divided. One portion of the tumor sample was flash frozen to allow for possible future paclitaxel quantification, and the remainder was fixed in formalin. Results were graphed using KaleidaGraph 4.1 (Synergy Software, Reading, Pennsylvania) and statistical data was obtained utilizing GraphPad Prism 6.0 (GraphPad Software, Inc., La Jolla, California).

Chapter 3

Results

3.1 Dynamic Light Scattering Characterization

Aggregation measurements of the hydrodynamic diameter (D_h) of compounds is comparable to previous results with fullerenes and of the same order of magnitude.[20,84,85] Results obtained by Zakharian *et al.* for hydrophobic C_{60}-paclitaxel liposomes show that $D_h \approx 130$ nm, independent of suspension concentration, while Laus *et al.* demonstrate larger D_h values for extremely hydrophilic endohedral fullerene derivatives (D_h=810.7 nm for $Gd@C_{60}(OH)_x$, D_h=720.6 nm for $Gd@C_{60}[C(COOH)_2]_{10}$). The aggregation results for the water-soluble compound **9** are evident, in that although chemically similar in nature to hydrophobic C_{60}-paclitaxel, the water-solubilizing groups attached not only increase its hydrophilicity, but also its mass and volume. Thus measured aggregate sizes increase as the water-solubilizing groups attached allow the serinol-C_{60}-paclitaxel-2′-poly(ethylene glycol) ester derivative to more closely approximate the hydrophilic nature of $C_{60}(OH)_x$.

In measuring the unconjugated fullerene, compound **5**, a small measurement at ~5000 nm was found in only one of the three scans and is an H_2O artifact that inconsistently appears periodically. Additionally, the distribution in measured sizes of compound **9** shows a slight tail, with a minor aggregate size of about 10% the intensity of the main size, centered around D_h=78.82 nm. This distribution, however, is not considered bimodal and demonstrates that the sample is completely aggregated in

solution. Mean intensities of the measured hydrodynamic diameters are provided in **Appendix A5.**

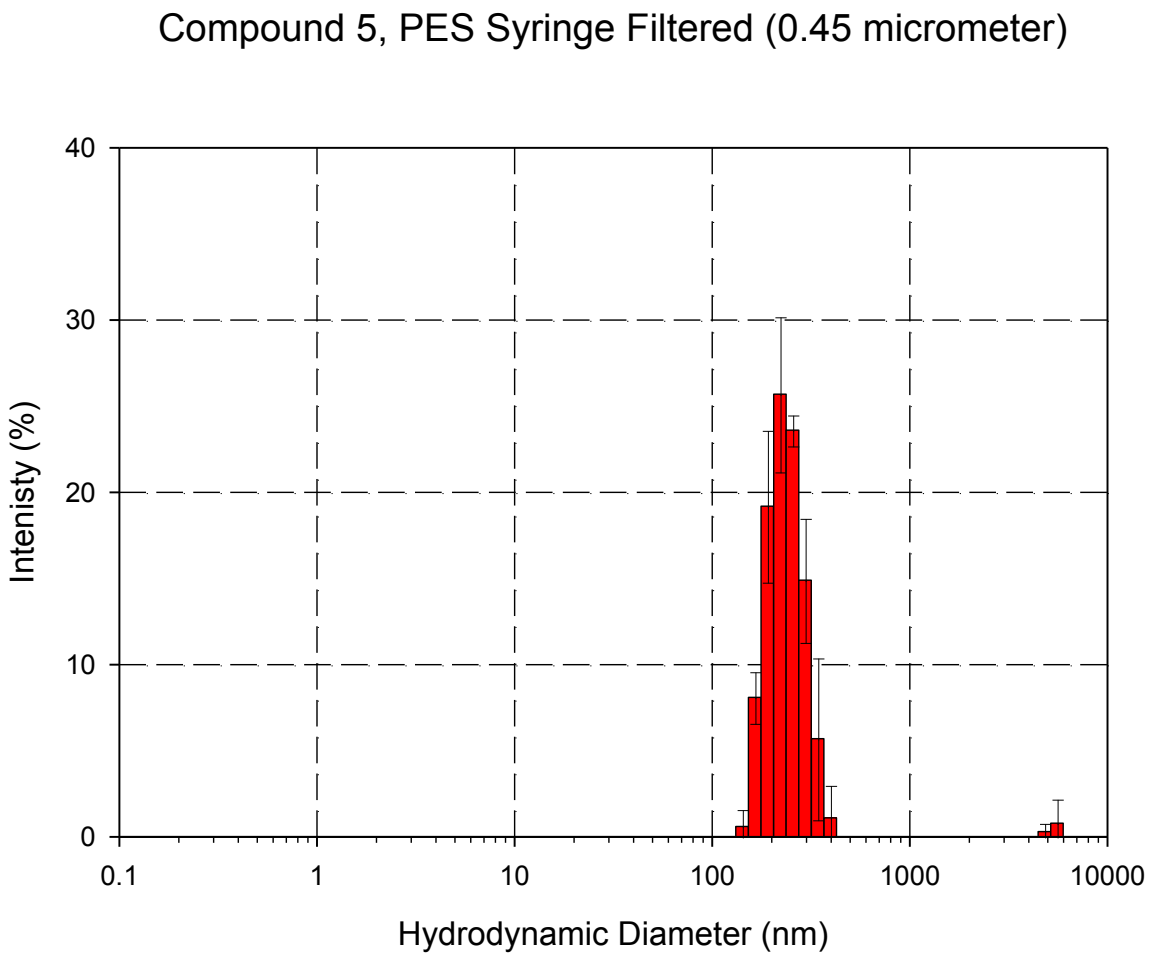

Figure 3.1.1: DLS Histogram of particle aggregation size in aqueous solution of water-soluble unconjugated serinol-C_{60} (**5**, 61.1 μg/mL). Error bars represent +/- one standard deviation.

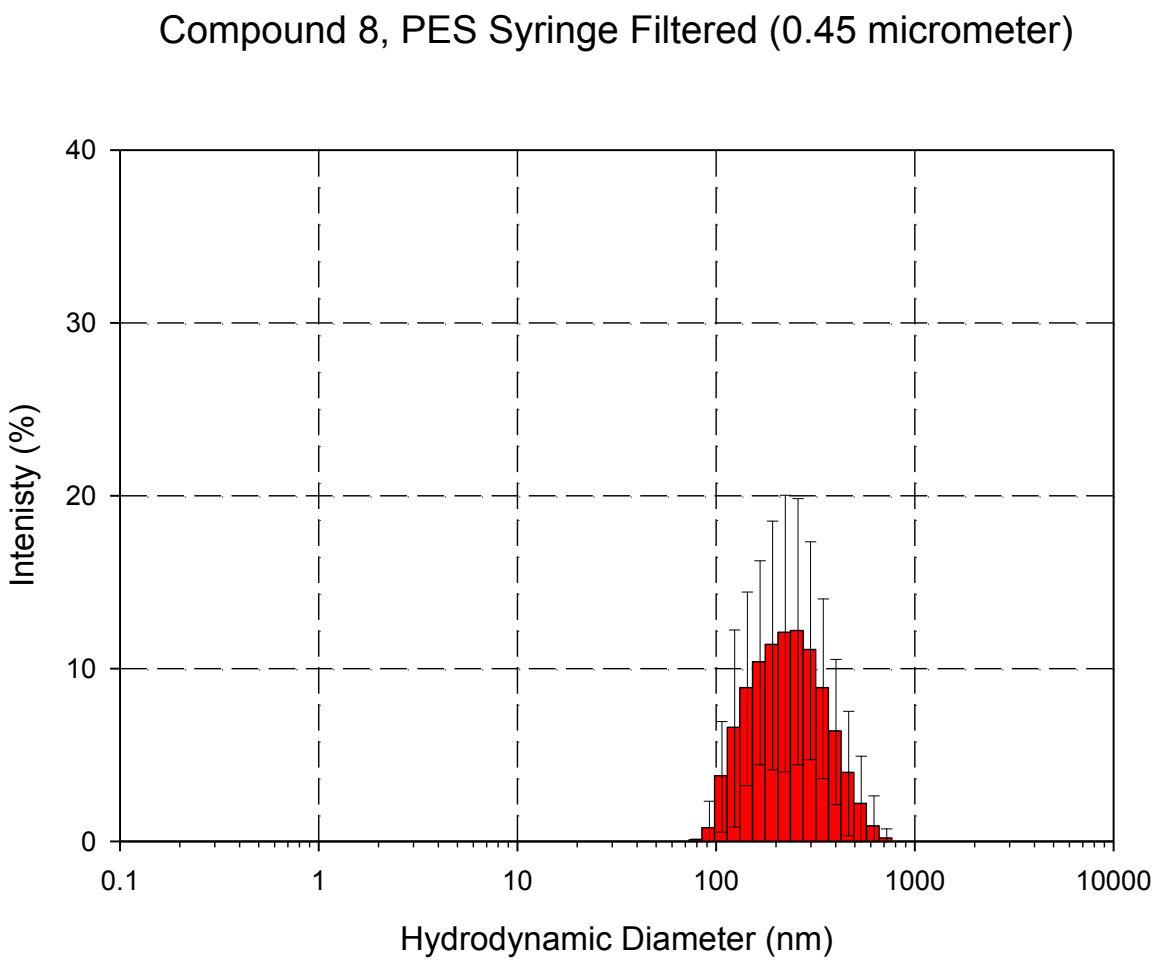

Figure 3.1.2: DLS Histogram of particle aggregation size in aqueous solution of paclitaxel-2′-poly(ethylene glycol) ester derivative (**8**, 40.4 μg/mL). Error bars represent +/- one standard deviation.

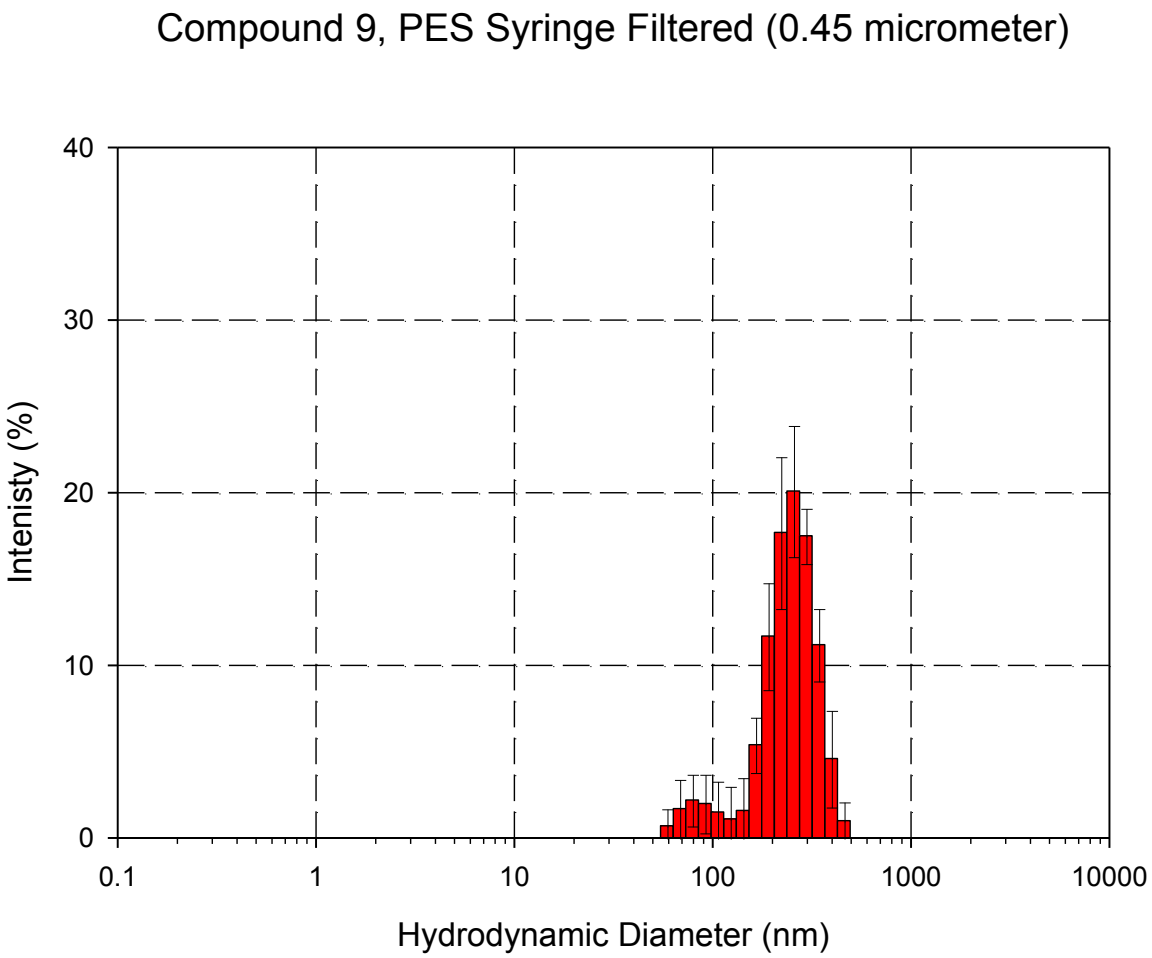

Figure 3.1.3: DLS Histogram of particle aggregation size in aqueous solution of serinol-C_{60}-paclitaxel-2′-poly(ethylene glycol) ester derivative (**9**, 100 μg/mL). Error bars represent +/- one standard deviation.

	Compound 5	Compound 8	Compound 9
Concentration (μg/mL)	61.1	40.4	100
Average Hydrodynamic Diameter (D_h, nm)	294.2	247.6	244.5

Table 3.1.1: Average hydrodynamic diameter sizes for molar equivalent concentration solutions of serinol-C_{60}-paclitaxel-2′-poly(ethylene glycol) ester derivative (compound **9**) and its synthetic precursors (compounds **5** and **8**).

3.2 *In Vitro* Studies of $Gd@C_{60}(OH)_x$ and C_{60}-Paclitaxel Derivatives

3.2.1 *In Vitro* Cytotoxicity of Serinol-C_{60}-Paclitaxel-2'-Succinate Derivative (Compound 7) and Serinol-C_{60}-Paclitaxel-2′-Poly(ethylene glycol) Ester Derivative (Compound 9)

Cytotoxicity results of the studies performed on oncology cell lines revealed a puzzling contrast (Figure **3.2.1**). Primarily, it was confirmed that when quantifiable, measurements of cytotoxicity within the first 4 and 8 hour time points were negligible. Additionally, an IC_{50} value for the control water-soluble fullerene compound **10** was negligible due to no observable cytotoxic activity. Secondly, paclitaxel showed consistent cytotoxicity across all three cell lines. However, compound **7** and PEG-Paclitaxel (compound **8**) demonstrate, that once the paclitaxel is conjugated, its cytotoxicity markedly decreases and its IC_{50} increases. Finally, compound **9** showed the surprising result that once paclitaxel is conjugated to a water-soluble fullerene via a 2'-poly(ethylene glycol) ester bond, its efficacy increases significantly over paclitaxel itself.

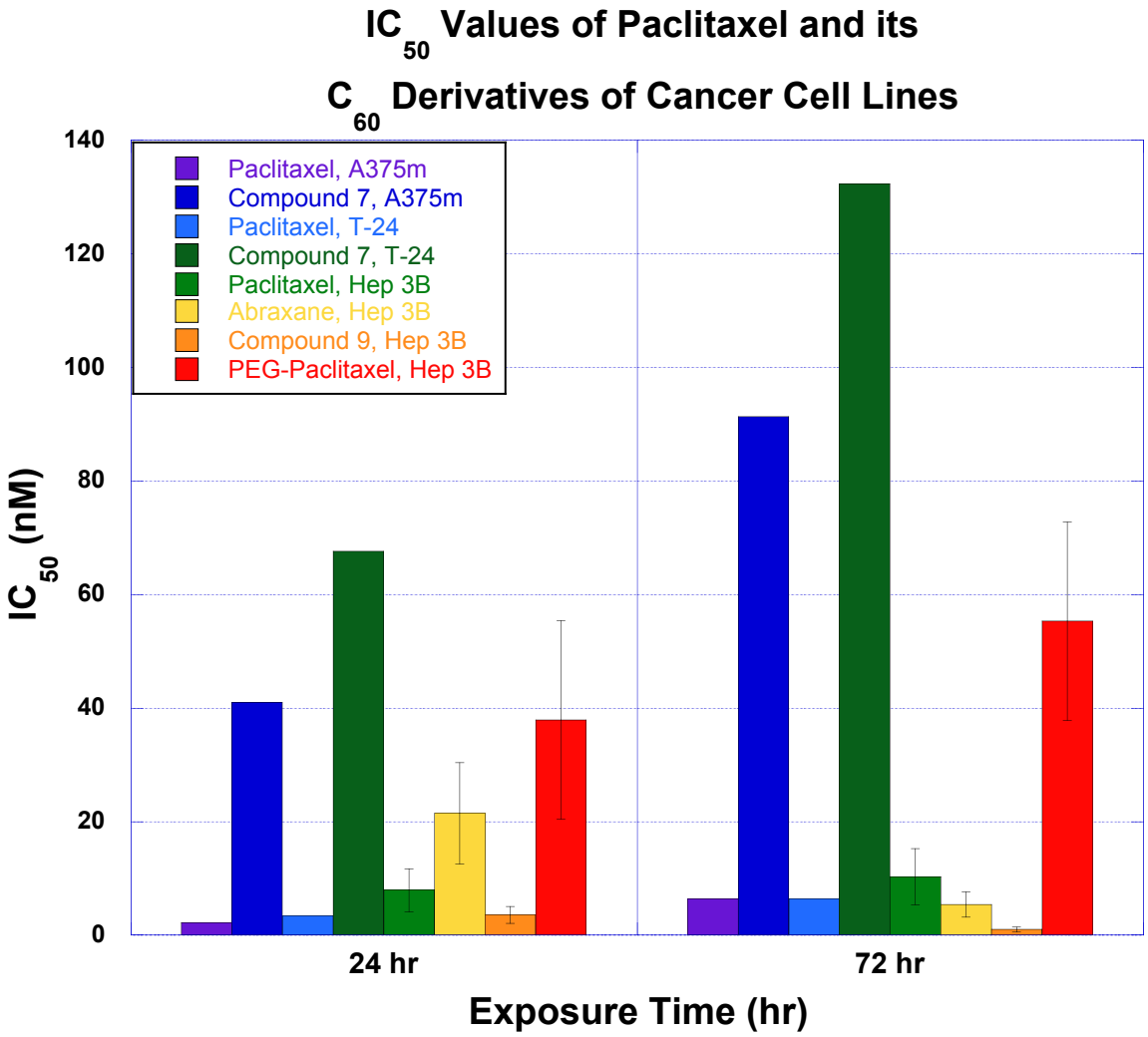

Figure 3.2.1: *In Vitro* Timed Pulse Cytotoxicity assay of paclitaxel, compound **7**, compound **9**, Abraxane and PEG-paclitaxel in A375m, T-24 and Hep 3B cancer cell lines. Almost all measurements for the 4 and 8 hour timepoints, as well as those for the compound **10** control provided R^2 values less than 0.80, indicating limited toxicity, and were thus excluded from the figure. Where indicated, error bars represent +/- one standard deviation.

3.2.2 *In Vitro* Studies of Metallofullerene Immunoconjugates

3.2.2.1 ELISA Testing of the Gd@C_{60}-mAb Immunoconjugates

To determine whether specific binding was retained upon fullerene conjugation, the ELISA binding curves and IP(50) values, which reflect binding efficiencies, were determined for both the Gd@C_{60}–(ZME-018) and Gd@C_{60}-(MuIgG) immunoconjugates in both A375m and T-24 cell lines (**Figure 3.2.2**). IP(50) values in the A375m cell line, for the Gd@C_{60}–(ZME-018) immunoconjugate (IP(50)=44.8 ng/mL) and non-conjugated ZME-018 (IP(50)=43.9 ng/mL) were practically identical, reflecting unchanged specific targeting of the antibody upon conjugation. Comparing the targeting of Gd@C_{60}–(ZME-018) to the negative nonspecific Gd@C_{60}-(MuIgG) immunoconjugate (IP(50)=1228 ng/mL) to A375m cells, the binding was nearly 800 times more efficient, indicating that Gd@C_{60}–(ZME-018) clearly retains cell specificity over a non-targeting mAb. Finally, to measure any increase in nonspecific immunoconjugate binding, the IP(50) value of Gd@C_{60}–(ZME-018) was determined for T24 (human bladder carcinoma) cells. At IP(50)=13,320 ng/mL, this represents a measurable increase in nonspecific binding over the unmeasurable IP(50) value of unconjugated ZME-018 mAb. However, the difference between specific and nonspecific binding is still greater by a factor of almost 300. The results shown here indicate little change in the specific binding of the Gd@C_{60}-(ZME-018) immunoconjugate from the original, unconjugated ZME-018 antibody.

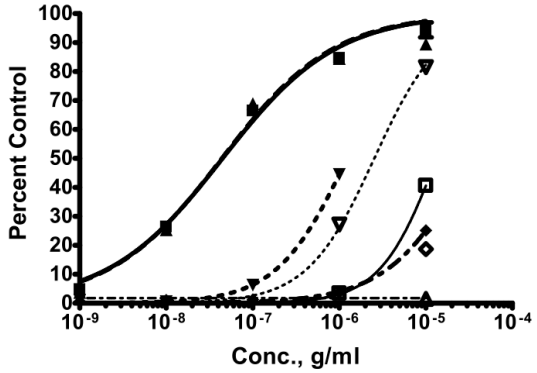

Cell Line	Sample	IC(50), ng/ml
A375m	ZME-GdC60	44.8
A375m	ZME	43.9
A375m	muIgG-GdC60	1228
A375m	muIgG	33790
T-24	ZME-GdC60	13320
T-24	ZME	NA
T-24	muIgG-GdC60	2537
T-24	muIgG	NA

Figure 3.2.2: ELISA (Dry-cell) A375m (+) and T-24 (-): Two hour incubation, dead cell tests of the Gd@C_{60}-immunoconjugates

3.2.2.2 Determination of Gd^{3+}-ion concentration for the Gd@C_{60}-(ZME-018) Immunoconjugates in A375m Melanoma Cells

ICP-MS determined the [Gd^{3+}] of each fullerene immunoconjugate sample, whereupon the total fullerene concentration (assuming only 41.9% of the sample is Gd@$C_{60}(OH)_x$) in the sample and the total fullerene (Gd@$C_{60}(OH)_x$+$C_{60}(OH)_x$):mAb ratio were calculated (**Tables 3.2.1** and **3.2.2**). The results showed a relatively close adherence to the 5:1 ratio in which the fullerene and mAb were combined, though measured drops in the ratio could be due to fullerene lost over the course of the experiment, possible through separation on the Sephadex column.

mAb Conjugate	mAb Concentration (nM)[1]	Gd@C_{60} Concentration (nM)	Total Fullerene (Gd@C_{60}+C_{60}) Concentration (nM)[2]	Total Fullerene:mAb Ratio
Gd@C_{60}-(ZME-018)	0.667	1.42	3.39	5.09
Gd@C_{60}-(MuIgG)	0.667	1.39	3.30	4.96

Table 3.2.1: ICP-MS results for the Gd@$C_{60}(OH)_x$ immunoconjugates and the calculated Gd@C_{60}+C_{60}:mAb ratio for Experiment 1.

mAb Conjugate	mAb Concentration (nM)[1]	Gd@C_{60} Concentration (nM)	Total Fullerene (Gd@C_{60}+C_{60}) Concentration (nM)[2]	Total Fullerene:mAb Ratio
Gd@C_{60}-(ZME-018)	0.667	1.34	3.19	4.78
Gd@C_{60}-(MuIgG)	0.667	1.35	3.23	4.85

Table 3.2.2: ICP-MS results for the Gd@$C_{60}(OH)_x$ immunoconjugates and the calculated Gd@C_{60}+C_{60}:mAb ratio for Experiment 2.

1) Determined by BioRad protein assay.

2) Determined assuming the composition of metallofullerene in the mAb sample contained 41.9% Gd@C_{60}(OH)x and 58.1% $C_{60}(OH)_x$.

For the time-dependent cell internalization experiments, the Gd^{3+}-ion concentration for both the Gd@C_{60}-(ZME-018) and Gd@C_{60}-(MuIgG) samples were each determined ten times using ICP-MS for the experiment run in duplicate (**Tables A6.1** and **A6.2**). For Experiment 1, the Gd@C_{60}-(ZME-018) immunoconjugate exhibited an increase in delivery of Gd@C_{60} to the A375m cells, peaking in concentration of 9.38×10^{13} Gd@C_{60}+C_{60} molecules/cell at the two hour time point (**Table A6.1**) and then

slowly declining to an average of 4.75×10^{13} Gd@C_{60} molecules/cell after 24 hr (**Figure 3.2.3**). Experiment 2 yielded similar results, with the Gd@C_{60}-(ZME-018) immunoconjugate peaking in concentration at 9.34×10^{13} Gd@C_{60}+C_{60} molecules/cell at the two hour time point (**Table A6.2**) and then slowly declining to an average of 4.31×10^{13} Gd@C_{60} molecules/cell after 24 hr (**Figure 3.2.3**). Results from both of these experiments indicate a significant preferential internalization for the targeting Gd@C_{60}-(ZME-018) to A375m cells over the non-targeting controls.

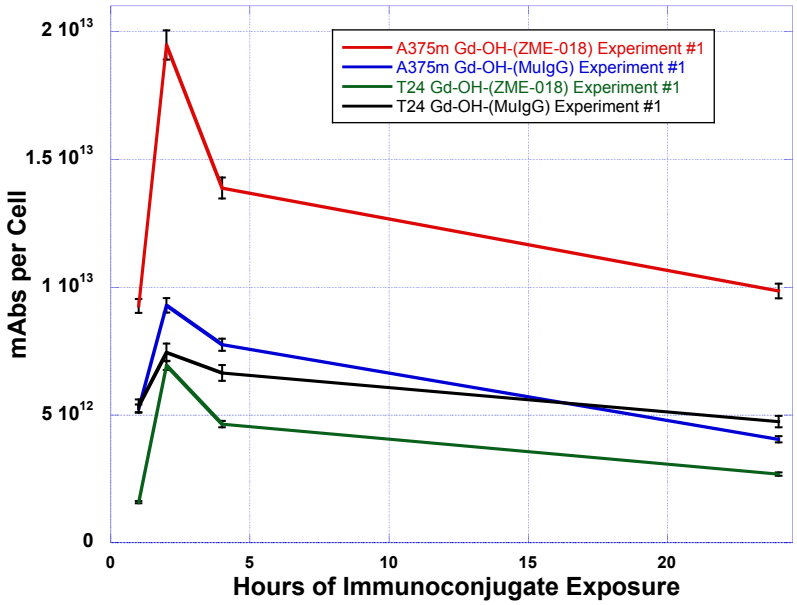

Figure 3.2.3: Internalization of Gd@C_{60}-mAb immunoconjugates into cells over time (Experiment 1). Error bars represent one +/- one standard deviation for ten individual [Gd^{3+}] determinations for each time point.

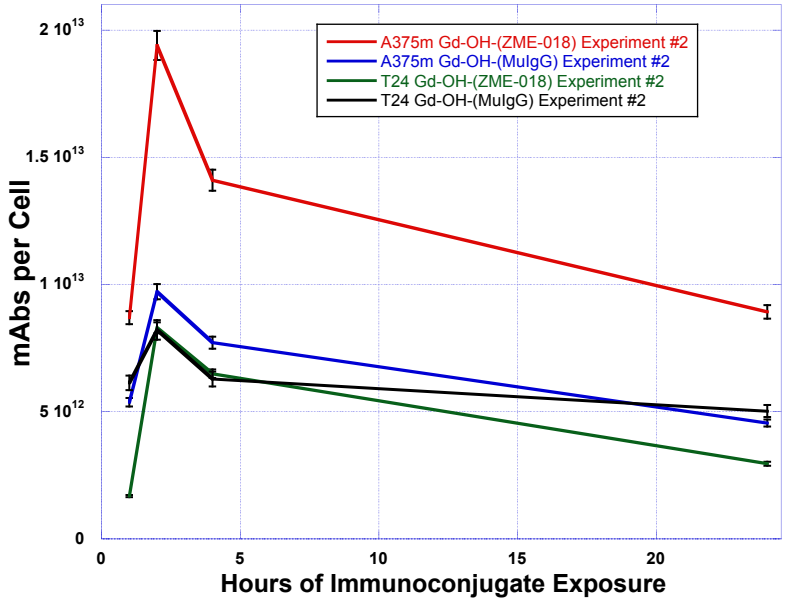

Figure 3.2.4: Internalization of Gd@C_{60}-mAb immunoconjugates into cells over time (Experiment 2). Error bars represent one +/- one standard deviation for ten individual [Gd^{3+}] determinations for each time point.

3.2.3 *In Vitro* Studies of C_{60}-Paclitaxel Immunoconjugates

3.2.3.1 Serinol-C_{60}-Paclitaxel-2'-Succinate Derivative Immunoconjugate Preparation

To quantitatively confirm conjugation of compound 7 to both ZME-018 and MuIgG, UV-Vis spectra (**Figure 3.2.4**) of the naked antibodies and their Compound **7**-immunoconjugates were obtained, as well as compound **7**. Using Beer's Law ($A=\varepsilon lc$) to calculate the additional absorbance produced from the fullerene component of the immunoconjugate, the ratios of **7**:ZME-018 and **7**:MuIgG were determined to be 4.86 and 5.24 respectively.

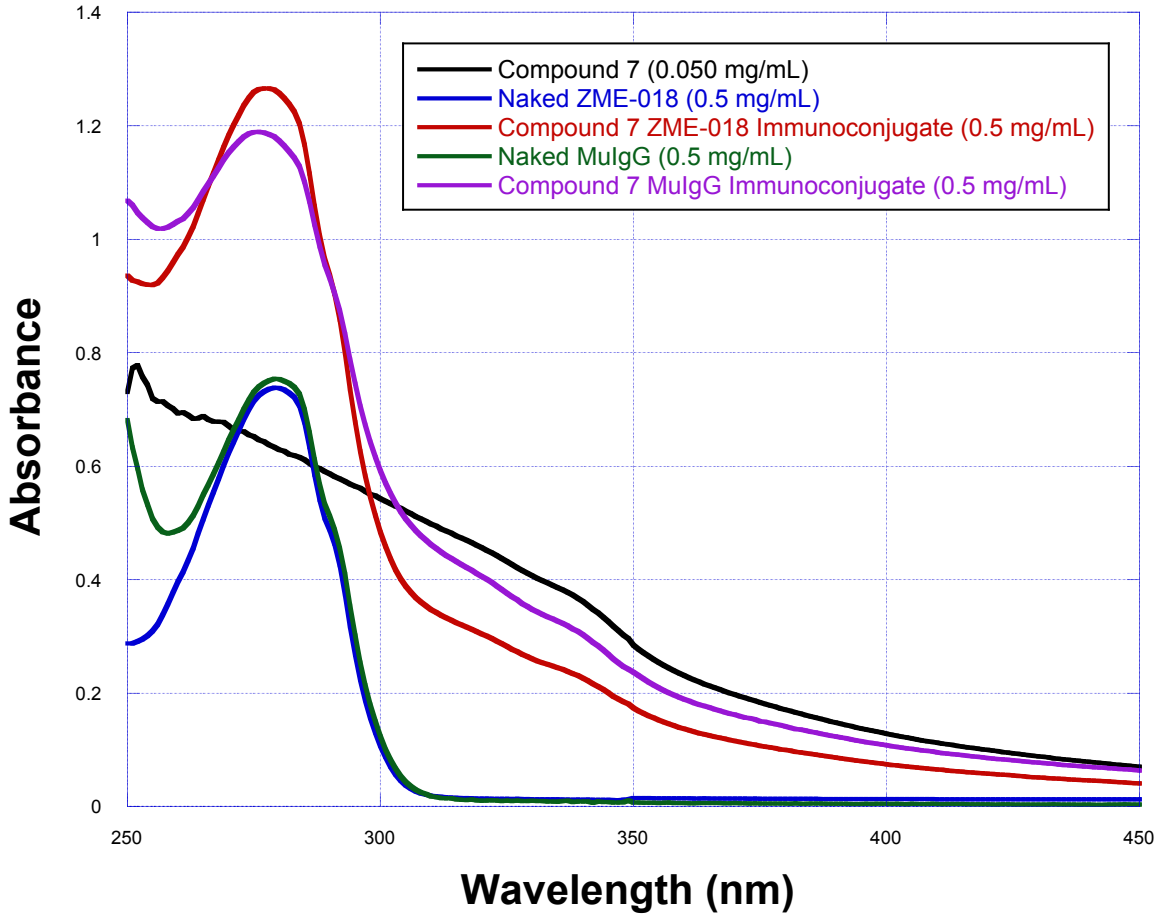

Figure 3.2.5: UV-Vis spectra comparing the two immunoconjugates to the two naked antibodies. The immunoconjugates exhibited increased absorbance from 250-450 nm, especially at shorter wavelengths.

3.2.3.2 *In Vitro* Timed Pulse Experiment for the Serinol-C_{60}-Paclitaxel-2'-Succinate Derivative Immunoconjugates

Results from cytotoxicity studies for compound **7** demonstrated some intriguing results. First, as determined in **3.2.1**, conjugation of paclitaxel to water-soluble C_{60} via succinic acid decreases the cytotoxicity of paclitaxel. This result, however, is in accordance with previous studies.[20,82] Second, upon conjugation of compound **7** to the

mAb, all visible targeting behavior of the antibody was lost. The Compound 7-(ZME-018), which targets A375m cells, showed a 50% increase in the IC_{50} over the non-targeting MuIgG control immunoconjugate. These results were additionally reflected in the control T-24 cells, where the MuIgG immunoconjugate showed greater cytotoxicity than the ZME-018. Since neither the ZME-018 or MuIgG antibody targets T-24 cells, no measurable difference in cytotoxicity should be demonstrated between the immunoconjugates.

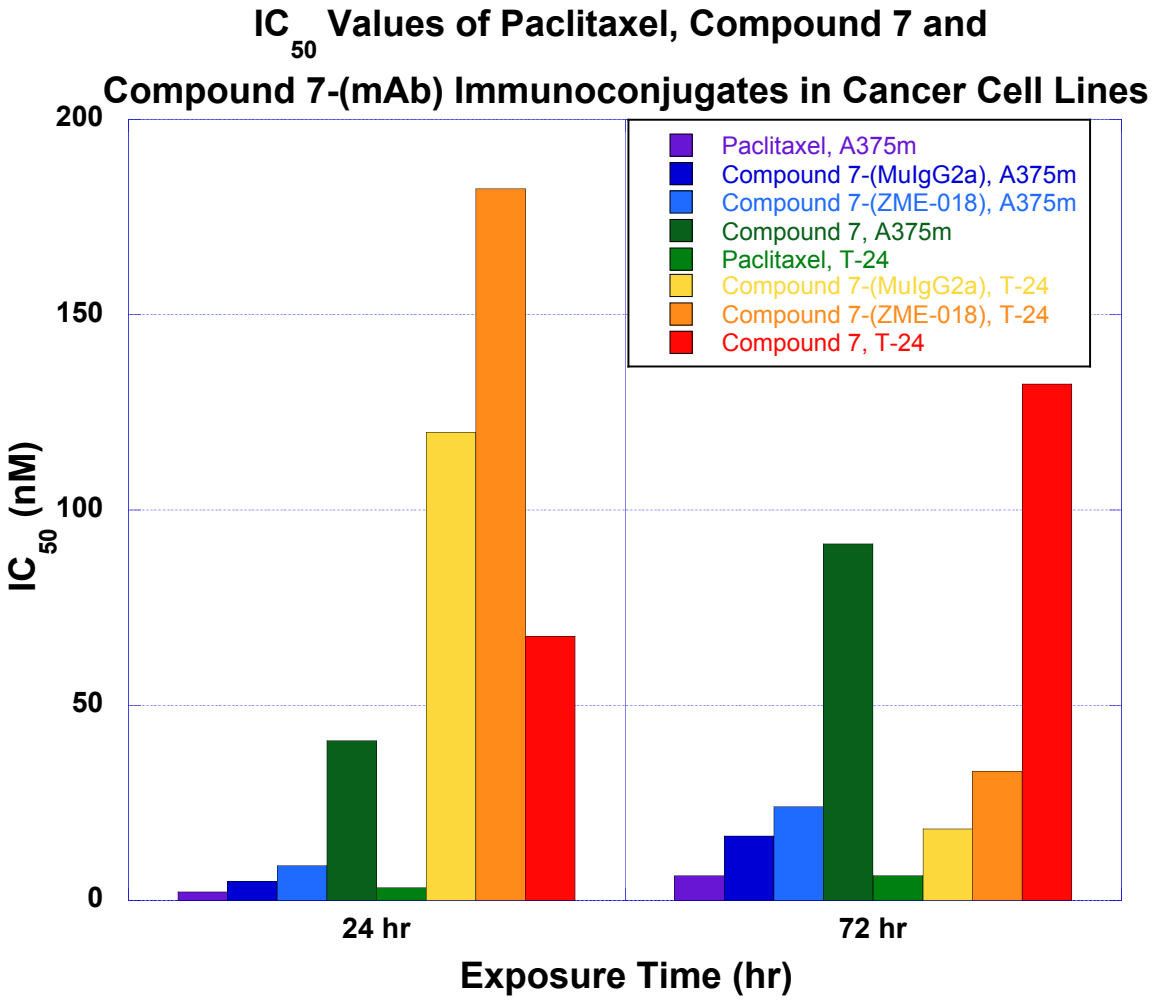

Figure 3.2.6: *In Vitro* Timed Pulse Cytotoxicity assay of paclitaxel, compound **7** and immunoconjugates in A375m melanoma and T-24 bladder carcinoma cell lines. Almost

all measurements within the 4 and 8 hour timepoints provided R^2 values less than 0.90, excluding them from the figure.

3.3 *In Vivo* Studies of a C_{60}-Paclitaxel Derivative

Throughout the course of *in vivo* testing, most of the animal masses remained relatively unchanged, with both the averages and standard deviations holding steady. However, there was a noticeable decline over time, in the body masses of the Abraxane group, a trend which by day 7 triggered the veterinary staff to give gel food to all mice, excluding the experimental (compound **9**) group, in order to help them better cope with weight loss. Masses of murine subjects during the course of the experiment are provided in **Appendix A7**.

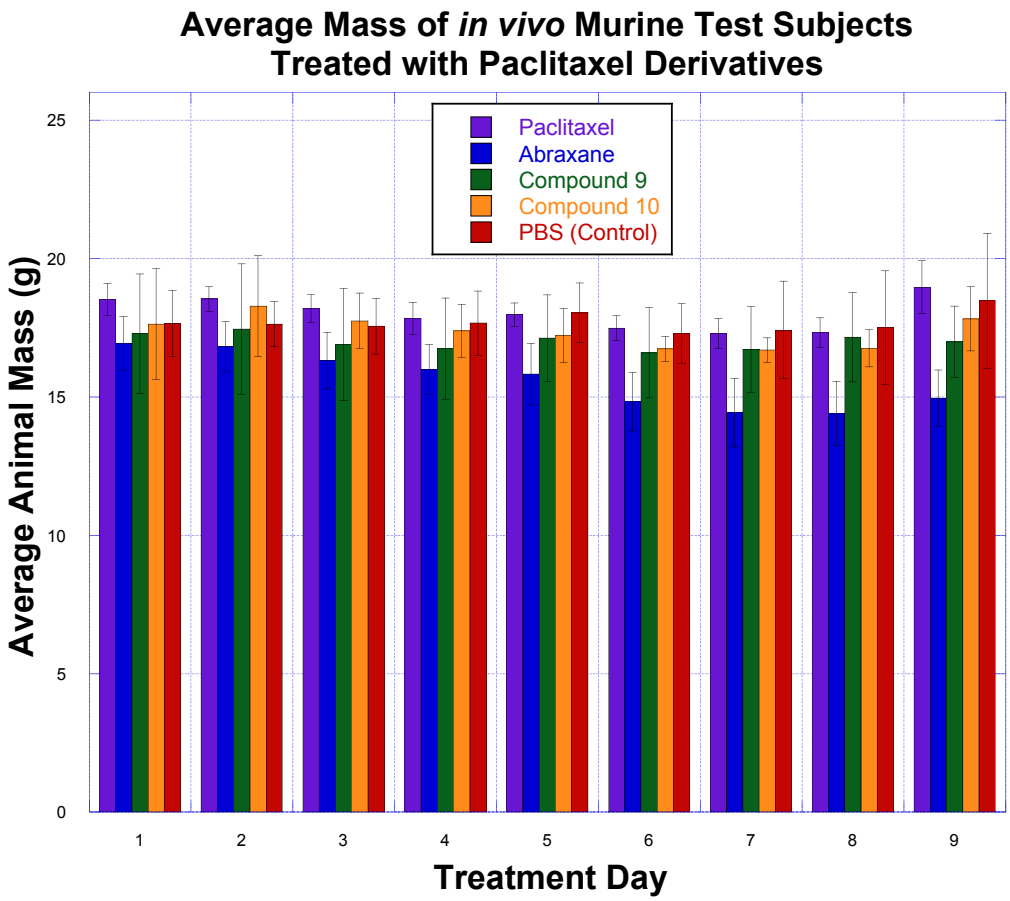

Figure 3.3.1: Average mass of *in vivo* murine test subjects during treatment with paclitaxel derivatives. Error bars represent +/- one standard deviation.

Overall, the subject tumor mass results appear to better reflect the treatment efficacy than results measured in murine body mass. While the control samples, compound **10** and PBS, predictably show the greatest increase in tumor mass, with one PBS subject dying on day 4, and one undergoing euthanization on day 6, due to excessive tumor burden. Of the five materials tested, paclitaxel remains the most effective at controlling overall tumor growth. Interestingly, the subject group administered compound

9, the experimental fullerene sample, showed resulting tumor masses comparable to the clinically-approved Abraxane.

To determine whether the *in vivo* results demonstrate that compound **9** is significantly different from PBS control when administered to murine subjects, a two-tailed t-test was performed, with the null hypothesis being that there is no difference in tumor mass between the compound **9** and PBS control groups. Statistical calculations of compound **9** versus the PBS control show a P value of 0.0869, indicating a retention of the null hypothesis on the 95% confidence level. Interestingly, comparison of FDA-approved Abraxane with PBS control shows a P value of 0.0840, a value close to 0.0869, and one that also fails to demonstrate a difference in treatments on the 95% confidence level. The source of these failures most likely stems from the small number of subjects in each treatment group, leading to a large standard deviation in the measurements and thus difficulty ascertaining whether the observations reflect a truly significant difference between the treatment and control groups.

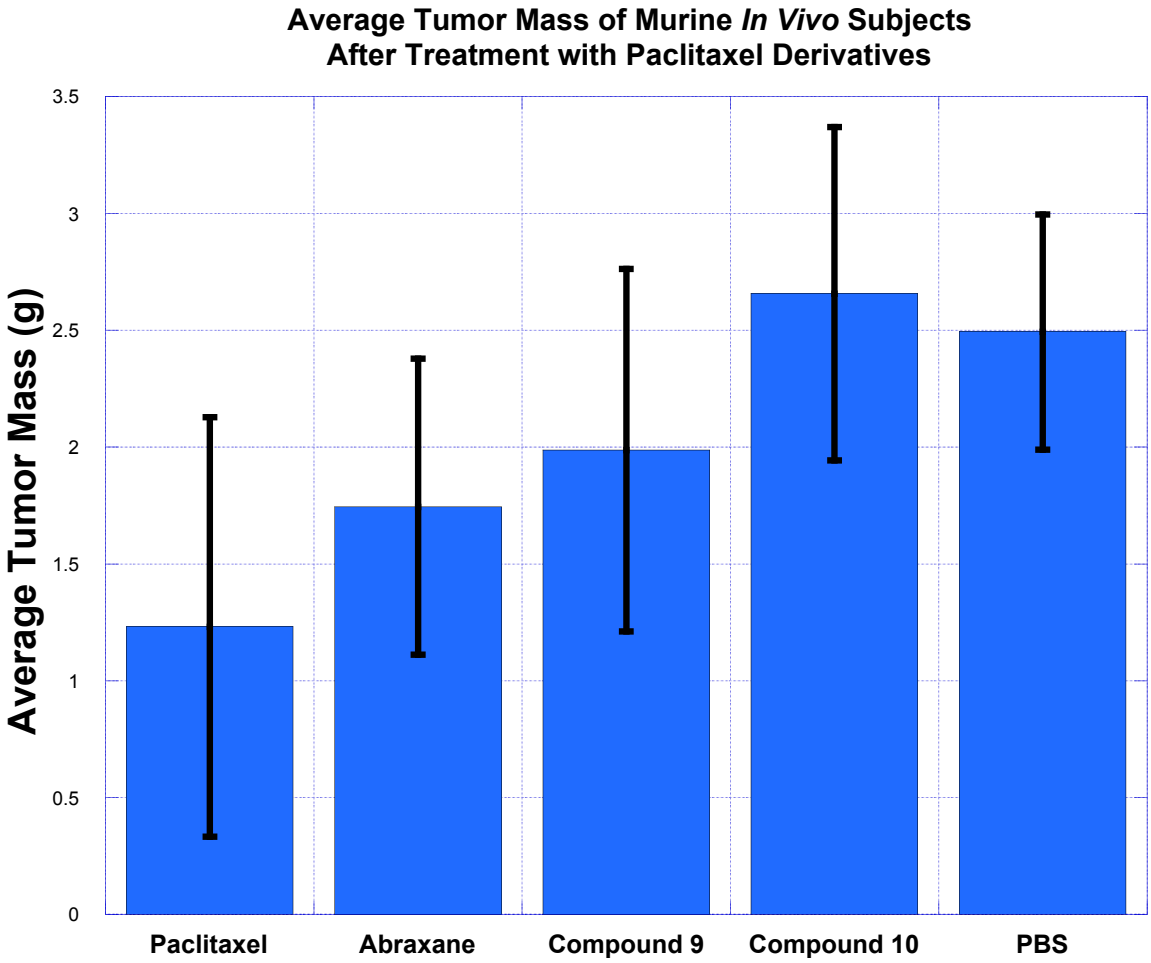

Figure 3.3.2: Average tumor mass in murine test subjects after treatment with paclitaxel derivatives. Error bars represent +/- one standard deviation.

Chapter 4

Discussion

Currently, the development of a paclitaxel-C_{60} conjugate described in this thesis serves as a contribution to the growing library of research utilizing fullerenes as therapy modalities. However, as the first well-characterized, water-soluble C_{60} conjugate for specific use as a drug delivery vehicle, the potential is great for the development of new fullerene conjugates and therapeutic development of FIT.

The synthetic hurdles for compounds **7** and **9** were formidable in achieving the final product derivatives. Although the initial step of synthesizing paclitaxel-2'-succinate was facile, its conjugation to **5** was plagued by low yields and difficult to purify, making it unsuitable for *in vivo* testing. By using a well-documented synthesis to conjugate poly(ethylene glycol) to paclitaxel, and then covalently attaching the conjugate to water-soluble C_{60}, a system has been developed for producing water-soluble fullerene derivatives in sufficient quantities for drug delivery. In particular contrast to other fullerene-drug conjugates,[38,39,40,41] compounds **7** and **9** are uniform and well characterized, a requisite for therapies seeking FDA approval for clinical use.

In the development of FIT, conjugating water-soluble paclitaxel-C_{60} derivatives to antibodies reveal the need for further investigation. Our initial studies, utilizing $Gd@C_{60}(OH)_x$, determined that C_{60}-mAb immunoconjugates maintain selective binding and internalize into A375m melanoma cells, taking $Gd@C_{60}(OH)_x$ with them. However, when replicating these internalization experiments with compound **7**, cytotoxicity was

maintained, though there was no demonstrated significant difference between targeted A375m and control T-24 bladder carcinoma cells.

In these experiments, the loss of specific delivery of paclitaxel, but maintenance of overall cytotoxicity, is attributable to one of two factors. The first possibility is that paclitaxel is being prematurely liberated from the fullerene before it can properly internalize into the cell, either via esterase activity or spontaneous ester hydrolysis. Addressing this possibility requires either a more biostable linker at paclitaxel's 2' hydroxyl, or conjugating an ester linkage to either the 1- or 7- hydroxyl on paclitaxel.

Chemistry provides only a limited number of biolabile linkers that are strong enough for eventual delivery under biological conditions, yet labile enough for eventual release, usually triggered either by a drop in pH (consistent with cancer cells) or enzymatic activity. The first candidate for a stronger linker would be an ester linker α-substituted with aliphatic groups. This approach would maintain similar chemistry to that already developed above, but electrostatic induction from electron donating aliphatics would serve to strengthen the adjacent ester bond, thus making the paclitaxel less labile. Additional approaches include replacing the 2'-ester bond with a carbamate or carbonate ester bond for greater stability. These classes of bonds are frequently used in pharmaceutical chemistry due to their simultaneous biostability and lability, but their formation and purification can be challenging and would most likely prove difficult for a molecule such as paclitaxel. The additional possibility also exists for utilizing either of paclitaxels 1- or 7-hydroxyls. This approach, however, is challenged by both the significant steric unreactivity of paclitaxel's 1-hydroxyl, thus rendering esterification

difficult, and the marked decrease in activity of 7-hydroxy esters due to overstability.[86,87,88]

Another possible explanation for the limited activity demonstrated by compound **7**-mAb immunoconjugates is that while **7** is stable in associating with mAbs in PBS solution, introduction into medium disrupts the supramolecular forces holding the fullerene to the mAb. If the fullerene conjugate is semi-labile in the presence of other proteins, this too would explain the results of the immunoconjugate, where cytotoxicity is maintained, yet selective activity for A375m cells is not.

While either premature 2'-ester hydrolysis or antibody-fullerene dissociation is a viable possibility, a previous study demonstrated similar results, where paclitaxel-2'-succinate was conjugated to the anti-epidermal growth factor receptor antibody cetuximab (C225) for *in vivo* treatment of A431 human epithelial carcinomas.[89] In the study, while the antibody-drug conjugate retained binding and cell internalization properties, tumor growth inhibition between the paclitaxel-C225 conjugate and naked C225 was not significantly different. This led the study's authors to conclude that either only a small quantity of antibody-delivered paclitaxel was being internalized into the tumor cells, or that paclitaxel was being prematurely released from the antibody, before targeted delivery to cells.

Future work to determine the reason behind loss of activity in the fullerene immunoconjugate can be performed by first covalently attaching the fullerene to the mAb for direct delivery and internalization into targeted cells. This strategy is already employed for clinical antibody-drug conjugates, and could be taken advantage through

the following. By reacting 2-iminothiolane (Traut's reagent) with an antibody sample, each individual antibody is covalently labeled with an average of 5 free thiols. For the fullerene, by functionalizing both arms of the linker malonate with protected amines, a second group is introduced for controlled fullerene functionalization. Whereby a paclitaxel (or other proposed chemotherapeutic) molecule may be attached to one arm of the linker malonate, the amine on the other malonate arm can be combined with the reactive linker 3-(2-Pyridyldithio)propionic acid (SPDP), producing a terminal thiol for antibody functionalization via disulfide bond. Once covalently attached to the mAb, if cytotoxicity of a paclitaxel-C_{60} derivative maintained the same blanket specificity for both targeted and non-targeted cells, varying the linker used to attach paclitaxel to C_{60} would be the next step towards development of FIT.

Given the previous success of using $Gd@C_{60}(OH)_x$-mAb immunoconjugates for cell internalization, the most likely cause to describe the lack of cytotoxic specificity seen in the results would be from spontaneous ester hydrolysis, releasing paclitaxel into solution before cell internalization. Although paclitaxel itself already contains four ester bonds, α-hydroxy acid esters, such as the one used to link paclitaxel to C_{60}, can be notoriously labile in solution, thus contribution to an explanation as to why overall cytotoxicity of paclitaxel is preserved, but indiscriminate between the targeted A375m and control T-24 cells.

Due to the synthetic hurdles of compound **7**, especially a low production yield, it was determined to be necessary to pursue another derivative, compound **9**, to achieve the end goal of obtaining enough product for *in vivo* testing. Additionally, compared to

paclitaxel and FDA-approved Abraxane, *in vitro* testing of conjugate **9** yielded excellent results, showing 10.1× and 5.29× better cytoxicity than paclitaxel and Abraxane, respectively. *In vivo* testing of compound **9** in a murine model showed tumor volume reduction similar to FDA-approved Abraxane, without the associated weight-loss, begging further investigation for compound **9** as a therapy for both antibody-drug conjugation and as a stand alone water-soluble form for delivery of hydrophobic paclitaxel.

Future work is still necessary to fulfill the fullerene immunotherapy (FIT) vision of a comprehensive fullerene-antibody conjugate for targeted drug delivery. The work in this thesis suggests that $Gd@C_{60}(OH)_x$ immunoconjugates do, indeed, internalize into target cells, without covalent attachment. However, successive work is based on the assumption that water-soluble $C_{60}(OH)_x$ and serinol-C_{60} derivatives behave similarly in solution. To better understand the loss of targeting behavior seen in the immunoconjugate, the system needs to be better characterized by uncovering the reason behind loss of specific delivery to targeted cells. This should first be accomplished by using SPDP or another biochemical moiety to covalently attach compound **9** to the targeting vector, preventing loss of the potentially labile fullerene to surrounding media proteins. If subsequent results prove to be similar to those already seen in this work, then it is reasonable to assume that cytotoxicity loss is due to premature release of paclitaxel, before it can be delivered and internalized into the targeted cell. To solve this problem, a more stable linker will be necessary, such as a substituted ester or a carbamate or

carbonate ester linker to create a stronger, biologically-labile covalent bond to affix paclitaxel to C_{60}.

Developing linker technology for effective conjugation of drugs to antibodies is currently an important area of focus in pharmaceuticals. Acid-labile hydrazones were initially championed for their stability in neutral blood plasma and ability to hydrolyze at acidic pHs, such as those produced by anaerobic metabolism found in cancer cells. However, the 48-72 hour half-life for drug release of hydrazones *in vivo* does not appear to be long enough for optimal therapy, compared to the 6-10 days found for their peptide counterparts.[90] The use of peptide-based linkers is proving to be a significant advantage over traditional hydrolytic or reductively labile linkers, since hydrolysis is enzymatic. This allows for individual preferential selection of linkers hydrolyzed by enzymes expressed or overexpressed in tumor cells or tumor masses. Using these peptide sequences for intracellular drug release, antibody-drug conjugates have been prepared using doxorubicin,[91] mitomycin C,[92] camptothecin,[93] talisomycin,[94] and auristatin derivatives.[93,95-97] As these peptide linkers become more specialized and developed for specific cancer lines, successful development of fullerene immunotherapy may eventually utilize one of these linkers to either anchor chemotherapeutic drugs to a fullerene or a fullerene conjugate to a targeting antibody.

Peptide linkers have been used for paclitaxel before. Firestone *et al.* reported a paclitaxel-peptide conjugate for antibody conjugation as early as 1994, using a peptide linker analogous to that of FDA-approved brentuximab vedotin.[98] Further development to conjugate the paclitaxel to an antibody never took place, possibly once it became evident

in the interim that for antibody-drug conjugates to be effective in human clinical use, drug IC_{50} values must be at least 10-100 pM, making paclitaxel (IC_{50}≈1-10 nM) possibly unsuitable.[99]

The main success of this thesis is the progress made toward further development of FIT and the potential translation of FIT into the clinic. Using $Gd@C_{60}(OH)_x$, the basic premise of using FIT to deliver fullerenes to targeted cells has been realized. The next step toward development of a therapeutic fullerene-antibody immunoconjugate is to transition from endohedral $Gd@C_{60}$ to the paclitaxel-C_{60} conjugate. However, by using the carbon-cage structure of C_{60} to constructing a water-soluble scaffold to covalently functionalize lipophilic paclitaxel, a new biologically-inert modality has been achieved to overcome the usual problem of pharmaceuticals in solubility, a challenge that currently limits approximately 40% of therapies from even reaching clinical trials.[100] Finally, the results documented in this work shifted the onus of FIT from a theoretical concept to a realistic goal of applied science awaiting final developmental refinement.

References

(1) Kroto, H.W.; Heath, J.R.; O'Brien, S.C.; Curl, R.F.; Smalley, R.E. *Nature.* **1985,** *318,* 162.

(2) Iijima, S. *Nature.* **1991,** *354,* 56.

(3) Haddon, R.C.; Hebard, A.F.; Rosseinski, M.J.; Murphy, D.W.; Duclos, S.J.; Lyons, K.B.; Miller, B.; Zahurak, J.M.; Tycko, R.; Dabbagh, G.; Thiel, F.A. *Nature.* **1991,** *350,* 320.

(4) Bakry, R.; Vallant, R.M.; Najam-ul-Hag, M.; Rainer, M.; Szabo, Z.; Huck, C.W.; Bonn, G.K. *Int. J. Nanomedicine.* **2007,** *2,* 639.

(5) Kokubo, K.; Matsubayashi, K.; Tategaki, H.; Takada, H.; Oshima, T. *ACS Nano.* **2008,** *2,* 327.

(6) Larnparth, I.; Hirsch, A. *Chem. Commun.* **1994,** *14,* 1727.

(7) Wharton, T.; Wilson, L.J.; *Bioorg. Med. Chem.* **2002**, *10,* 3545.

(8) Flahaut, E.; Durrieu, M.C.; Remy-Zolghadri, M.; Bareille, R.; Baquey, C. *J. Mater. Sci.* **2006,** *41,* 2411.

(9) Pantarotto, D.; Partidos, C.D.; Graff, R.; Hoebeke, J.; Briand, J.; Prato, M. *J. Am. Chem. Soc.* **2003,** *125,* 6160.

(10) Prato, M.; Da Ros, T. *Chem. Commun.* **1999,** *8,* 663.

(11) Hartman, K.B.; Hamlin, D.K.; Wilbur, D.S.; Wilson, L.J. *Small*. **2007,** *3,* 1496.

(12) Tóth, É.; Bolskar, R.D.; Helm, L.; Wilson, L.J.; Merbach, A.E. *J. Phys. Chem. C.* **2007,** *111,* 5633.

(13) Friedman, S.H.; DeCamp, D.L.; Sijbesma, R.P.; Srdanov, G.; Wudl, F.; Keyon, G.L. *J. Am. Chem. Soc.* **1993,** *115,* 6506.

(14) Baati, T.; Bourasset, F.; Gharbi, N.; Njim, L.; Abderrabba, M.; Kerkeni, A.; Szwarc, H.; Moussa, F. *Biomaterials.* **2012,** *33,* 4936.

(15) Mirakyan, A.L.; Wilson, L.J. *J. Chem. Soc. Perkin Trans. II.* **2002,** 1173.

(16) Tokuyama, H.; Yamago, S.; Nakamura, E.; Shiraki, T.; Sugiura, Y. *J. Am. Chem. Soc.* **1993,** *115,* 7918.

(17) Tóth, É.; Bolskar, R.D.; Borel, A.; González, G.; Helm, L.; Merbach, A.E.; Sitharaman, B.; Wilson, L.J. *J. Am. Chem. Soc.* **2005,** *127,* 799.

(18) Nakamura, E.; Isobe, H.; Tomita, N.; Sawamura, M.; Jinno, S.; Okayama, H. *Angew. Chem., Int. Ed.* **2000,** *39,* 4254.

(19) Wharton, T.; Wilson, L.J. *Bioorg. Med. Chem.* **2002,** *10,* 3545.

(20) Zakharian, T.Y.; Seryshev, A.; Sitharaman, B.; Gilbert, B.E.; Knight, V.; Wilson, L.J. *J. Am. Chem. Soc.* **2005,** *127,* 12508.

(21) Durdagi, S.; Supuran, C.T.; Strom, T.A.; Doostdar, N.; Kumar, M.K.; Barron, A.R.; Mavromoustkos, T.; Papdopoulos, M.G. *J. Chem. Inf. Model.* **2009,** *49,* 1139.

(22) Tanimoto, S.; Sakai, S.; Matsumura, S.; Takahashi, D.; Toshima, K. *Chem. Commun.* **2008,** 5767.

(23) Marchesan, S.; Da Ros, T.; Spalluto, G.; Balzarini, J.; Prato, M. *Bioorg. Med. Chem. Lett.* **2005,** *15,* 3615.

(24) Taylor, R.; Walton, D.R.M. *Nature.* **1993,** *363,* 685.

(25) Dugan, L.L.; Turetsky, D.M.; Du, C.; Lobner, D.; Wheeler, M.; Almli, C.R.; Shen, F.; Luh, T.; Choi, D.W.; Lin, T-S. *Proc. Natl. Acad. Sci. USA.* **1997,** *94,* 9434.

(26) Dugan, L.L.; Lovett, E.; Almli, C.R.; Lin, T-S.; Choi, D.W. *Proc. Electrochem. Soc.* **1998,** *98,* 1236.

(27) Quick, K.L.; Ali, S.S.;Arch, R.; Xiong, C.; Wozniak, D.; Dugan, L.L. *Neurobiol. Aging.* **2008,** *29,* 117.

(28) Yamakoshi, Y.; Umezawa, N.; Ryu, A.; Arakane, K.; Miyata, N.; Goda, Y.; Masumizu, T.; Nagano, T. *J. Am. Chem. Soc.* **2003,** *125,* 12803.

(29) Tokuyama, H.; Yamago, S.; Nakamura, E.; Shiraki, T.; Sugiura, Y. *J. Am. Chem. Soc.* **1993,** *115,* 7918.

(30) Liu, J.; Ohta, S.-I.; Sonoda, A.; Yamada, M.; Yamamoto, M.; Nitta, N.; Murata, K.; Tabata, Y. *J. Control. Release.* **2007,** *117,* 104.

(31) Hotze, E.M.; Labille, J.; Alvarez, P.; Wiesner, M.R. *Environ. Sci. Technol.* **2008,** *42,* 4175.

(32) Lee, J.; Mackeyev, Y.; Cho, M.; Wilson, L.J.; Kim, J.-H.; Alvarez, P.J.J. *Environ. Sci. Technol.* **2010,** *44,* 9488.

(33) Heath, J.R.; O'Brien, S.C.; Zhang, Q.; Liu, Y.; Curl, R.F.; Tittel, F.K.; Smalley, R.E. *J. Am. Chem. Soc.* **1985,** *107,* 7779.

(34) Bolskar, R.D.; Benedetto, A.F.; Husebo, L.O.; Price, R.E.; Jackson, E.F.; Wallace, S.; Wilson, L.J.; Alford, J.M. *J. Am. Chem. Soc.* **2003,** *125,* 5471.

(35) Mikawa, M.; Kato, H.; Okumura, M.; Narataki, M.; Kanazawa, Y.; Miwa, N.; Shinohara, H. *Bioconjugate Chem.* **2001,** *12,* 510.

(36) Kato, H.; Kanazawa, Y.; Okumura, M.; Taninaka, A.; Yokawa, T.; Shinohara, H. *J. Am. Chem. Soc.* **2003,** *125,* 4391.

(37) Shu, C.; Corwin, F.D.; Zhang, J.; Chen, Z.; Reid, J.E.;Sun, M.; Xu, W.; Sim, J.H.; Wang, C.; Fatouros, P.P.; Esker, A.R.; Gibson, H.W.; Dorn, H.C. *Bioconjugate Chem.* **2009,** *20,* 1186.

(38) Braun, M.; Atalick, S.; Guldi, D.M.; Lanig, H.; Brettreich, M.; Burghardt, S.; Hatzimarinaki, M.; Ravanelli, E.; Prato, M.; van Eldik, R.; Hirsch, A. *Chem. Eur. J.* **2003,** *9,* 3867.

(39) Partha, R.; Lackey, M.; Hirsch, A.; Casscells, S.W.; Conyers, J.L. *J. Nanobiotechnol.* **2007,** *5,* 1.

(40) Partha, R.; Mitchell, L.R.; Lyon, J.L.; Joshi, P.P.; Conyers, J.L. *ACS Nano.* **2008,** *2,* 1950.

(41) Chaudhuri, P.; Paraskar, A.; Soni, S.; Mashelkar, R.A.; Sengupta, S. *ACS Nano.* **2009,** *3,* 2505.

(42) Ferrari, M. *Curr. Opin. Chem. Biol.* **2005,** *9,* 343.

(43) Jaracz, S.; Chen, J.; Kuznetsova, L.V.; Ojima, I. *Bioorg. Med. Chem.* **2005,** *13,* 5043.

(44) Casadevall, A.; Dadachova, E.; Pirofski, L. *Nat. Rev. Microbiol.* **2004,** *2,* 695.

(45) Wu, A.; Senter, P.D. *Nat. Biotechnol.* **2005,** *23,* 1137.

(46) Adams, G.P.; Weiner, L. *Nat. Biotechnol.* **2005,** *23,* 1147.

(47) Safavi, A.; Georg, G.I.; Velde, D.V.; Raisch, K.P.; Safavy, K.; Carpenter, M.; Wang, W.; Bonner, J.A.; Khazaeli, M.B.; Bauchsbaum, D.J. *Bioconjugate Chem.* **2004,** *15,* 1264.

(48) Guillemard, V.; Saragovi, H.U. *Cancer Res.* **2001,** *61,* 694.

(49) Safavy, A.; Raisch, K.P.; Khazaeli, M.B.; Buchsbaum, D.J.; Bonner, J.A. *J. Med. Chem.* **1999,** *42,* 4919.

(50) Luo, Y.; Prestwich, G.D. *Bioconjugate Chem.* **1999,** *10,* 755.

(51) Witzig, T.E.; White, C.A.; Wiseman, G.A.; Gordon, L.I.; Emmanouilides, C.; Raubitschek, A.; Janakiraman, N.; Gutheil, J.; Schilder, R.J.; Spies, S.; Silverman, D.H.; Parker, E.; Grillo-López, A.J. *J. Clin. Oncol.* **1999,** *17,* 3793.

(52) Witzig, T.E.; Gordon, L.I.; Cabanillas, F.; Czuczman, M.S.; Emmanouilides, C.; Joyce, R.; Pohlman, B.L.; Bartlett, N.L.; Wiseman, G.A.; Padre, N.; Grillo-López A.J.; Multani, P.; White, C.A. *J. Clin. Oncol.* **2002,** *20,* 2453.

(53) Witzig, T.E.; Flinn, I.W.; Gordon, L.I.; Emmanouilides, C.; Czuczman, M.S.; Saleh, M.N.; Cripe, L.; Wiseman, G.; Olejnik, T.; Multani, P.S.; White, C.A. *J. Clin. Oncol.* **2002,** *20,* 3262.

(54) Buchegger, F.; Antonescu, C.; Delaloye, A.B.; Helg, C.; Kovacsovics, T.; Kosinski, M.; Mach, J.; Ketterer, N. *Br. J. Canc.* **2006,** *94,* 1770.

(55) Francisco, J.A.; Cerveny, C.G.; Meyer, D.L.; Mixan, B.J.; Klussman, K.; Chace, D.F.; Rejniak, S.X.; Gordon, K.A.; DeBlanc, R.; Toki, B.E.; Law, C.-L.; Doronina, S.O.; Siegall, C.B.; Senter, P.D.; Wahl, A.F. *Blood.* **2003,** *102,* 1458.

(56) Hamann, P.R.; Hinman, L.M.; Hollander, I.; Beyer, C.F.; Lindh, D.; Holcomb, R.; Hallett, W.; Tsou, H.R.; Upeslacis, J.; Shochat, D.; Mountain, A.; Flowers, D.A.; Bernstein, I. *Bioconjugate Chem.* **2002,** *13,* 47.

(57) Wani, M.C.; Taylor, H.L.; Wall, M.E.; Coggon, P.; McPhail, A.T. *J. Am. Chem. Soc.* **1971,** *93,* 2325.

(58) Goodman, J.; Walsh, V. *The Story of Taxol: Nature and Politics in the Pursuit of an Anti-Cancer Drug,* 1st ed.; Cambridge University Press: Cambridge, England, 2001.

(59) Holton, R.A.; Somoza, C.; Kim, H.B.; Liang, F.; Biediger, R.J.; Boatman, P.D.; Shindo, M.; Smith, C.C.; Kim, S. *J. Am. Chem. Soc.* **1994,** *116,* 1597.

(60) Schiff, P.B.; Fant, J.; Horwitz, S.B. *Nature.* **1979,** *277,* 665.

(61) Löwe, J.; Li, H.; Downing, K.H.; Nogales, E. *J. Mol. Biol.* **2001,** *313,* 1045.

(62) Choy, H. *Oncology.* **1999,** *10,* 23.

(63) Tishler, R.B.; Schiff, P.B.; Geard, C.R.; Hall, E.J. *Int. J. Radiat. Oncol. Biol. Phys.* **1992,** *22,* 613.

(64) Tan, M.; Jing, T.; Lan, K.H.; Neal, C.I.; Li, P.; Lee, S.; Fang, D.; Nagata, Y.; Liu, J.; Arlinghaus, R.; Hung, M.C.; Yu, D. *Mol. Cell.* **2002,** *9,* 993.

(65) Dorr, R.T. *Ann. Pharmacother.* **1994,** *28,* 11.

(66) Li, C.; Yu, D.-F.; Newman, R.A.; Cabral, F.; Stephens, L.C.; Hunter, N.; Milas, L.; Wallace, S. *Cancer Res.* **1998,** *58,* 2404.

(67) Greenwald, R.B.; Gilbert, C.W.; Pendri, A.; Conover, C.D.; Xia, J.; Martinez, A. *J. Med. Chem.* **1996,** *39,* 424.

(68) Berger, C.S. *Gd@C_{60}-(ZME-018) Immunoconjugate Targeting of A375 Melanoma Cells.* Master's Dissertation, Rice University, Houston, Texas, 2010.

(69) Berger, C.S.; Marks, J.W.; Bolskar, R.D.; Rosenblum, M.G;.Wilson, L.J. *Transl. Oncol.* **2011,** *4,* 350.

(70) Mujoo, K.; Cheung, K.; Murray, J.L.; Rosenblum, M.G. *Cancer Immunol. Immunother.* **1995,** *40,* 339.

(71) Krizan, Z.; Murray, J.L.; Hersh, E.M.; Rosenblum, M.G.; Glenn, H.J.; Gschwind, C.R.; Carlo, D.J. *Cancer Res.* **1985,** *45,* 4904.

(72) Chan, S.M.; Hoffer, P.B.; Maric, N.; Zoghbi, S.S.; Kirkwood, J.M.; Ernstoff, M.S.; Duray, P.H.; Gerich, B. *J. Nucl. Med.* **1987,** *28,* 1441.

(73) Macey, D.J.; Denardo, S.J.; Denardo, G.L.; Goodnight, J.K.; Unger, M.W. *Am. J. Physiol. Imaging.* **1988,** *3,* 1.

(74) Koizumi, M.; Endo, K.; Watanabe, Y.; Saga, T.; Sakahara, H.; Konishi, J. *Jpn. J. Canc. Res.* **1988,** *79,* 973.

(75) Rosenblum, M.G.; Cheung, L.; Mujoo, K.; Murray, J.L. *Cancer Immunol. Immunother.* **1995,** *40,* 322.

(76) Kirkwood, J.M.; Neumann, R.D.; Zoghbi, S.S.; Ernstoff, M.S.; Cornelius, E.A.; Shaw, C.; Ziyadeh, T.; Fine, J.A.; Unger, M.W. *J. Clin. Oncol.* **1987,** *8,* 1247.

(77) Rosenblum, M.G.; Murray, J.L.; Cheung, L.; Rifkin, R.; Salmon, S.; Bartholomew, R.A. *Mol. Biother.* **1991,** *3,* 6.

(78) Rosenblum, M.G.; Cheung, L.H.; Liu, Y.; Marks, J.W. *Cancer Res.* **2003,** *63,* 3995.

(79) Bolskar, R.D. *Nanomed.* **2008,** *3,* 201.

(80) Mattingly, P.G. *Synthesis-Stuttgart.* **1990,** *4,* 366.

(81) Deutsch, H.M.; Glinski, J.A.; Hernandez, M.; Haugwitz, R.D.; Narayanan, V.L.; Suffness, M.; Zalkow, L.H. *J. Med. Chem.* **1989,** *32,* 788.

(82) Greenwald, R.B.; Gilbert, C.W.; Pendri, A.; Conover, C.D.; Xia, J.; Martinez, A. *J. Med. Chem.* **1996,** *39,* 424.

(83) Ashcroft, J.M.; Tsyboulski, D.A.; Hartman, K.B.; Zakharian, T.Y.; Marks, J.W.; Weisman, R.B.; Rosenblum, M.G.; Wilson, L.J. *Chem. Commun.* **2006**, *28,* 3004.

(84) Laus, S.; Sitharaman, B.; Tóth, É.; Bolskar, R.D.; Helm, L.; Asokan, S.; Wong, M.S.; Wilson, L.J.; Merbach, A.E. *J. Am. Chem. Soc.* **2005,** *127,* 9368.

(85) Grattoni, A.; Fine, D.; Zabre, E.; Ziemys, A.; Gill, J.; Mackeyev, Y.; Cheney, M.A.; Danila, D.C.; Hosali, S.; Wilson, L.J.; Hussain, F.; Ferrari, M. *ACS Nano.* **2011,** *5,* 9382.

(86) Sugahara, S.; Kajiki, M.; Kuriyama, H.; Kobayashi, T.R. *Biol. Pharm. Bull.* **2002,** *25,* 632.

(87) Mathew, A.E.; Mejillano, M.R.; Nath, J.P.; Himes, R.H.; Stella, V.J. *J. Med. Chem.* **1992,** *35,* 145.

(88) Gibson, J.D.; Khanal, B.P.; Zubarev, E.R. *J. Am. Chem. Soc.* **2007,** *129,* 11653.

(89) Safavy, A.; Bonner, J.; Waksal, H.W.; Buchsbaum, D.J.; Gillespie, G.Y.; Khazaeli, M.B.; Arani, R.; Chen, D.-T.; Carpenter, M.; Raisch, K.P. *Bioconjugate Chem.* **2003**, *14*, 302.

(90) Boghaert, E.R.; Khandke, K.M.; Sridharan, L.: Dougher, M.; DiJoseph, J.F.; Kunz, A.; Hamann, P.R.; Moran, J.; Chaudhary, I.; Damle, N.K. *Cancer Chemother. Pharmacol.* **2008**, *61*, 1027.

(91) Dubowchik, G.M.; Firestone, R.A. *Bioorg. Med. Chem. Lett.* **1998**, *8*, 3341.

(92) Dubowchik, G.M.; Mosure, K.; Knipe, J.O.; Firestone, R.A. *Bioorg. Med. Chem. Lett.* **1998**, *8*, 3347.

(93) Walker, M.A.; Dubowchik, G.M.; Hofstead, S.J.; Trail, P.A.; Firestone, R.A. *Bioorg. Med. Chem. Lett.* **2002**, *12*, 217.

(94) Walker, M.A.; King, H.D.; Dalterio, R.A.; Trail, P.A.; Firestone, R.A.; Dubowchik, G.M. *Bioorg. Med. Chem. Lett.* **2004**, *14*, 4323.

(95) Jedema, I.; Barge, R.M.; van der Velden, V.H.; Nijmeijer, B.A.; van Dongen, J.J.; Willemze, R.; Falkenburg, J.H. *Leukemia*, **2004**, *18*, 316.

(96) Doronina, S.O.; Mendelsohn, B.A.; Bovee, T.D.; Cerveny, C.G.; Alley, S.C.; Meyer, D.L.; Oflazoglu, E.; Toki, B.E.; Sanderson, R.J.; Zabinski, R.F.; Wahl, A.F.; Senter, P.D. *Bioconjug. Chem.* **2006**, *17*, 114.

(97) Francisco, J.A.; Cerveny, C.G.; Meyer, D.L.; Mixan, B.J.; Klussman, K.; Chace, D.F.; Rejniak, S.X.; Gordon, K.A.; DeBlanc, R.; Toki, B.E.; Law, C.L.; Doronina, S.O.; Siegall, C.B.; Senter, P.D.; Wahl, A.F. *Blood*, **2003**, *102*, 1458.

(98) Firestone, R.A.; Dubowchik, G.M. (Bristol Myers Squibb Co., USA). Lysosomal enzyme-cleavable antitumor drug conjugates. European Patent 0624377, November 15, 1994.

(99) Chari, R.V.J. *Adv. Drug. Deliv. Rev.* **1998**, *31*, 89.

(100) Jouyban, A. *Handbook of Solubility Data for Pharmaceuticals,* 1st ed.; CRC Press: Boca Raton, Florida, 2009.

Appendix

Appendix A1: Chemicals and their related information used in Section **2.3**

Chemical	Purity	CAS	Commercial Source
2-Aminoethanol	99%	141-43-5	Sigma-Aldrich, St. Louis, Missouri
Di-*tert*-butyl pyrocarbonate ($(Boc)_2O$)	99%	24424-99-5	Oakwood Products, Inc., West Columbia, South Carolina
Ethyl malonyl chloride	≥95%	36239-09-5	Fluka, GmbH, Buchs, Switzerland
Ethyldiisopropylamine (DIPEA, Hünig's base)	99%	7087-68-5	Alfa-Æsar, Ward Hill, Massachusetts
Ethyl acetate (EtOAc)	≥99.5%	141-78-6	Sigma-Aldrich, St. Louis, Missouri
Hexanes, mixture of isomers	≥98.5%		Sigma-Aldrich, St. Louis, Missouri
C_{60}	99+%	99685-96-8	MER Corp, Tucson, Arizona
Carbon Tetrabromide (CBr_4)	99%	558-13-4	Sigma-Aldrich, St. Louis, Missouri
1,8-diazabicyclo[5.4.0]undec-7-ene (DBU)	98%	6674-22-2	Sigma-Aldrich, St. Louis, Missouri
Toluene	≥99.5%	108-88-3	Sigma-Aldrich, St. Louis, Missouri
2-Amino-1,3-propanediol (Serinol)	98%	534-03-2	AK Scientific, Inc., Mountain View, California
Diethyl malonate	99%	105-53-3	Sigma-Aldrich, St. Louis, Missouri
2-Propanol (Isopropyl alcohol)	99.9%	67-63-0	Fisher, Pittsburgh, Pennsylvania
Pyridine	99.9%	110-86-1	Fisher, Pittsburgh, Pennsylvania
Acetic anhydride ($(Ac)_2O$)	99.7%	108-24-7	Fisher, Pittsburgh, Pennsylvania
Methanol (CH_3OH)	≥99.5%	67-56-1	Sigma-Aldrich, St. Louis, Missouri
Isopropyl ether	99+%	108-20-3	Acros, Geel, Belgium

tert-butylimino-tris(dimethylamino)phosphorane (phosphazene base P_1-*t*-Bu)	97+%	81675-81-2	Sigma-Aldrich, St. Louis, Missouri
Methylene chloride (CH_2Cl_2)	99.9%	75-09-2	Fisher, Pittsburgh, Pennsylvania
Chloroform ($CHCl_3$)	≥99.8%	67-66-3	Sigma-Aldrich, St. Louis, Missouri
Ethanol (CH_3CH_2OH)	100%	64-17-5	Decon Labs, King of Prussia, Pennsylvania
1,4-Dioxane	>99%	123-91-1	Mallinckrodt
Deionized water	>18 MOhm	7732-18-5	
Hydrochloric acid, *aq.*	37%	7647-01-0	EMD Chemicals, Geneva, Switzerland
Dimethyl formamide (DMF)	≥99.9%	68-12-2	Sigma-Aldrich, St. Louis, Missouri
Paclitaxel	98%	33069-62-4	AK Scientific, Inc., Mountain View, California
4-(Dimethylamino)pyridine	99%	1122-58-3	Sigma-Aldrich, St. Louis, Missouri
Succinic Anhydride	99%	108-30-5	Alfa-Æsar, Ward Hill, Massachusetts
Poly(ethylene glycol) bis(carboxymethyl) ether (Avg. M_n: 600 Da)		39927-08-7	Sigma-Aldrich, St. Louis, Missouri
Trichloroethylene	≥99.5%	79-01-6	Sigma-Aldrich, St. Louis, Missouri
N,N'-diisopropylcarbodiimide (DIC)	≥99%	693-13-0	Advanced ChemTech, Louisville, Kentucky
1-(3-Dimethylaminopropyl)-3-ethylcarbodiimide Hydrochloride (EDC)	98%	25952-53-8	TCI America, Portland, Oregon
1-Hydroxybenzotriazole hydrate (HOBt)	99%	123333-53-9	Fluka, GmbH, Buchs, Switzerland
2-(*N*-morpholino)ethanesulfonic acid (MES)	≥99%	4432-31-9	USB Corporation, Cleveland, Ohio

Appendix A2: Mass spectrometry data of compounds described in Section **2.3**
Compound 1: 2-((*Tert*-butoxycarbonyl)amino)ethyl ethyl malonate (**1**)

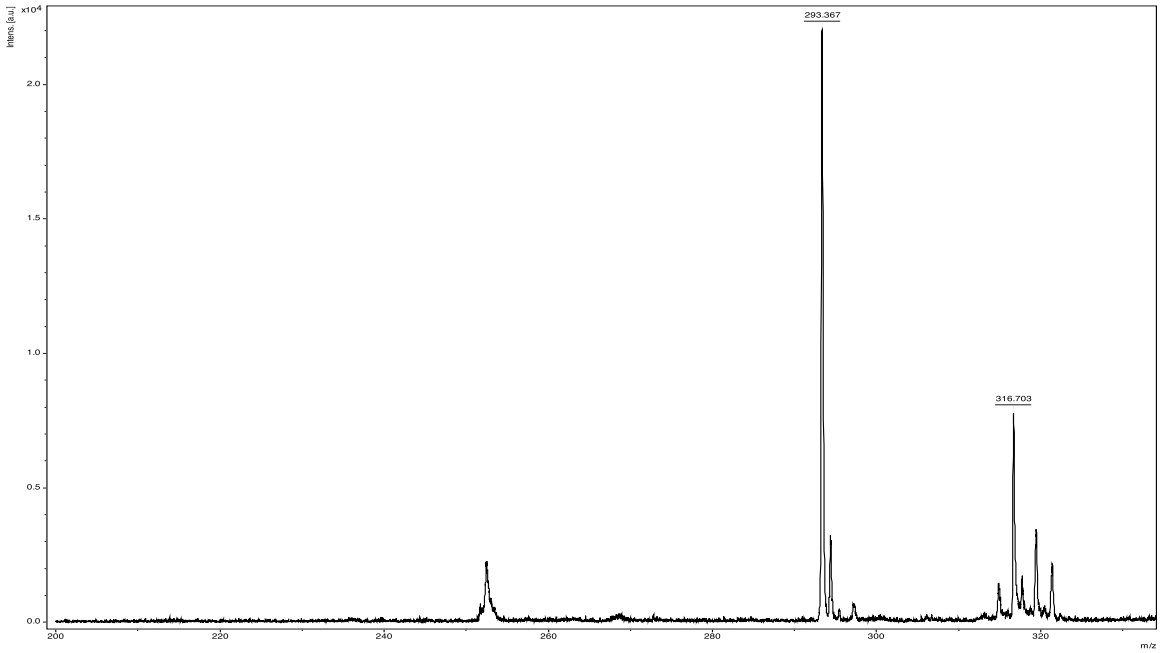

Figure A2.1.a: MALDI-TOF Spectrum of **1**, Matrix: sinapinic acid, positive mode

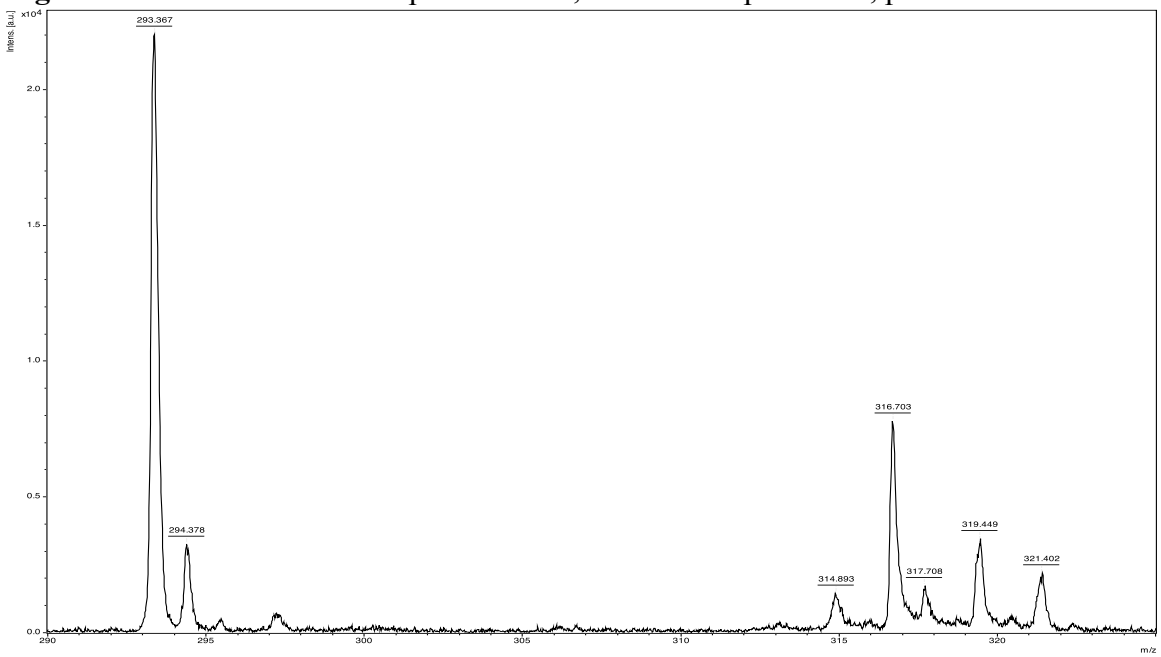

Figure A2.1.b: MALDI-TOF Spectrum of **1**, Matrix: sinapinic acid, positive mode

Compound 2: 3'-ethoxycarbonyl-3'-((2-((*tert*-butoxycarbonyl)amino)ethoxy)carbonyl)-[1,2](C_{60}-I_h)[5,6]fullerene (**2**)

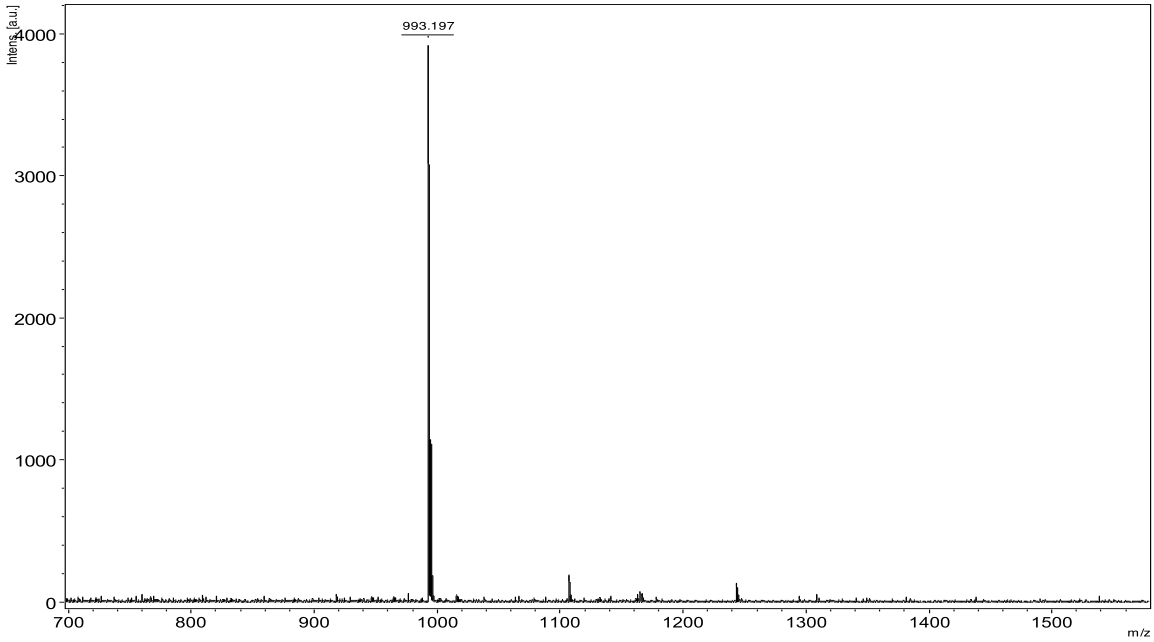

Figure A2.2: MALDI-TOF Spectrum of **2**, Matrix: trans-2-[3-(4-*tert*-Butylphenyl)-2-methyl-2-propenylidene]malononitrile, positive mode

Compound 3: Bis(2-acetoxy-1-acetoxymethylethylcarbamoyl)methane (**3**)

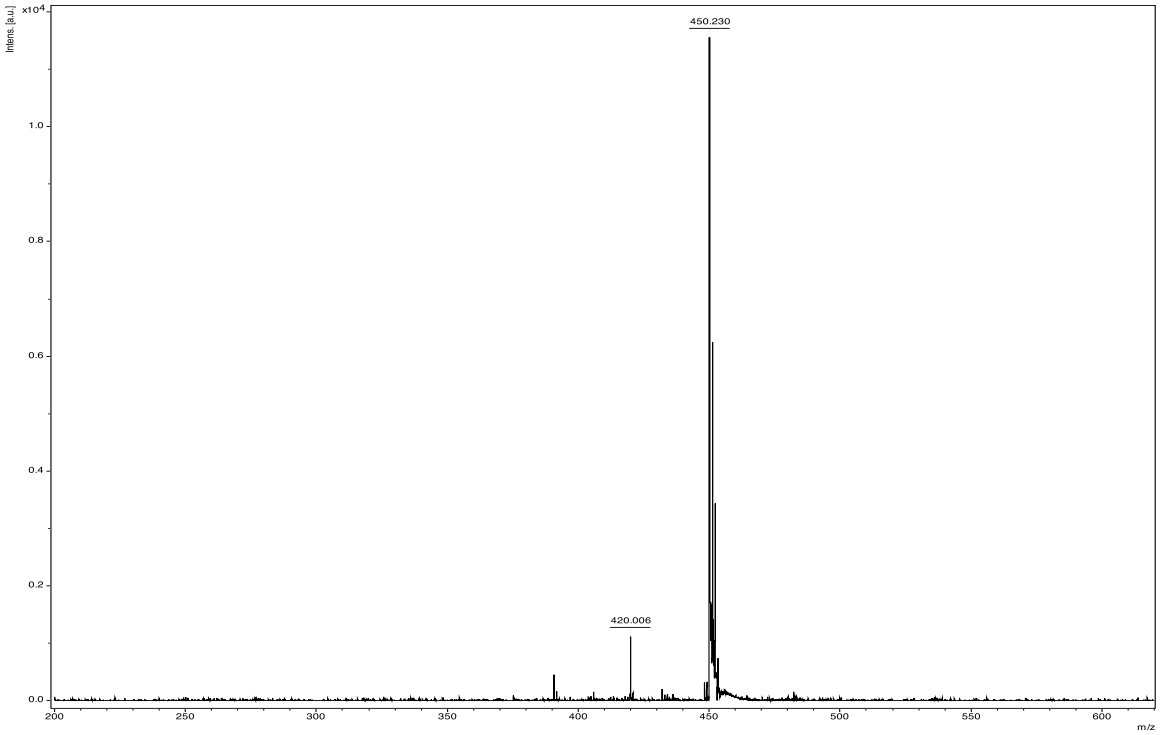

Figure A2.3.a: MALDI-TOF Spectrum of **3**, Matrix: sinapinic acid, positive mode

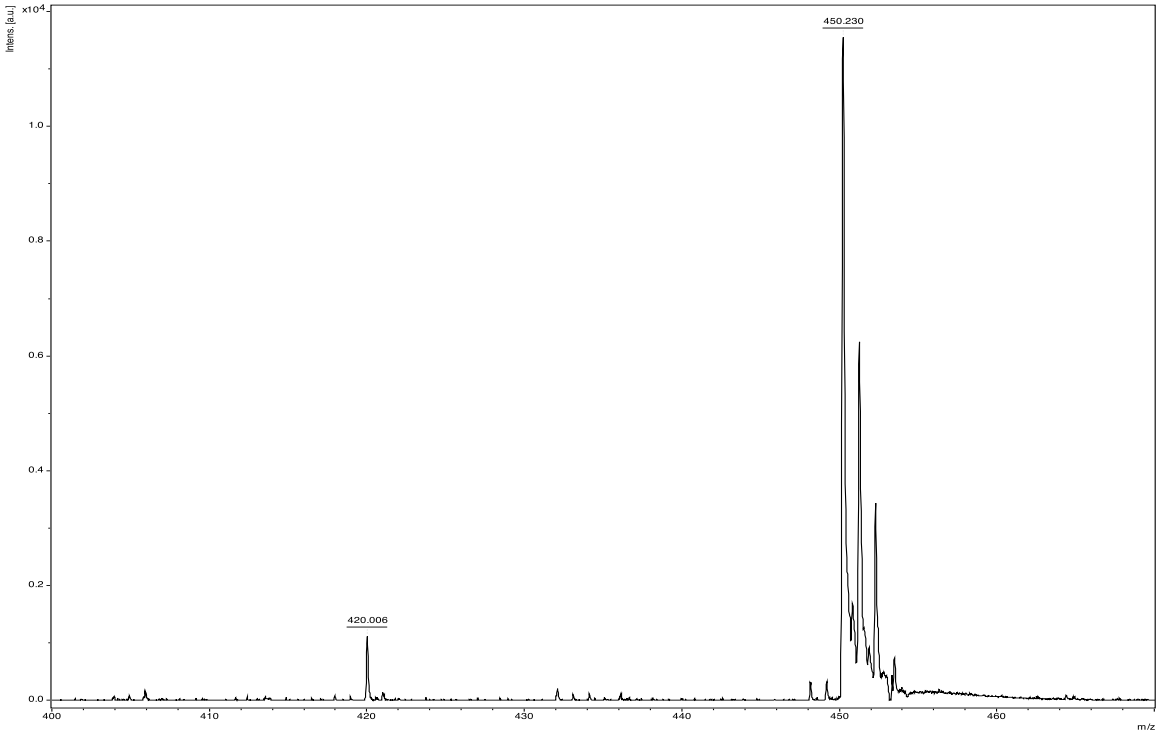

Figure S2.3.b: MALDI-TOF Spectrum of **3**, Matrix: sinapinic acid, positive mode

Compound 4: 3'-ethoxycarbonyl -3'-((2-((*tert*-butoxycarbonyl)amino)ethoxy)carbonyl)-3'', 3'', 3''', 3''', 3'''', 3'''', 3''''', 3''''', 3'''''', 3''''''-deca-(2-acetoxy-1-acetoxymethylethylcarbamoyl)-3'H, 3''H, 3'''H, 3''''H, 3'''''H, 3''''''H-hexacyclopropa[1,2:18,36:22,23:27,45:31,32:55,60](C_{60}-I_h)[5,6]fullerene (**4**)

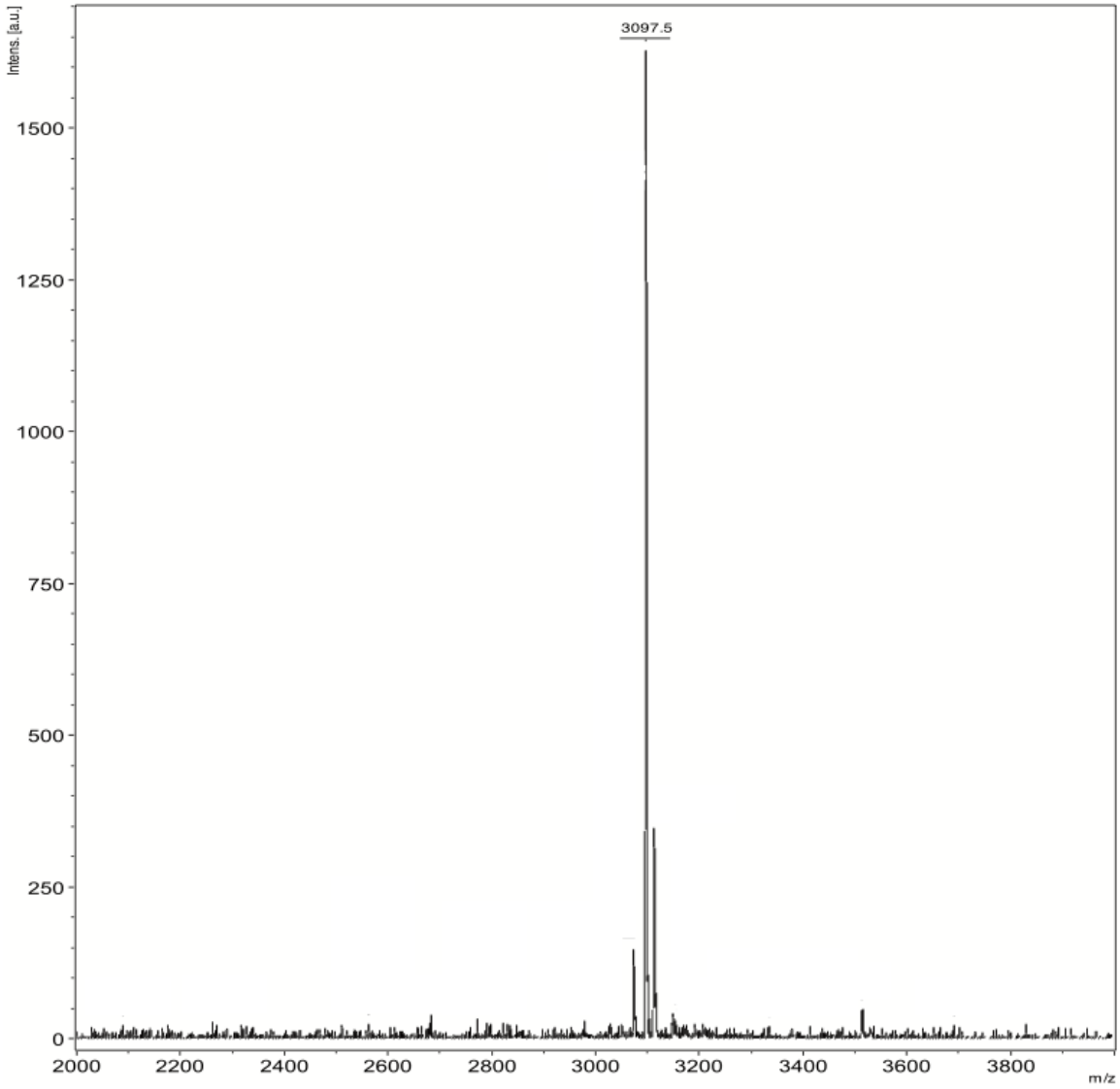

Figure A2.4.a: MALDI-TOF Spectrum of **4**, Matrix: trans-2-[3-(4-*tert*-Butylphenyl)-2-methyl-2-propenylidene]malononitrile, positive mode

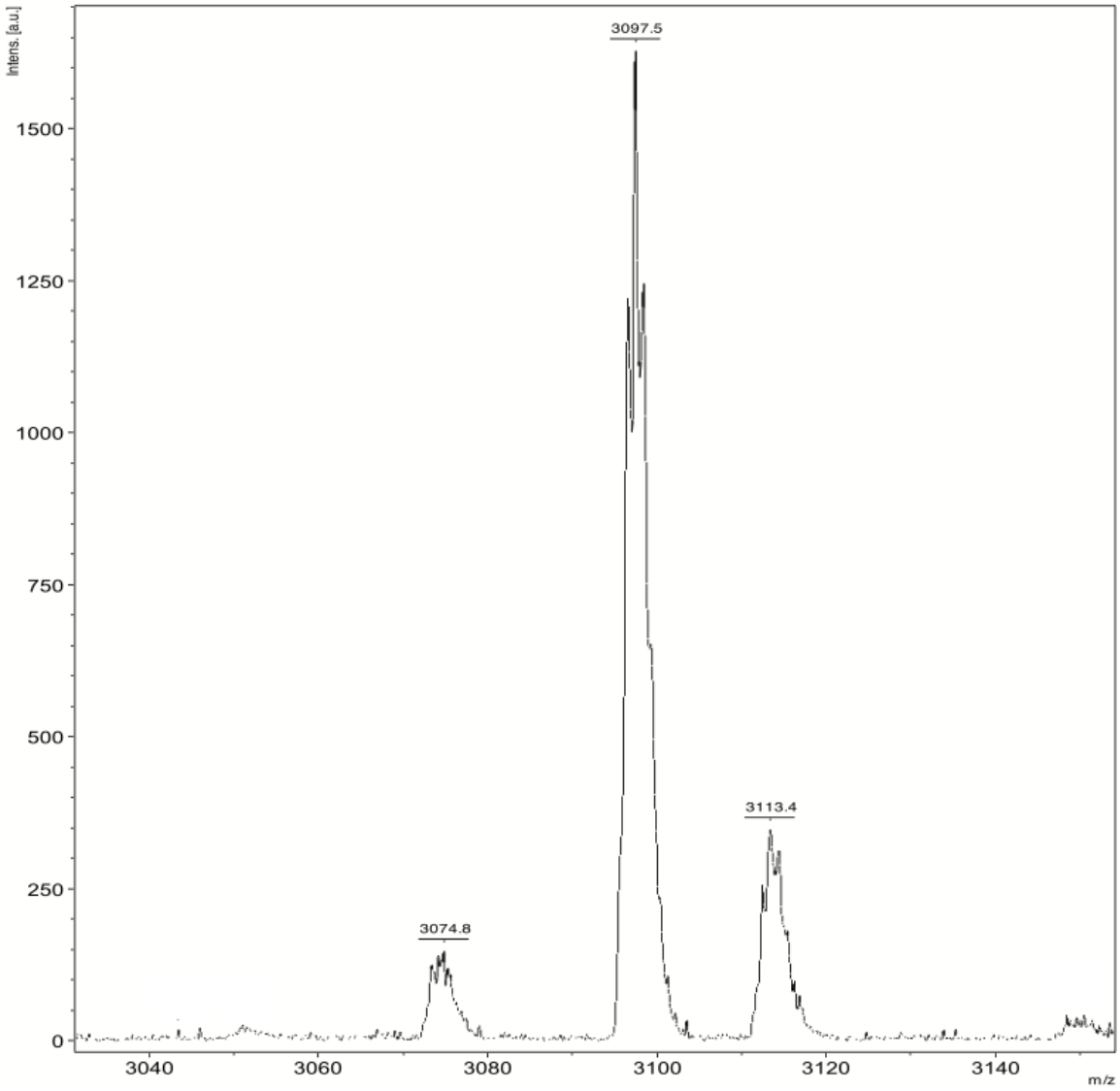

Figure A2.4.b: MALDI-TOF Spectrum of **4**, Matrix: trans-2-[3-(4-*tert*-Butylphenyl)-2-methyl-2-propenylidene]malononitrile, positive mode

Compound 5: 3’-ethoxycarbonyl-3’-((2-ammoniumethoxy)carbonyl)- 3'', 3'', 3''', 3''', 3'''', 3'''', 3''''', 3''''', 3'''''-deca-(2-hydroxy-1-(hydroxymethyl)ethylcarbamoyl)-3'H, 3"H, 3'''H, 3''''H, 3'''''H, 3'''''H-hexacyclopropa[1,2:18,36:22,23:27,45:31,32:55,60](C_{60}-I_h)[5,6]fullerene monohydrochloride (**5**)

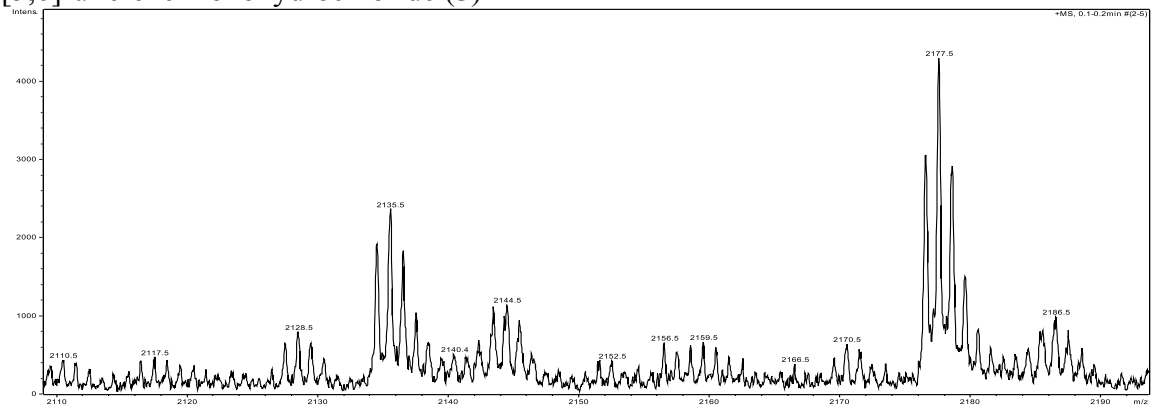

Figure A2.5: ESI-TOF Spectrum of **5**, positive mode

Compound 6: Paclitaxel-2′-Succinate (**6**)

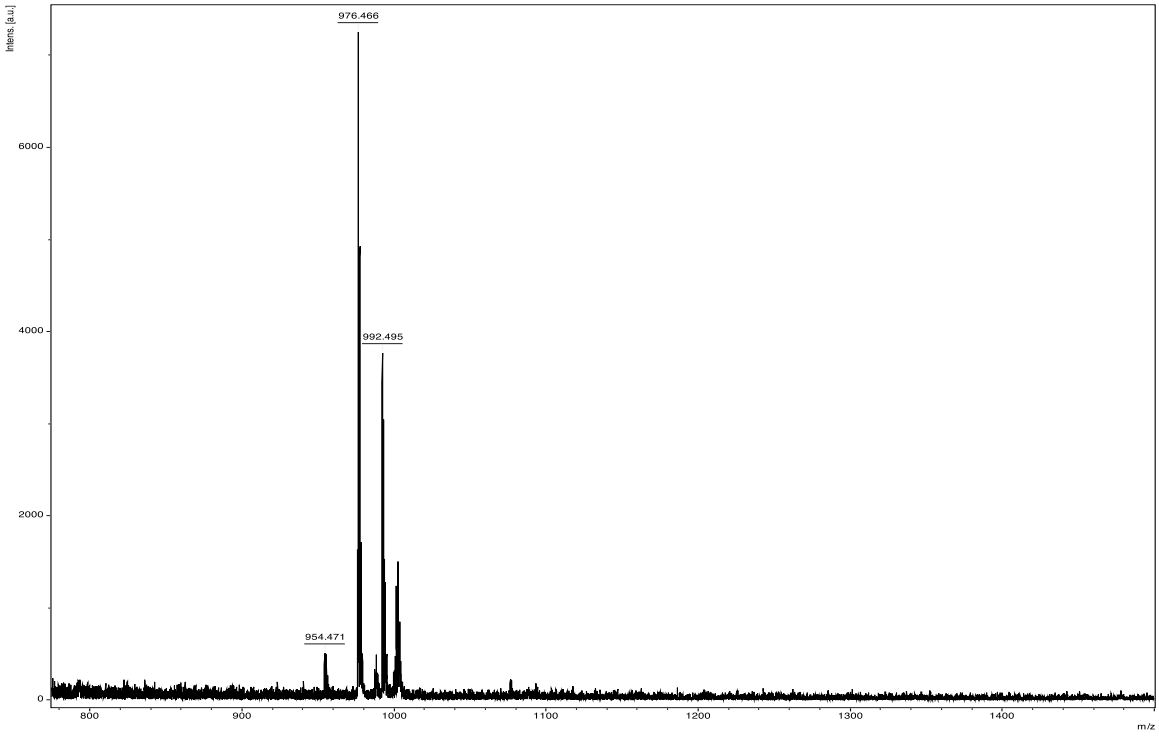

Figure A2.6: MALDI-TOF Spectrum of **6**, Matrix: trans-2-[3-(4-*tert*-Butylphenyl)-2-methyl-2-propenylidene]malononitrile, positive mode

Compound 7: Serinol-C_{60}-Paclitaxel-2'-Succinate Derivative (**7**)

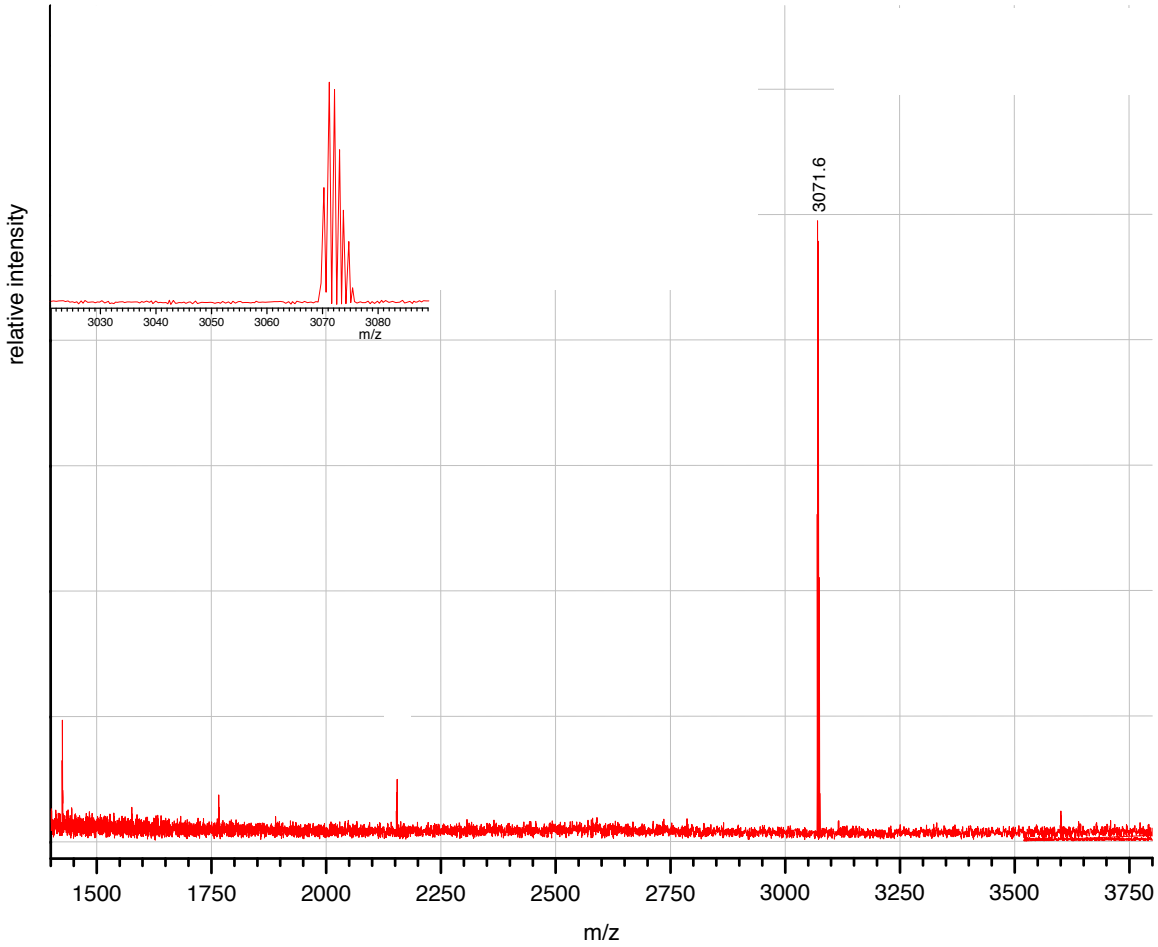

Figure A2.7: ESI-TOF Spectrum of **7**, positive mode

Compound 8: Paclitaxel-2′-Poly(ethylene glycol) Ester Derivative (**8**)

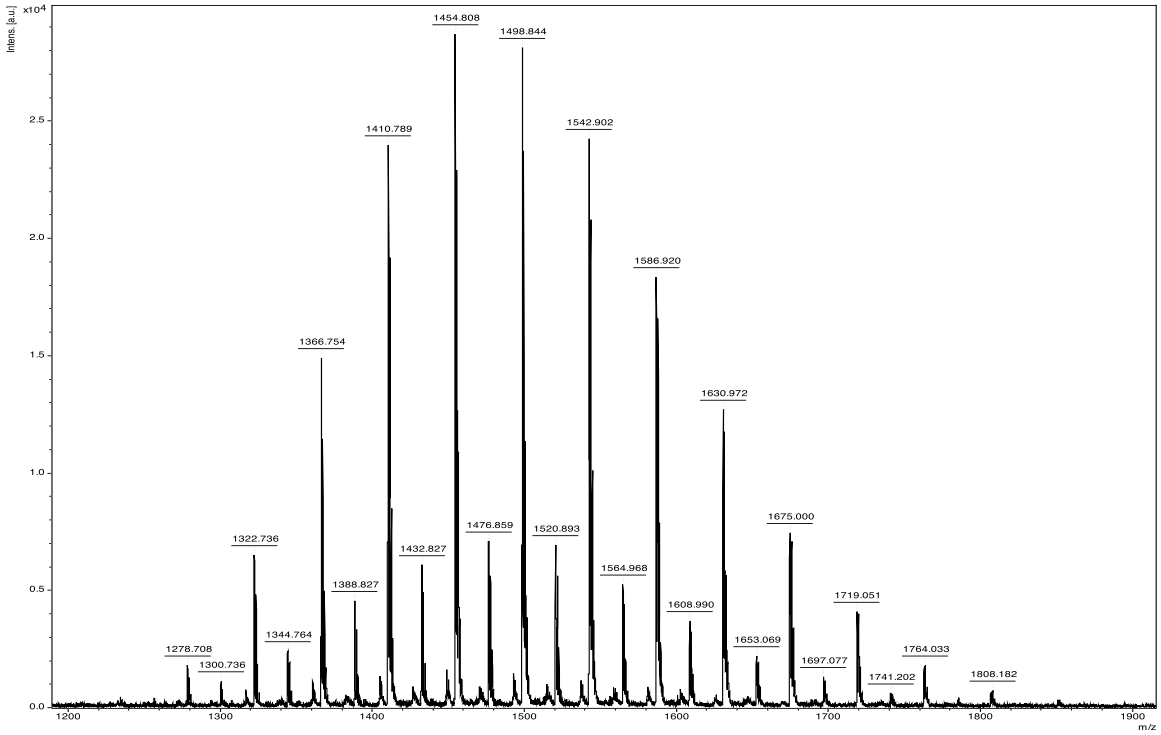

Figure A2.8: MALDI-TOF Spectrum of **8**, Matrix: trans-2-[3-(4-*tert*-Butylphenyl)-2-methyl-2-propenylidene]malononitrile, positive mode

Compound 9: Serinol-C_{60}-Paclitaxel-2′-Poly(ethylene glycol) Ester Derivative (**9**)

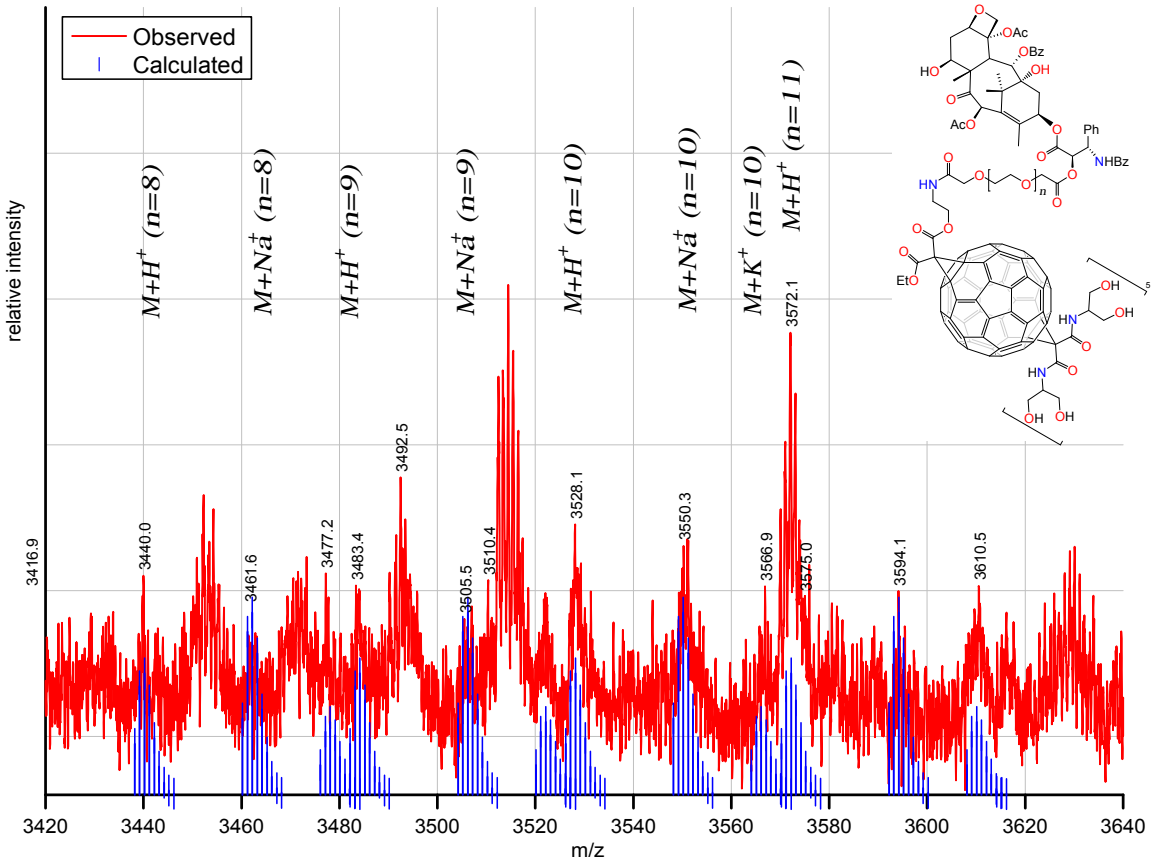

Figure A2.9: ESI-TOF Spectrum of **9**, positive mode

Compound 10: 3’, 3’’, 3’’, 3’’’, 3’’’, 3’’’’, 3’’’’, 3’’’’’, 3’’’’’, 3’’’’’’, 3’’’’’’-dodeca-(2-hydroxy-1-{hydroxymethyl}ethylcarbamoyl)-3’H, 3’’H, 3’’’H, 3’’’’H, 3’’’’’H, 3’’’’’’ H-hexacyclopropa[1,2:18,36:22,23:27,45:31,32:55,60](C$_{60}$-I$_h$)[5,6]fullerene (**10**)

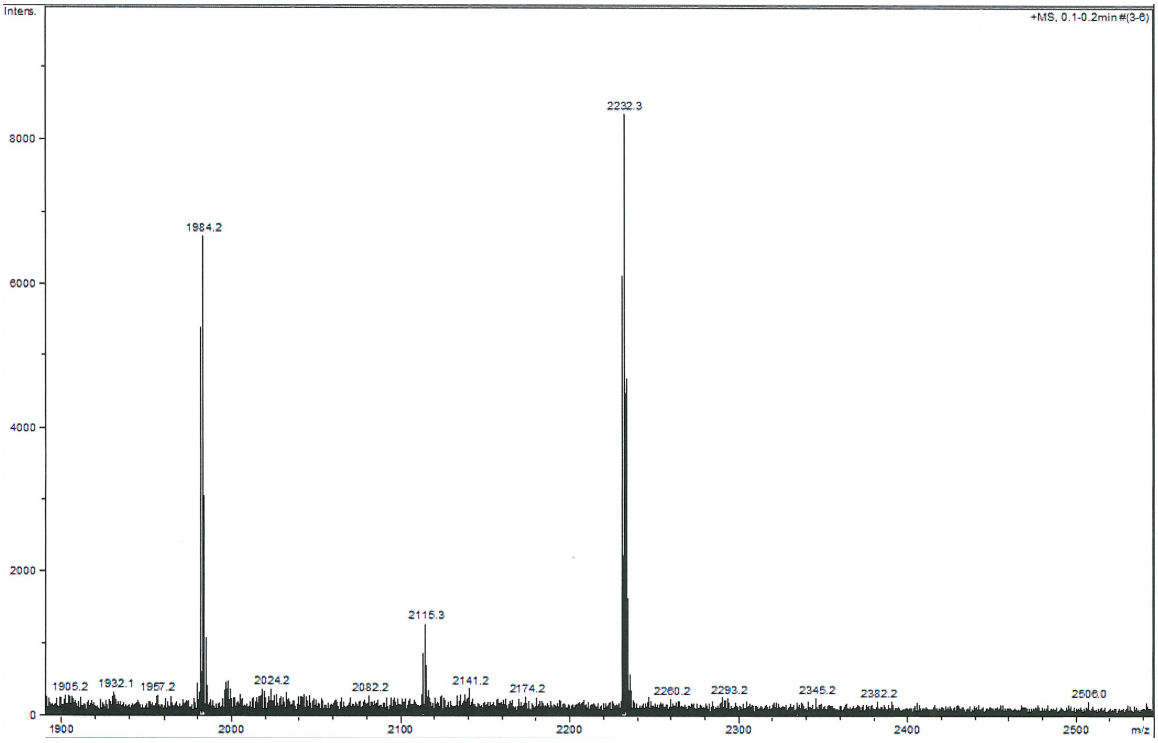

Figure A2.10: ESI-TOF Spectrum of **10**, positive mode

Appendix A3: Infrared spectroscopy data of compounds described in Section **2.3**
Compound 1: 2-((*Tert*-butoxycarbonyl)amino)ethyl ethyl malonate (**1**)

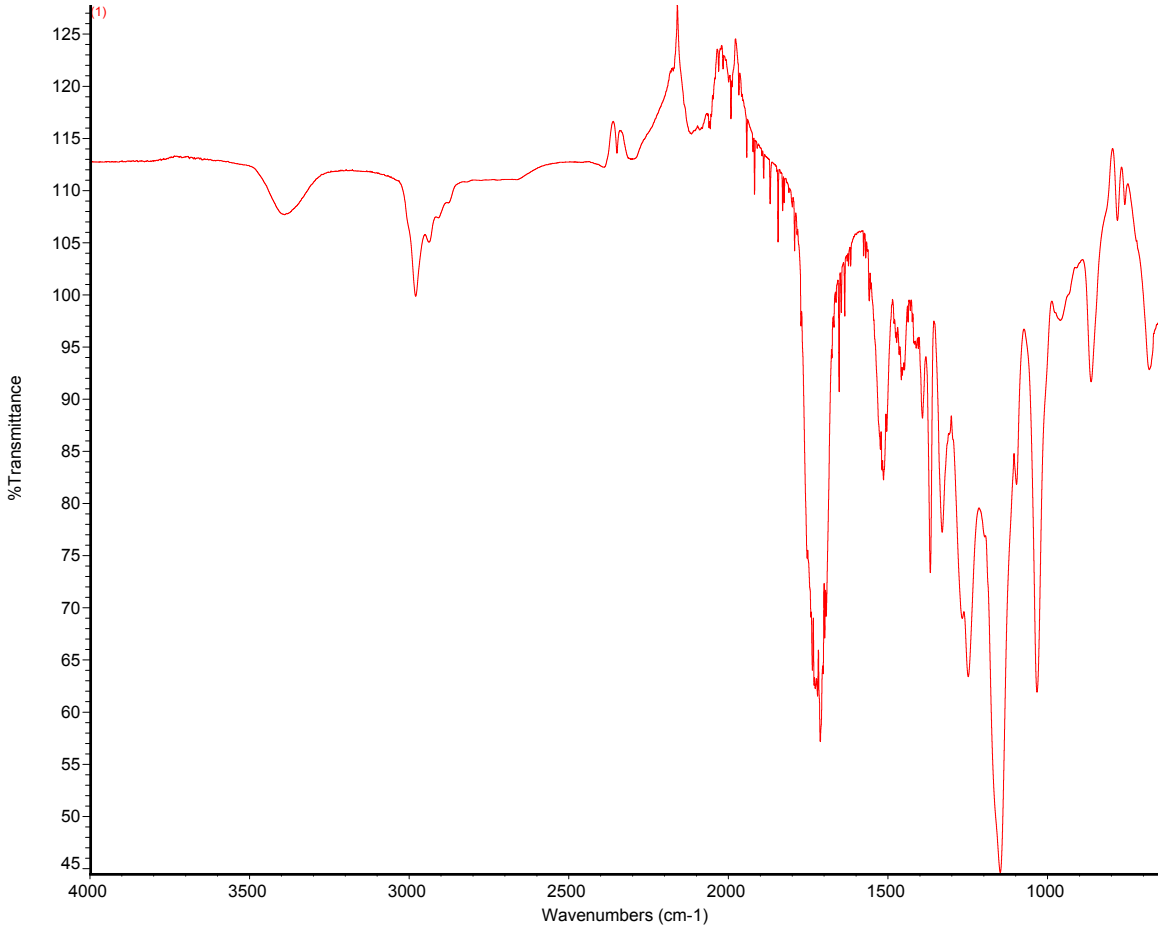

Figure A3.1: Infrared Transmission Spectrum of **1**

Compound 2: 3'-ethoxycarbonyl-3'-((2-((*tert*-butoxycarbonyl)amino)ethoxy)carbonyl)-[1,2](C_{60}-I_h)[5,6]fullerene (**2**)

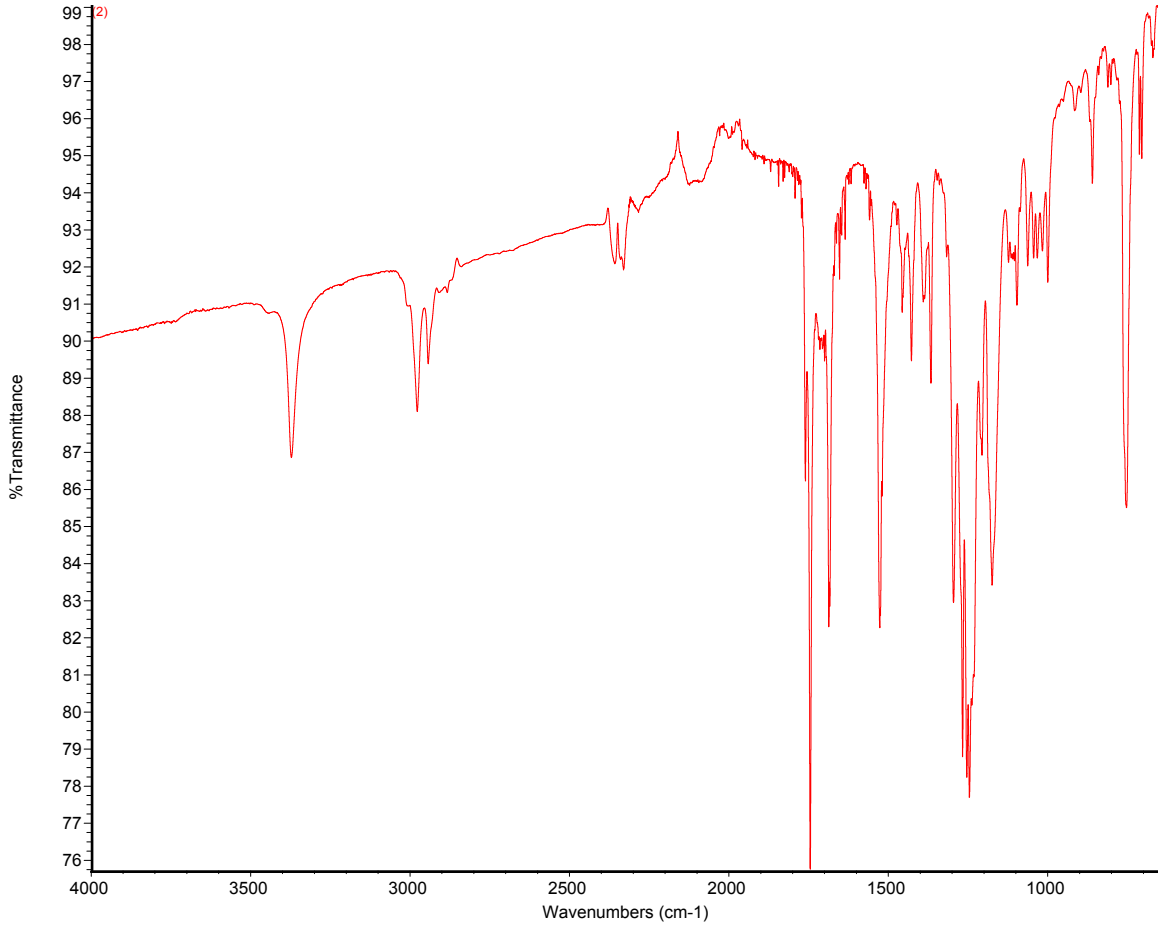

Figure A3.2: Infrared Transmission Spectrum of **2**

Compound 3: Bis(2-acetoxy-1-acetoxymethylethylcarbamoyl)methane (**3**)

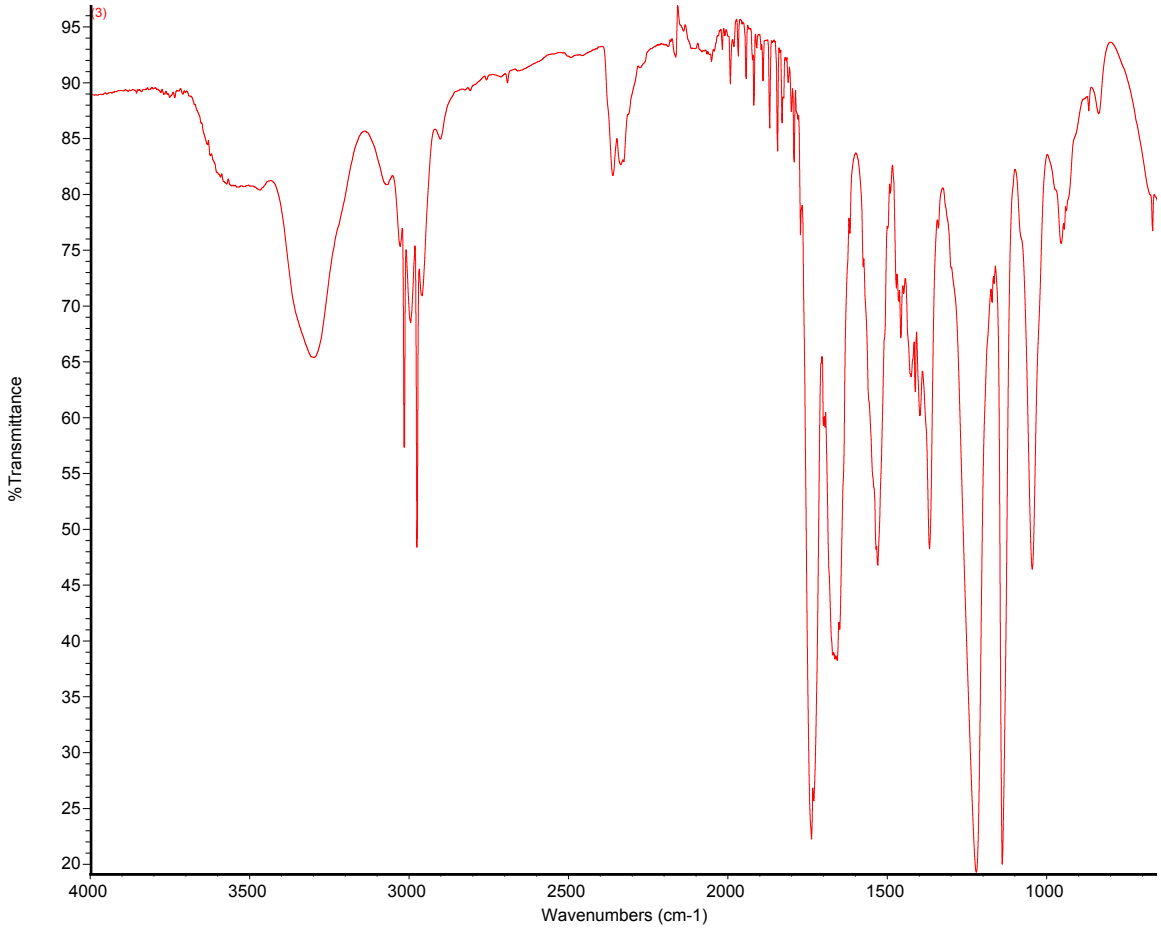

Figure A3.3: Infrared Transmission Spectrum of **3**

Compound 4: 3'-ethoxycarbonyl -3'-((2-((*tert*-butoxycarbonyl)amino)ethoxy)carbonyl)-3'', 3'', 3''', 3''', 3'''', 3'''', 3''''', 3''''', 3'''''', 3''''''-deca-(2-acetoxy-1-acetoxymethylethylcarbamoyl)-3'H, 3''H, 3'''H, 3''''H, 3'''''H, 3''''''H-hexacyclopropa[1,2:18,36:22,23:27,45:31,32:55,60](C_{60}-I_h)[5,6]fullerene (**4**)

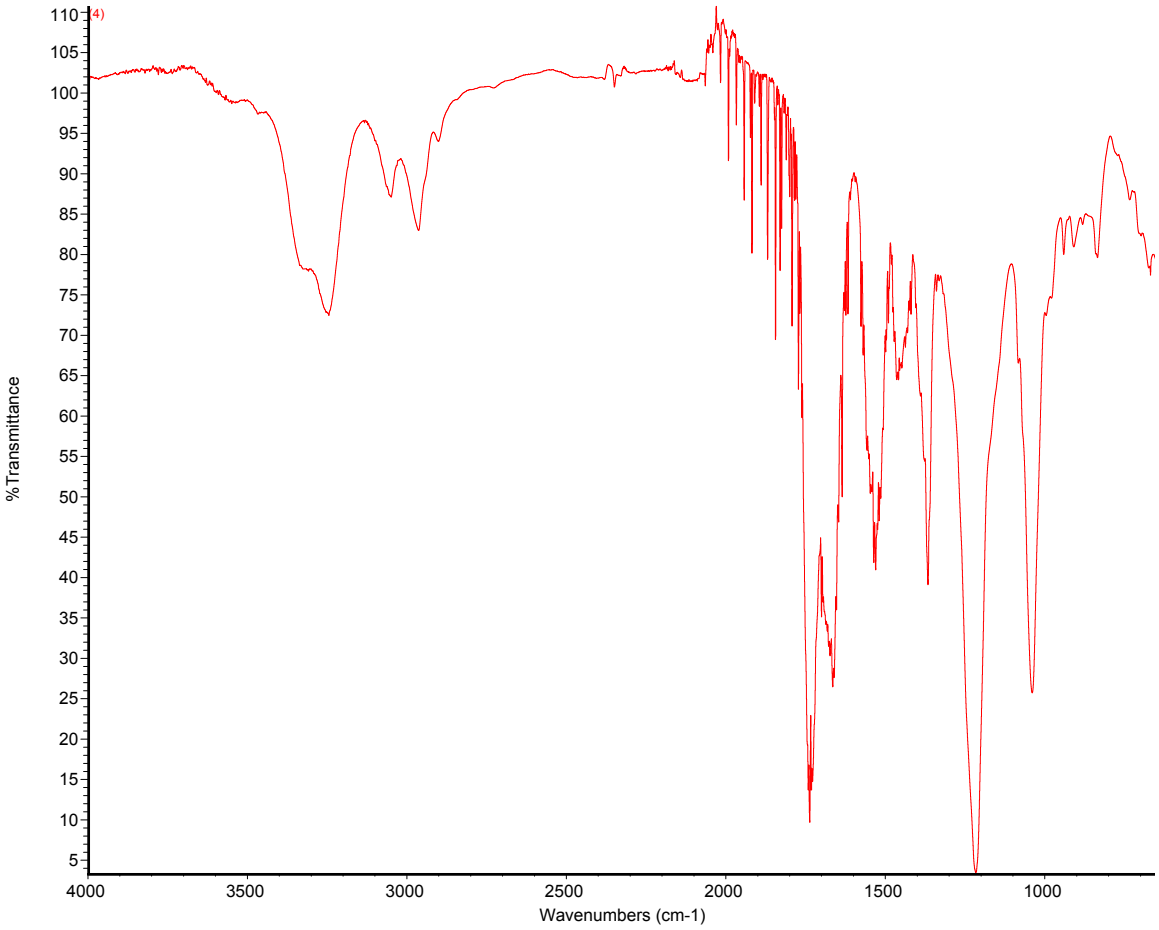

Figure A3.4: Infrared Transmission Spectrum of **4**

Compound 5: 3'-ethoxycarbonyl -3'-((2-((*tert*-butoxycarbonyl)amino)ethoxy)carbonyl)-3'', 3'', 3''', 3''', 3'''', 3'''', 3''''', 3''''', 3'''''', 3''''''-deca-(2-acetoxy-1-acetoxymethylethylcarbamoyl)-3'H, 3''H, 3'''H, 3''''H, 3'''''H, 3''''''H-hexacyclopropa[1,2:18,36:22,23:27,45:31,32:55,60](C$_{60}$-I$_h$)[5,6]fullerene (**5**)

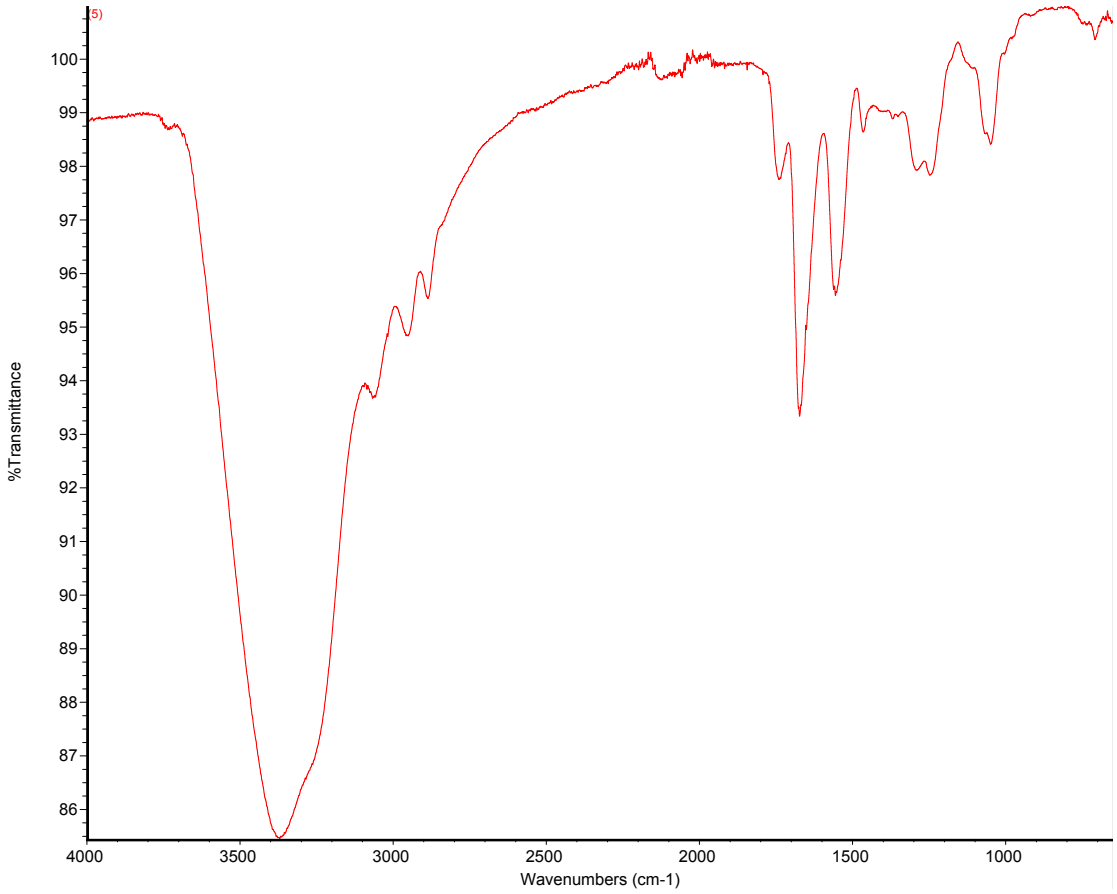

Figure A3.5.a: Infrared Transmission Spectrum of **5**

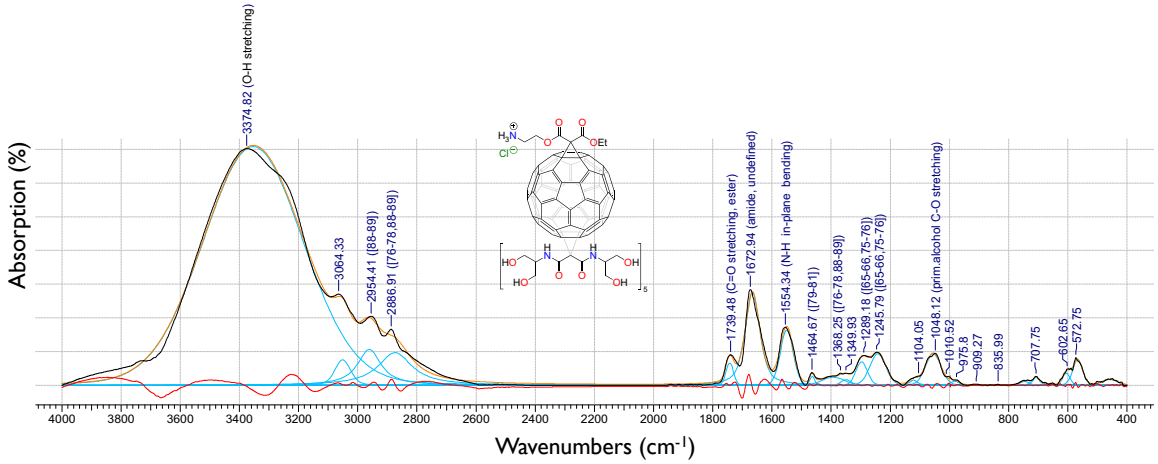

Figure A3.5.b: Analysis of Infrared Spectrum of **5**

Paclitaxel

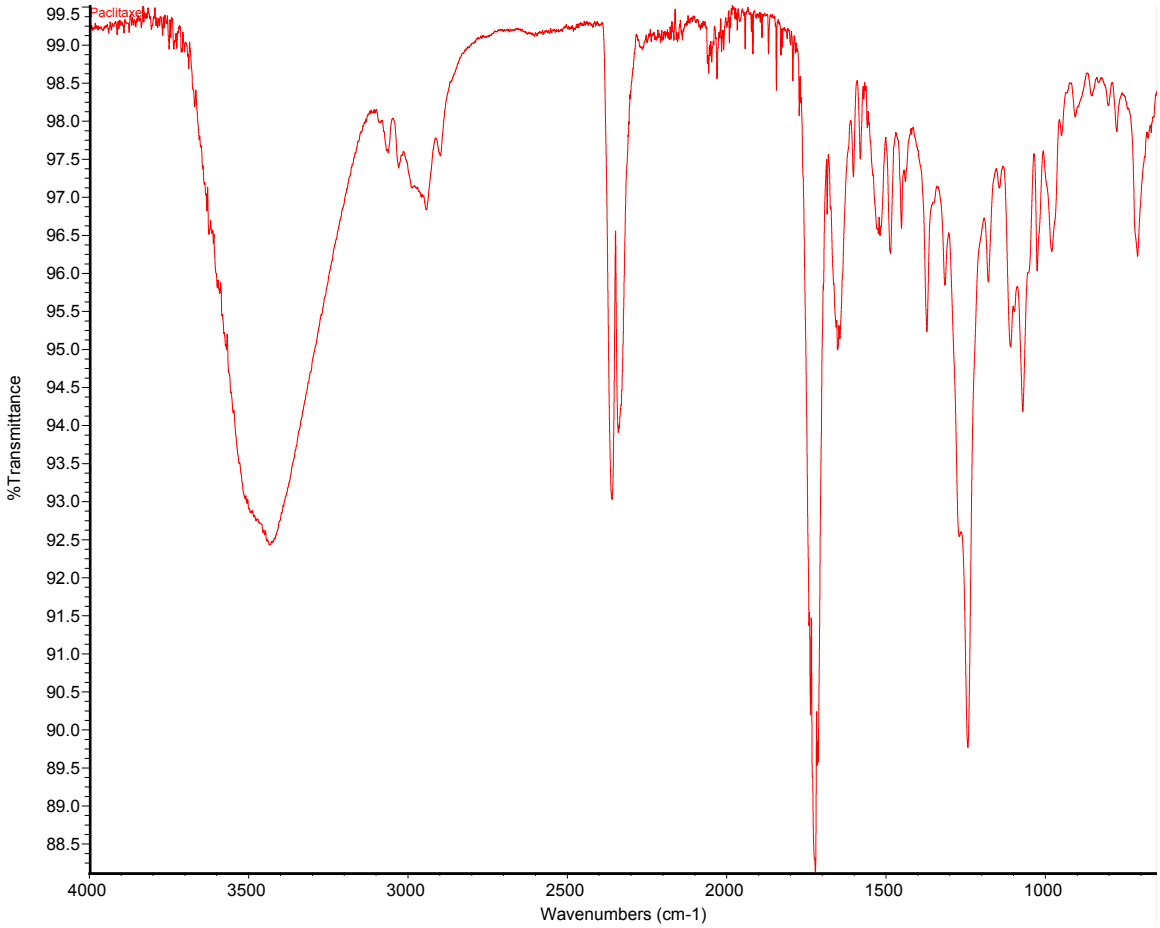

Figure A3.6.a: Infrared Transmission Spectrum of Paclitaxel

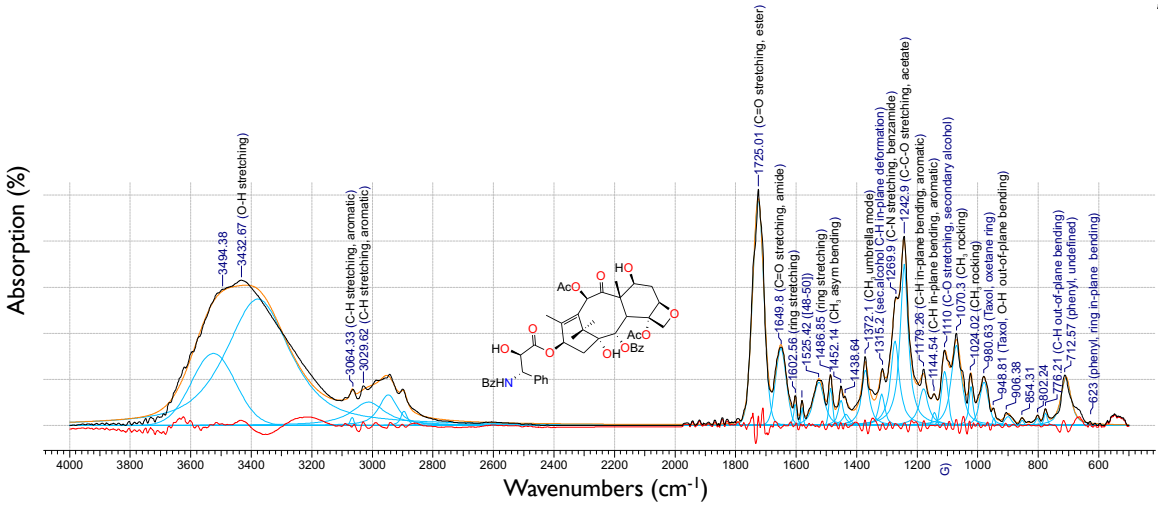

Figure A3.6.b: Analysis of Infrared Spectrum of Paclitaxel

Compound 6: Paclitaxel-2′-succinate

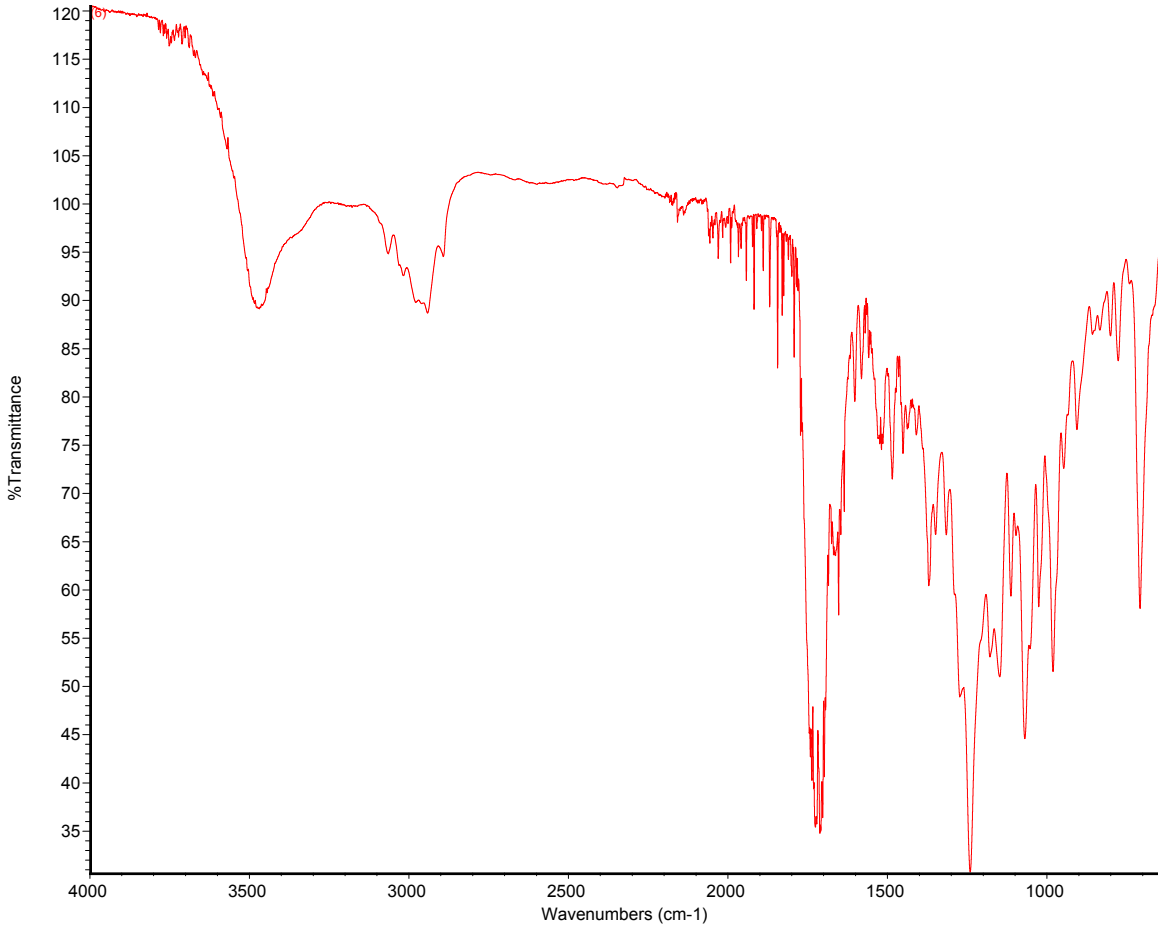

Figure A3.6.c: Infrared Transmission Spectrum of **6**

Compound 7: Serinol-C_{60}-Paclitaxel-2'-Succinate Derivative (**7**)

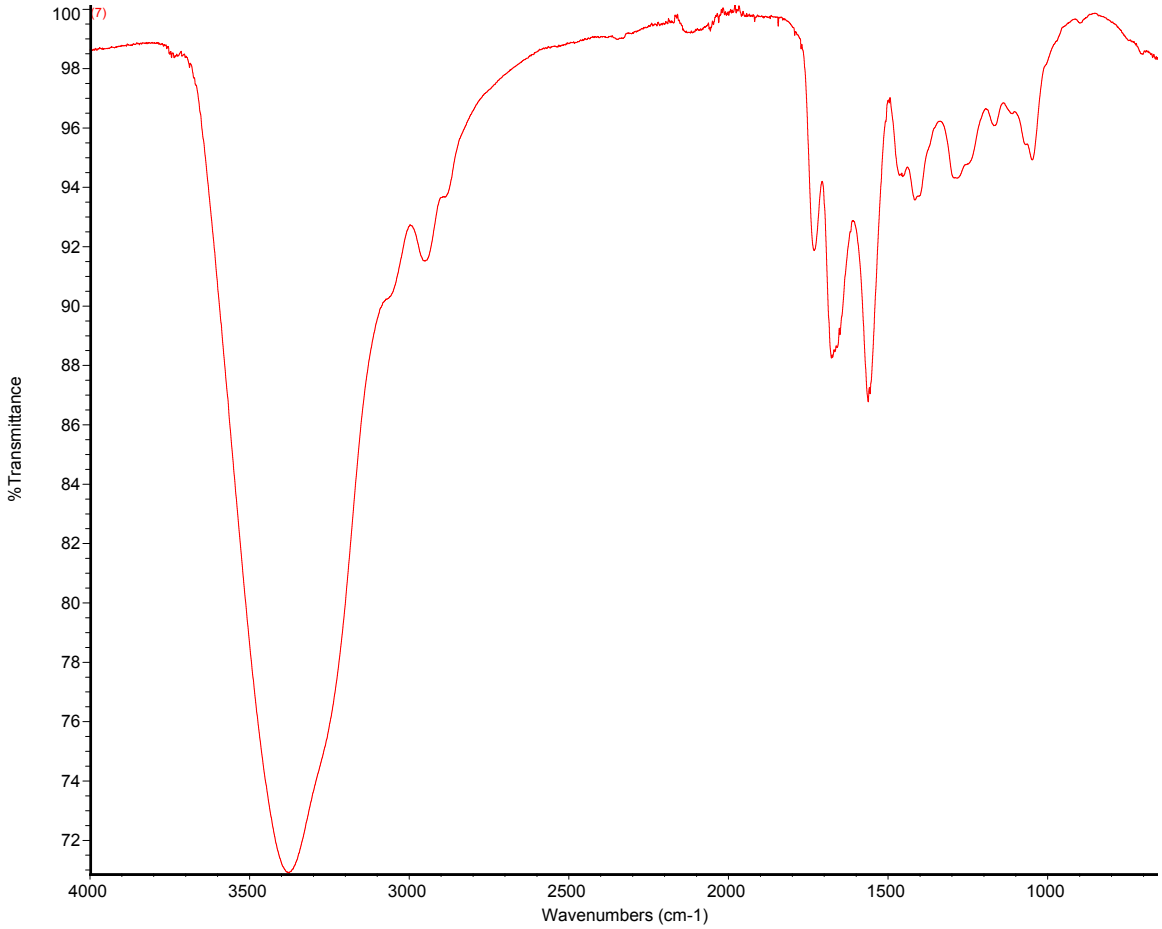

Figure A3.7: Infrared Transmission Spectrum of **7**

Compound 8: Paclitaxel-2′-Poly(ethylene glycol) Ester (**8**)

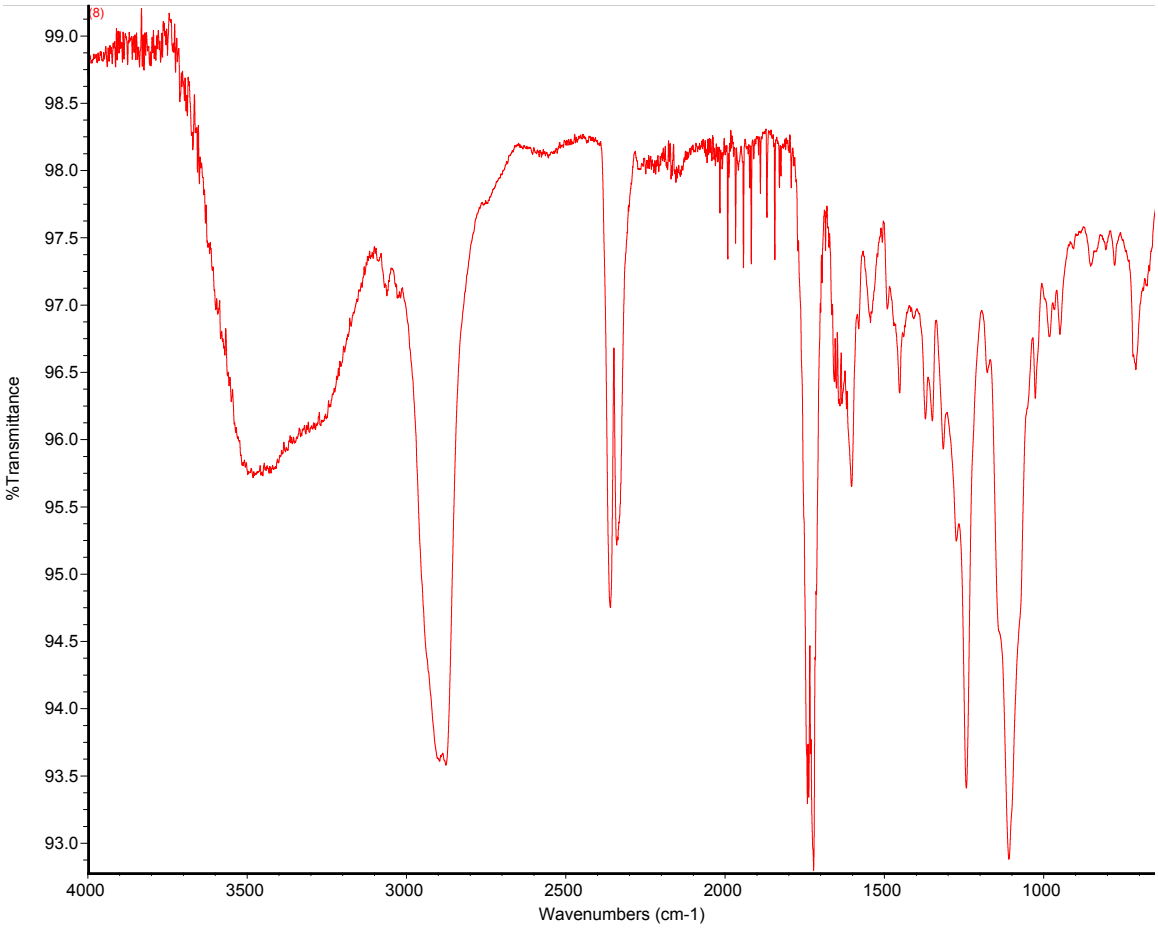

Figure A3.8.a: Infrared Transmission Spectrum of **8**

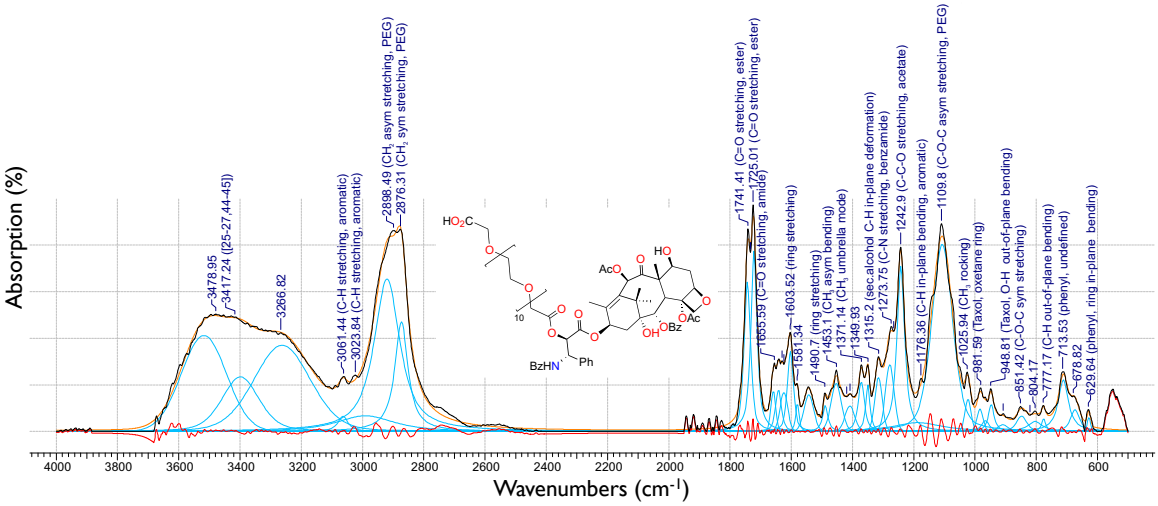

Figure A3.8.b: Analysis of Infrared Spectrum of **8**

Compound 9: Serinol-C_{60}-Paclitaxel-2′-Poly(ethylene glycol) Ester Derivative (**9**)

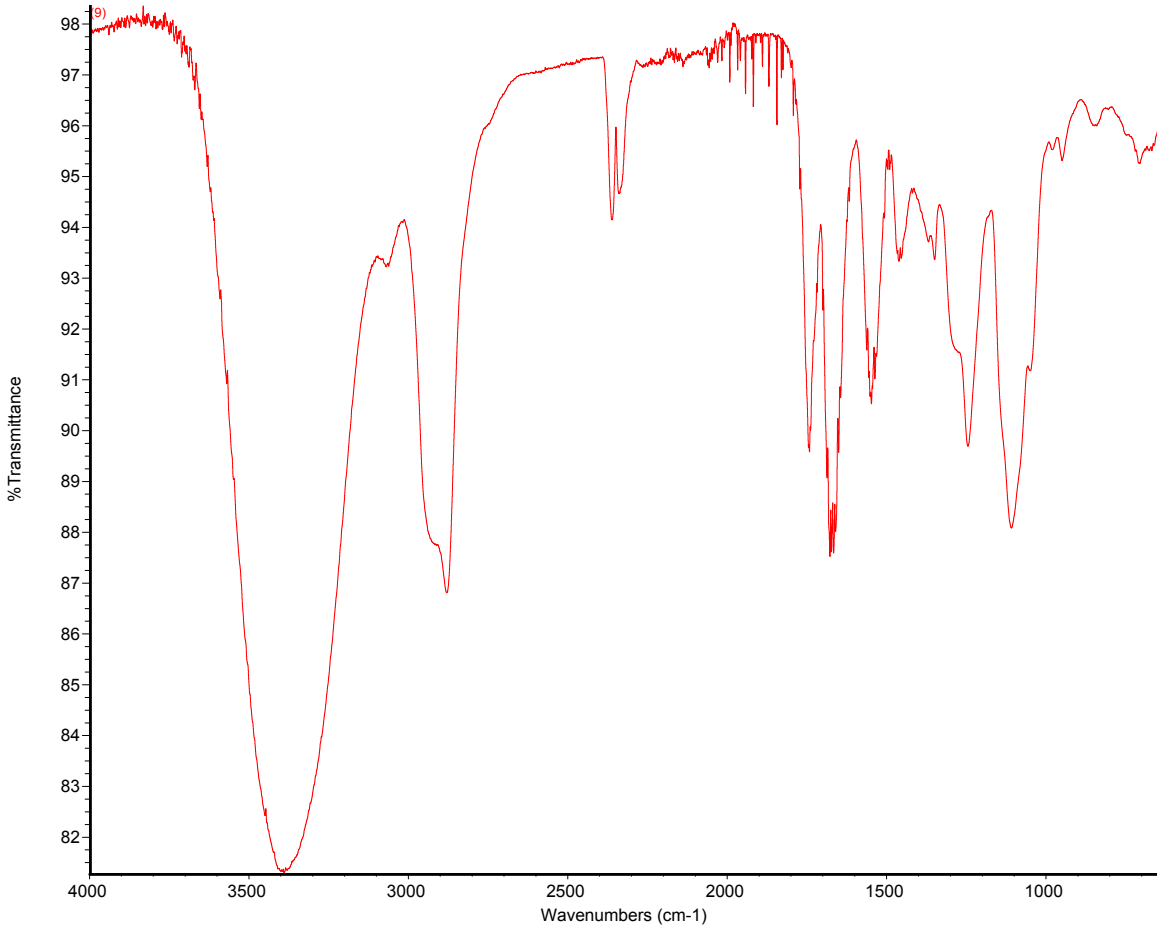

Figure A3.9.a: Infrared Transmission Spectrum of **9**

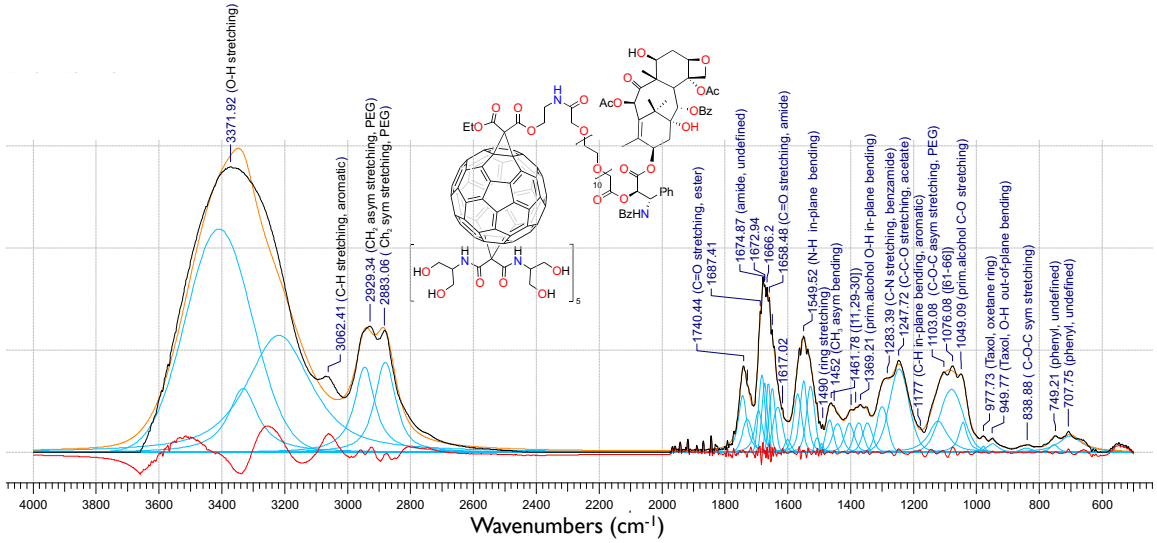

Figure A3.9.b: Analysis of Infrared Spectrum of **9**

Compound 10: 3’, 3’’, 3’’, 3’’’, 3’’’, 3’’’’, 3’’’’, 3’’’’’, 3’’’’’, 3’’’’’’, 3’’’’’’-dodeca-(2-hydroxy-1-{hydroxymethyl}ethylcarbamoyl)-3’H, 3’’H, 3’’’H, 3’’’’H, 3’’’’’H, 3’’’’’’ H-hexacyclopropa[1,2:18,36:22,23:27,45:31,32:55,60](C$_{60}$-I$_h$)[5,6]fullerene (**10**)

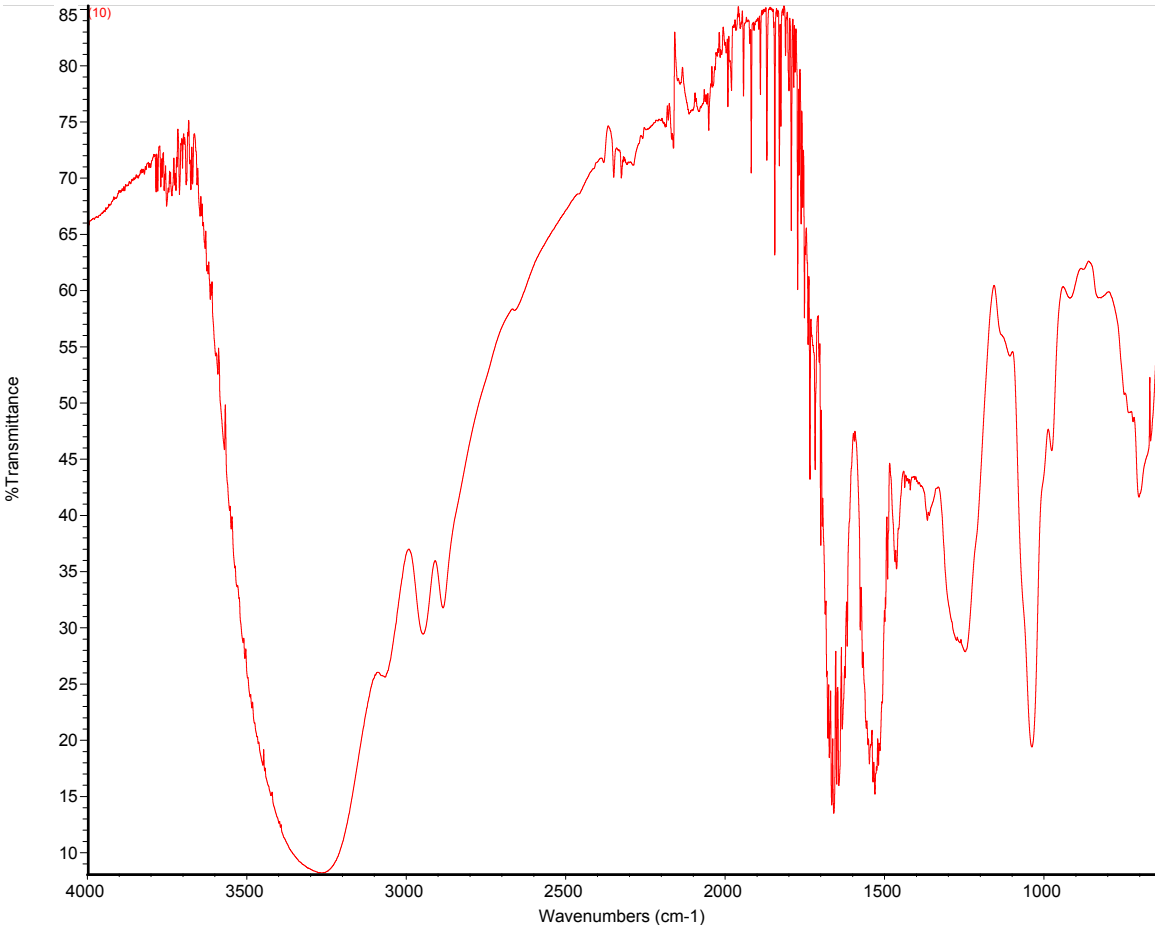

Figure A3.10: Infrared Transmission Spectrum of **10**

Appendix A4: ^{1}H and ^{13}C Nuclear Magnetic Resonance spectroscopy of compounds described in Section **2.3**

Compound 1: 2-((*Tert*-butoxycarbonyl)amino)ethyl ethyl malonate (**1**)

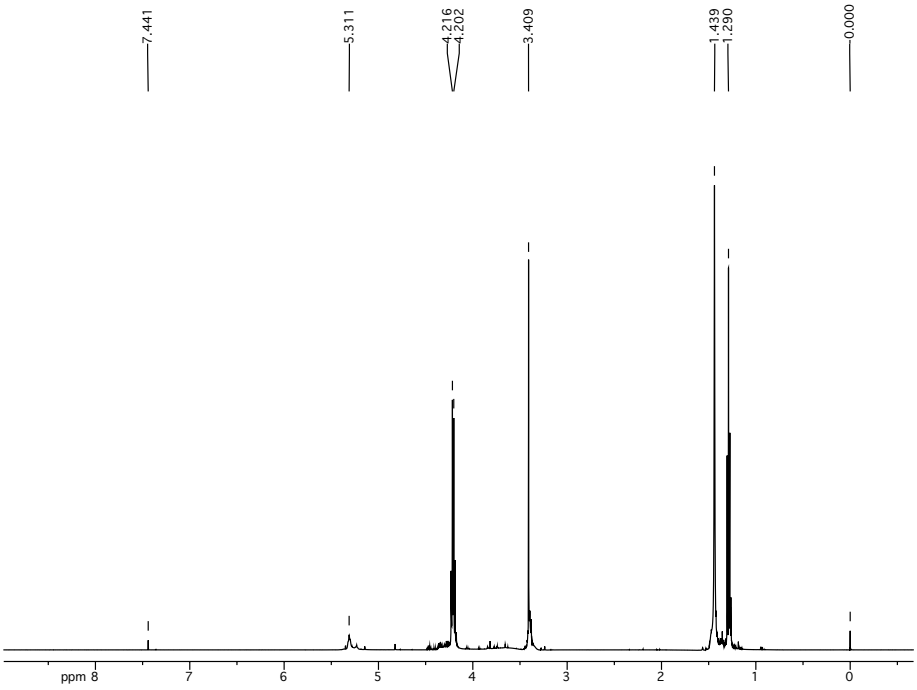

Figure A4.1.a: 500 MHz ^{1}H Spectrum of **1** in $CDCl_3$, 32 Scans

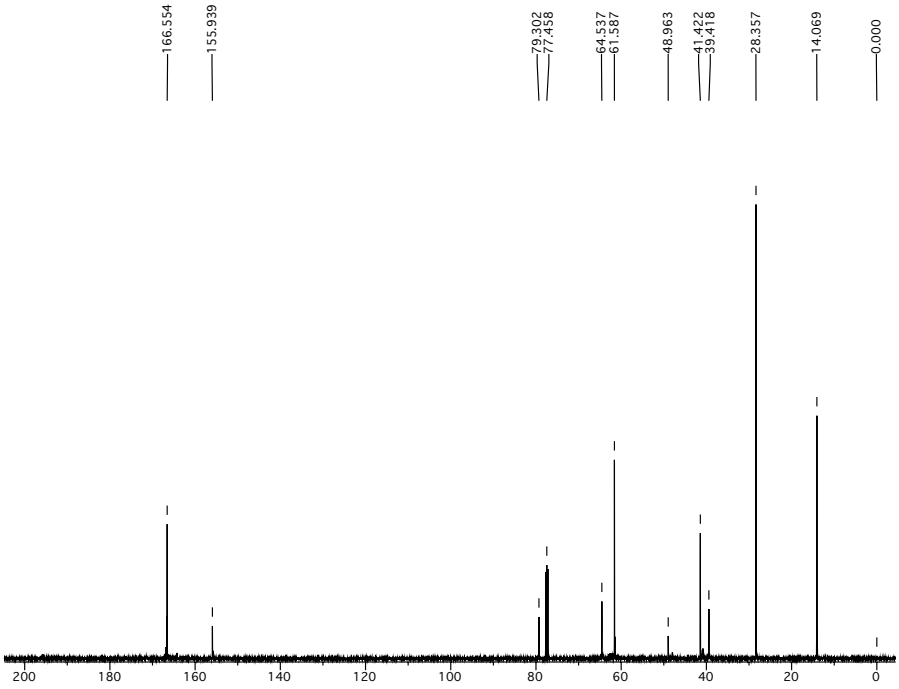

Figure A4.1.b: 500 MHz ^{13}C Spectrum of **1** in $CDCl_3$, 128 Scans

Compound 2: 3'-Ethoxycarbonyl-3'-((2-((*tert*-butoxycarbonyl)amino)ethoxy)carbonyl)-[1,2](C_{60}-I_h)[5,6]fullerene (**2**)

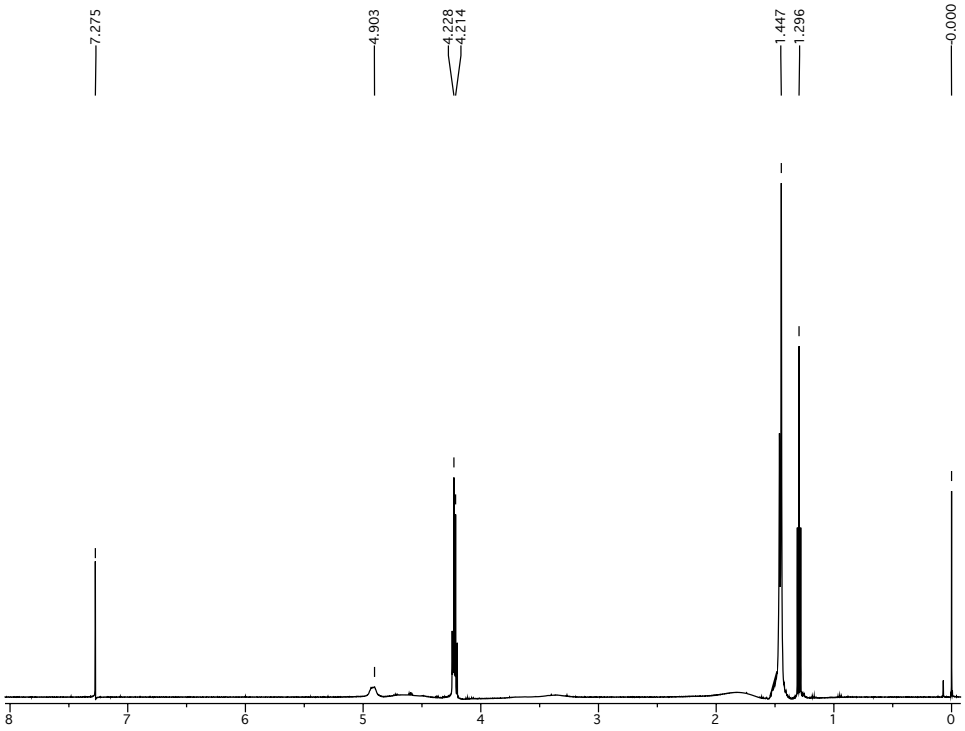

Figure A4.2.a: 500 MHz ^{1}H Spectrum of **2** in $CDCl_3$, 64 Scans

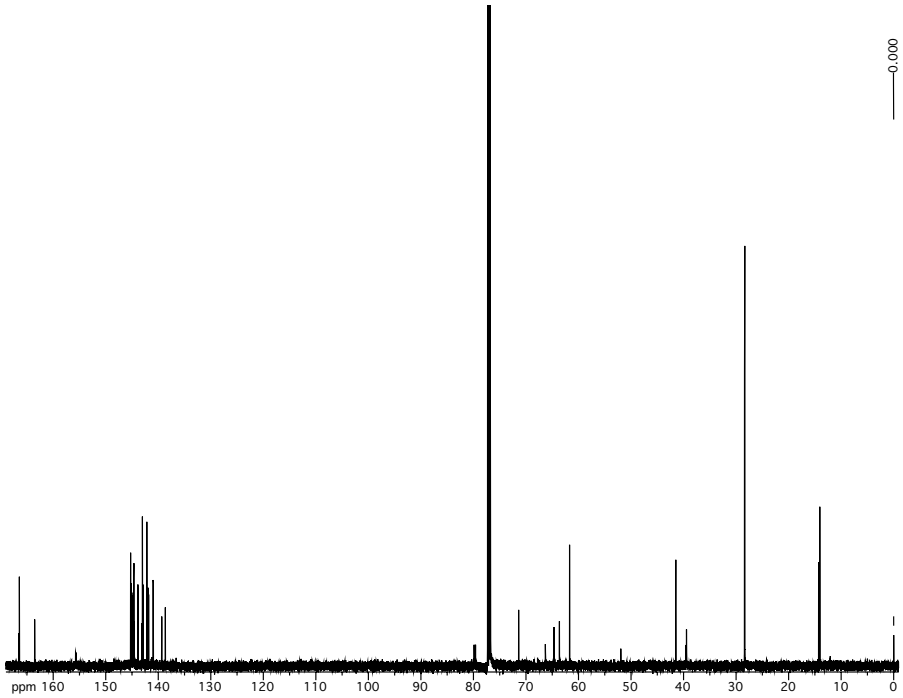

Figure A4.2.b: 500 MHz ^{13}C Spectrum of **2** in $CDCl_3$, 256 Scans

Compound 3: Bis(2-acetoxy-1-acetoxymethylethylcarbamoyl)methane (**3**)

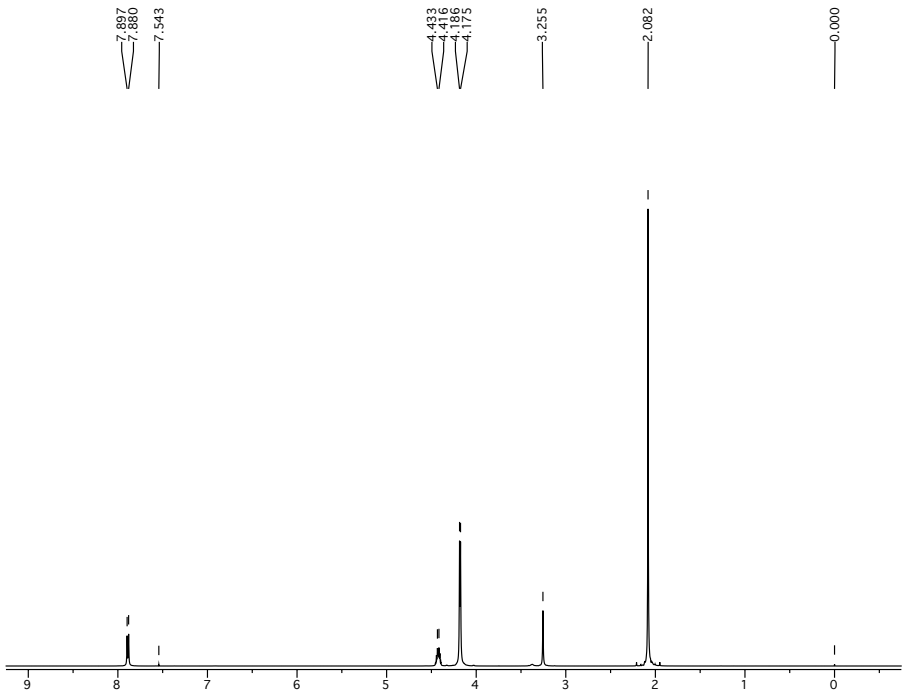

Figure A4.3.a: 500 MHz ^{1}H Spectrum of **3** in $CDCl_3$, 32 Scans

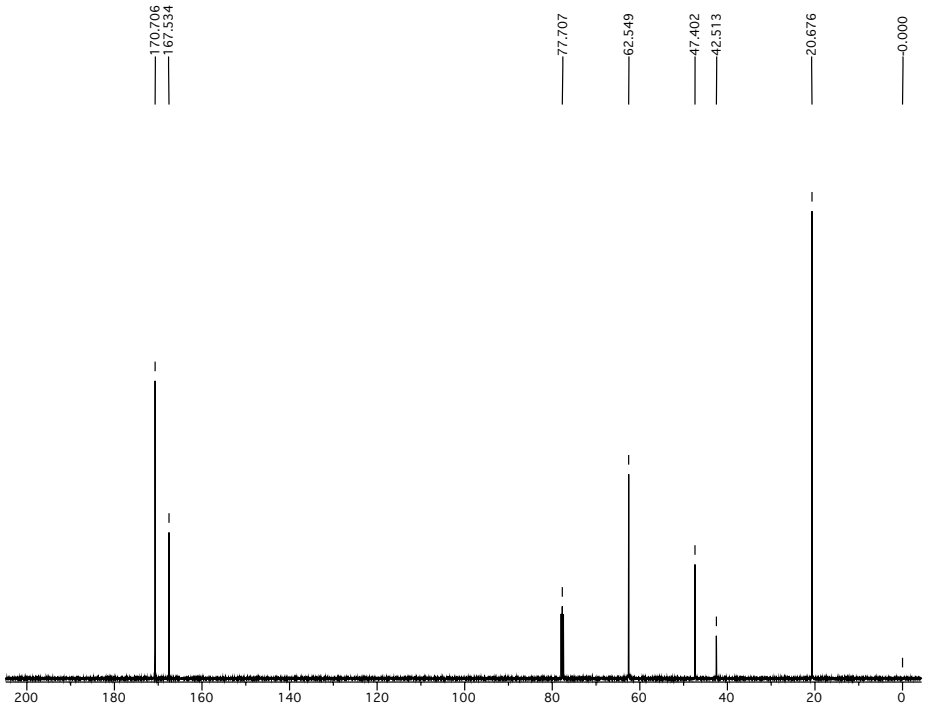

Figure A4.3.b: 500 MHz ^{13}C Spectrum of **3** in $CDCl_3$, 128 Scans

Paclitaxel

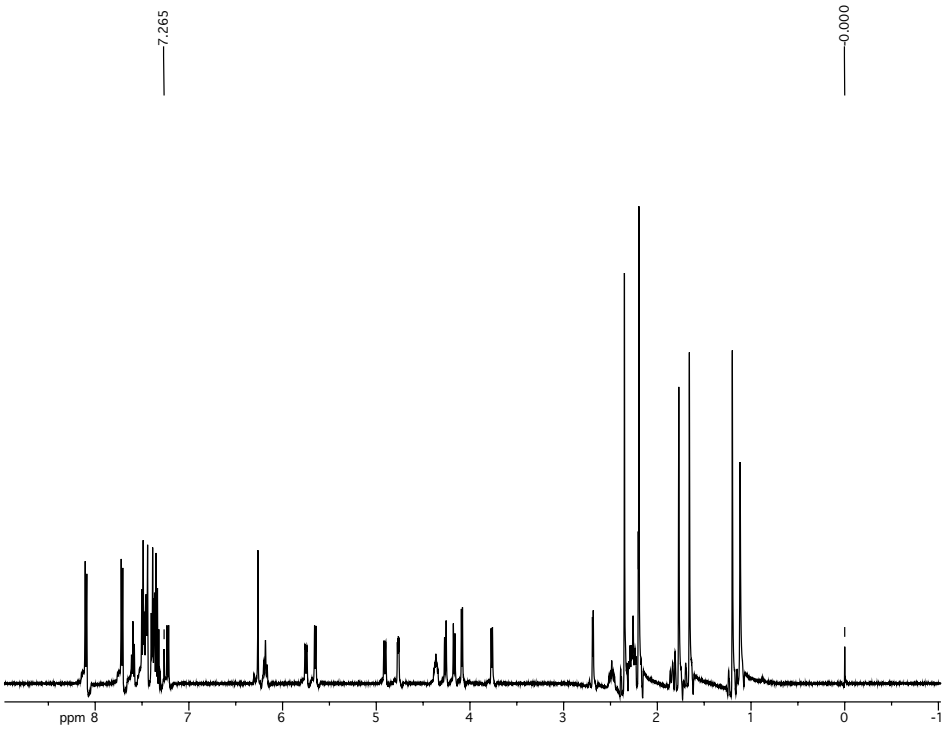

Figure A4.4.a: 500 MHz ^{1}H Spectrum of paclitaxel in $CDCl_3$, 32 Scans

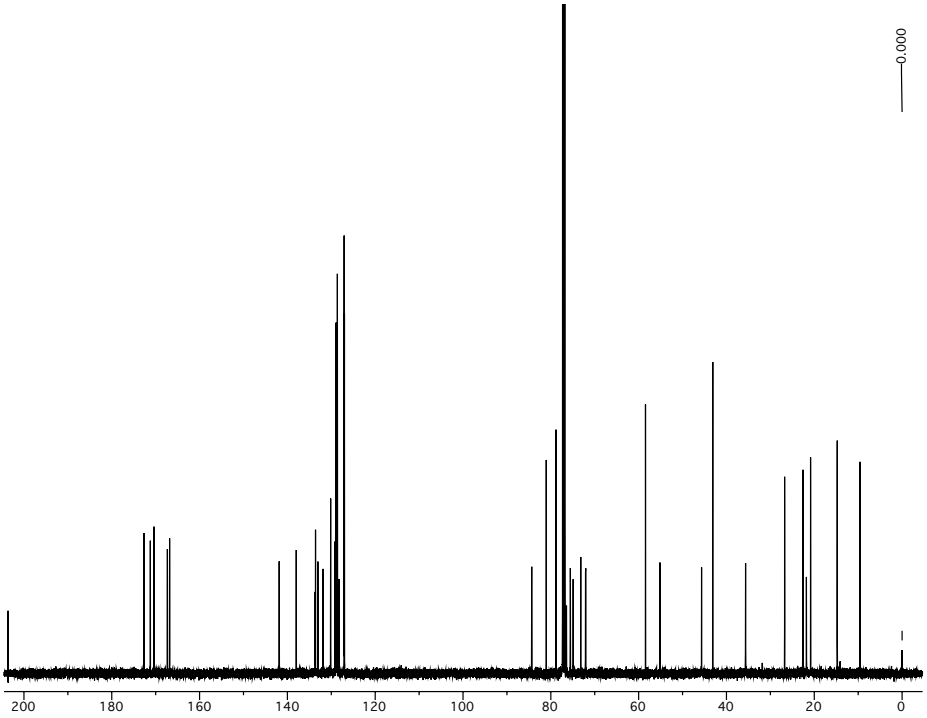

Figure A4.4.b: 500 MHz ^{13}C Spectrum of paclitaxel in $CDCl_3$, 256 Scans

Compound 6: Paclitaxel-2′-succinate (**6**)

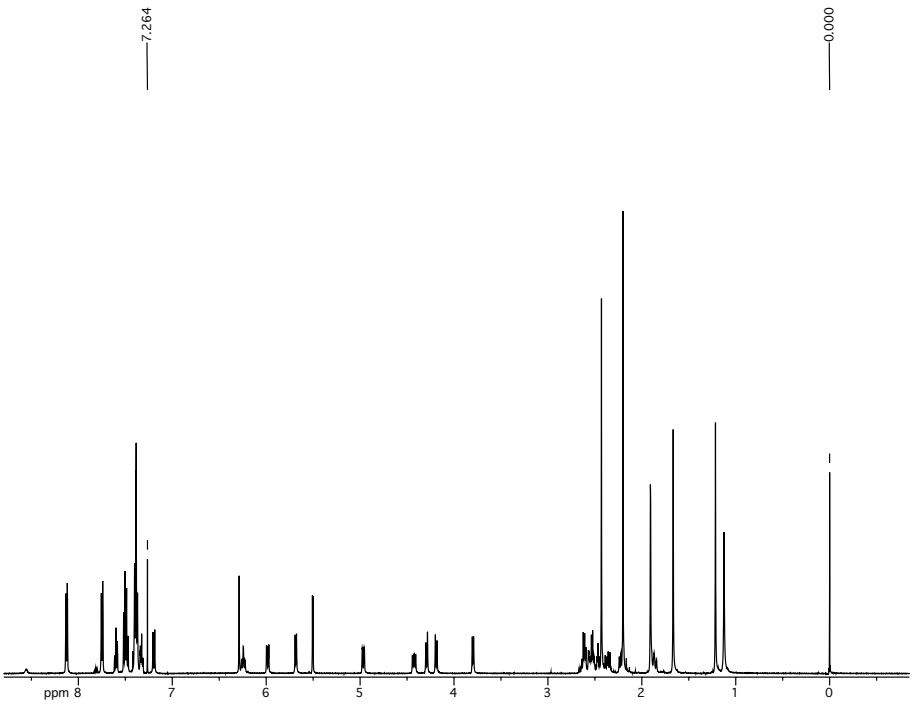

Figure A4.5.a: 500 MHz ^{1}H Spectrum of **6** in $CDCl_3$, 64 Scans

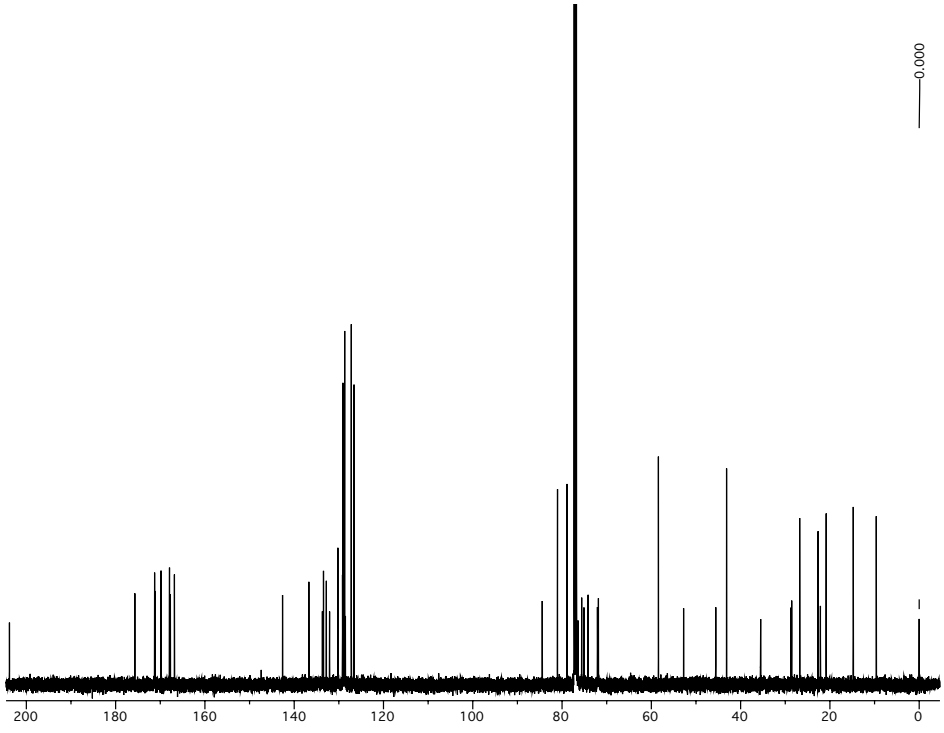

Figure A4.5.b: 500 MHz ^{13}C Spectrum of **6** in $CDCl_3$, 512 Scans

Compound 8: Paclitaxel-2′-Poly(ethylene glycol) Ester Derivative (**8**)

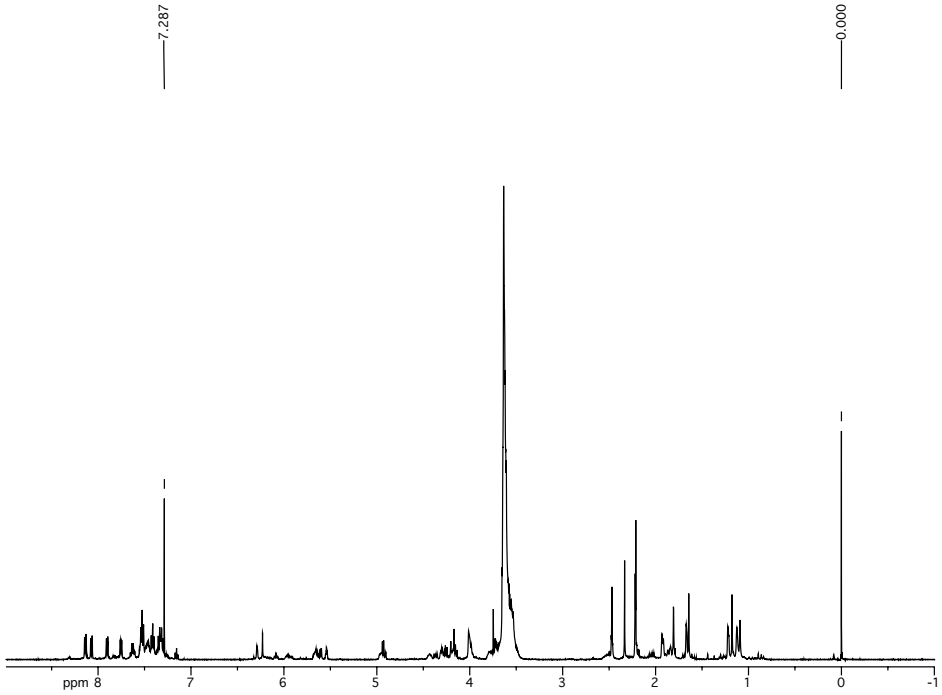

Figure A4.6.a: 500 MHz ^{1}H Spectrum of **8** in $CDCl_3$, 32 Scans

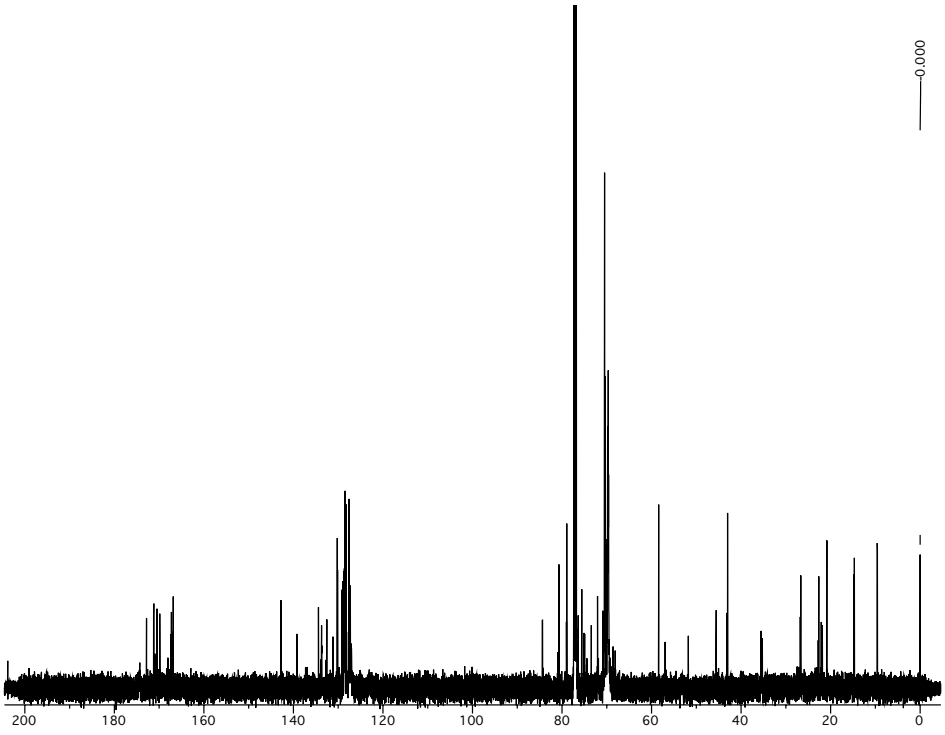

Figure A4.6.b: 500 MHz ^{13}C Spectrum of **8** in $CDCl_3$, 512 Scans

Appendix A5: Mean intensities of measured hydrodynamic diameters for Serinol-C_{60}-Paclitaxel-2′-Poly(ethylene glycol) Ester Derivative (compound **9**) and its synthetic precursors (compounds **5** and **8**). The hydrodynamic diameters provided are an abbreviation of the data to include only those results which show a measurable significant intensity.

	Normalized Mean Intensity (%)		
Hydrodynamic Diameter (nm)	**Compound 5**	**Compound 8**	**Compound 9**
58.77	0	0	0.7
68.06	0	0	1.7
78.82	0.1	0	2.2
91.28	0.8	0	2
105.7	3.8	0	1.5
122.4	6.6	0	1.1
141.8	8.9	0.6	1.6
164.2	10.4	8.1	5.4
190.1	11.4	19.2	11.7
220.2	12.1	25.7	17.7
255	12.2	23.6	20.1
295.3	11.1	14.9	17.5
342	8.9	5.7	11.2
396.1	6.4	1.1	4.6
458.7	4	0	1
531.2	2.2	0	0
615.1	0.9	0	0
712.4	0.2	0	0

Appendix A6: Cell internalization results over time for the Gd@C_{60}-(ZME-018) and Gd@C_{60}-(MuIgG) immunoconjugates into A375m and T24 cell lines

Table A6.1: Experiment 1

Cells, mAbs, Incubation Period	Gd Concentration in Sample (ppt)[1]	Number of Cells	Gd@C_{60}+C_{60} per cell	mAbs per cell
A375m, No mAb, 0 hr	0.0 (0.00)	6.75E+06	0.00E+00	0.00E+00
A375m, ZME-018, 1 hr	35.7 (0.98)	7.30E+06	4.46E+13	9.27E+12
A375m, ZME-018, 2 hr	97.5 (2.08)	9.50E+06	9.38E+13	1.95E+13
A375m, ZME-018, 4 hr	55.6 (2.63)	7.60E+06	6.68E+13	1.39E+13
A375m, ZME-018, 24 hr	62.3 (1.32)	1.20E+07	4.75E+13	9.85E+12
A375m, MuIgG, 1 hr	20.6 (0.86)	7.50E+06	2.51E+13	5.25E+12
A375m, MuIgG, 2 hr	39.3 (1.45)	8.10E+06	4.43E+13	9.29E+12
A375m, MuIgG, 4 hr	43.7 (1.29)	1.08E+07	3.70E+13	7.75E+12
A375m, MuIgG, 24 hr	19.7 (0.28)	9.30E+06	1.93E+13	4.05E+12
T24, No mAb, 0 hr	0.0 (0.00)	5.70E+06	0.00E+00	0.00E+00
T24, ZME-018, 1 hr	5.1 (0.12)	6.05E+06	7.66E+12	1.59E+12
T24, ZME-018, 2 hr	33.3 (1.20)	9.10E+06	3.34E+13	6.94E+12
T24, ZME-018, 4 hr	24.0 (0.71)	9.80E+06	2.24E+13	4.64E+12
T24, ZME-018, 24 hr	13.9 (0.20)	9.80E+06	1.30E+13	2.69E+12
T24, MuIgG, 1 hr	17.9 (0.73)	6.40E+06	2.56E+13	5.36E+12
T24, MuIgG, 2 hr	24.1 (1.35)	6.20E+06	3.55E+13	7.45E+12
T24, MuIgG, 4 hr	34.3 (1.74)	9.90E+06	3.17E+13	6.65E+12
T24, MuIgG, 24 hr	28.2 (1.08)	1.14E+07	2.26E+13	4.74E+12

1) Gd^{3+}-ion concentration in parts per trillion from the average of ten individual ICP-MS measurements per sample with the standard deviation in parentheses.

Table A6.2: Experiment 2

Cells, mAbs, Incubation Period	Gd Concentration in Sample (ppt)[1]	Number of Cells	$Gd@C_{60}+C_{60}$ per cell	mAbs per cell
A375m, No mAb, 0 hr	0.0 (0.00)	6.65E+06	0.00E+00	0.00E+00
A375m, ZME-018, 1 hr	19.8 (0.38)	4.30E+06	4.19E+13	8.70E+12
A375m, ZME-018, 2 hr	36.9 (1.73)	3.60E+06	9.34E+13	1.94E+13
A375m, ZME-018, 4 hr	33.5 (1.32)	4.50E+06	6.79E+13	1.41E+13
A375m, ZME-018, 24 hr	27.8 (0.90)	5.90E+06	4.31E+13	8.93E+12
A375m, MuIgG, 1 hr	18.6 (0.62)	6.55E+06	2.60E+13	5.38E+12
A375m, MuIgG, 2 hr	17.2 (0.39)	3.35E+06	4.69E+13	9.72E+12
A375m, MuIgG, 4 hr	23.9 (0.60)	5.85E+06	3.72E+13	7.72E+12
A375m, MuIgG, 24 hr	17.8 (0.89)	7.40E+06	2.20E+13	4.56E+12
T24, No mAb, 0 hr	0.0 (0.00)	1.43E+06	0.00E+00	0.00E+00
T24, ZME-018, 1 hr	1.9 (0.11)	2.12E+06	8.14E+12	1.69E+12
T24, ZME-018, 2 hr	14.5 (0.49)	3.30E+06	4.00E+13	8.30E+12
T24, ZME-018, 4 hr	11.6 (0.24)	3.38E+06	3.14E+13	6.50E+12
T24, ZME-018, 24 hr	3.6 (0.05)	2.32E+06	1.43E+13	2.96E+12
T24, MuIgG, 1 hr	10.2 (0.36)	3.15E+06	2.96E+13	6.14E+12
T24, MuIgG, 2 hr	11.1 (0.51)	2.55E+06	3.96E+13	8.22E+12
T24, MuIgG, 4 hr	9.1 (0.23)	2.75E+06	3.03E+13	6.29E+12
T24, MuIgG, 24 hr	8.6 (0.19)	3.25E+06	2.42E+13	5.03E+00

1) Gd^{3+}-ion concentration in parts per trillion from the average of ten individual ICP-MS measurements per sample with the standard deviation in parentheses.

Appendix A7: Mass (g) of murine test subjects through the course of *in vivo* treatment with paclitaxel derivatives

Day 1	Treatment Groups for *In Vivo* Studies of Murine Subjects				
	Paclitaxel	**Abraxane**	**Compound 9**	**Compound 10**	**PBS (Control)**
Subject 1	18.95	16.06	19.17	15.57	16.55
Subject 2	19.23	17.54	16.38	20.18	19.85
Subject 3	18.37	17.87	14.25	18.22	16.71
Subject 4	17.67	16.18	17.91	15.63	17.82
Subject 5	18.13	18.03	15.97	18.56	17.83
Subject 6	18.8	15.97	20.03		17.16
Mean	18.525	16.94167	17.285	17.632	17.653333
Median	18.585	16.86	17.145	18.22	17.49
Standard Deviation (Absolute)	0.5769489	0.970143	2.15584554	1.99744086	1.2029076
Standard Deviation (%)	3.1144339	5.72637	12.4723491	11.3284985	6.8140536

Table A7.1: Mass of murine test subjects after Day 1 of *in vivo* treatment with paclitaxel derivatives

Day 2	Treatment Groups for *In Vivo* Studies of Murine Subjects				
	Paclitaxel	**Abraxane**	**Compound 9**	**Compound 10**	**PBS (Control)**
Subject 1	18.17	16.32	16.77	18.66	17.93
Subject 2	17.95	17.42	18.95	16.48	18.03
Subject 3	19.13	17.23	13.96	19.26	17.38
Subject 4	18.91	15.48	18.04	16.4	18.89
Subject 5	18.45	16.52	16.18	20.6	16.84
Subject 6	18.62	17.97	20.78		16.75
Mean	18.53833	16.82333	17.4466667	18.28	17.636667
Median	18.535	16.875	17.405	18.66	17.655
Standard Deviation (Absolute)	0.44373	0.892876	2.3639938	1.82082399	0.8121987
Standard Deviation (%)	2.393583	5.307364	13.5498307	9.96074392	4.605171

Table A7.2: Mass of murine test subjects after Day 2 of *in vivo* treatment with paclitaxel derivatives

Day 3	Treatment Groups for *In Vivo* Studies of Murine Subjects				
	Paclitaxel	**Abraxane**	**Compound 9**	**Compound 10**	**PBS (Control)**
Subject 1	17.5	16.97	18.5	18.52	16.74
Subject 2	17.92	17.19	14.05	18.71	17.24
Subject 3	18.79	16.58	16.22	17.16	19.26
Subject 4	18.14	15.51	19.66	18.03	18.13
Subject 5	18.76	17	17.26	16.31	16.54
Subject 6	18.04	14.63	15.66		17.44
Mean	18.19167	16.31333	16.8916667	17.746	17.558333
Median	18.09	16.775	16.74	18.03	17.34
Standard Deviation (Absolute)	0.501774	1.021894	2.02135021	1.00181336	1.0044385
Standard Deviation (%)	2.75826	6.264162	11.9665528	5.64529108	5.7205799

Table A7.3: Mass of murine test subjects after Day 3 of *in vivo* treatment with paclitaxel derivatives

Day 4	Treatment Groups for *In Vivo* Studies of Murine Subjects				
	Paclitaxel	**Abraxane**	**Compound 9**	**Compound 10**	**PBS (Control)**
Subject 1	17.76	15.52	16.84	17.68	19.41
Subject 2	18.69	14.4	15.75	18.6	17.53
Subject 3	18.05	16.78	19.61	16.67	16.9
Subject 4	17.02	16.42	14.42	16.2	18.55
Subject 5	17.38	16.3	15.93	17.8	17.44
Subject 6	18.11	16.56	17.94		16.16
Mean	17.835	15.99667	16.7483333	17.39	17.665
Median	17.905	16.36	16.385	17.68	17.485
Standard Deviation (Absolute)	0.588175	0.892046	1.82784481	0.95535334	1.1616669
Standard Deviation (%)	3.29787	5.576451	10.9135923	5.49369372	6.5760934

Table A7.4: Mass of murine test subjects after Day 4 of *in vivo* treatment with paclitaxel derivatives

Day 5	Treatment Groups for *In Vivo* Studies of Murine Subjects				
	Paclitaxel	**Abraxane**	**Compound 9**	**Compound 10**	**PBS (Control)**
Subject 1	18.69	15.46	15.6	16.35	19.79
Subject 2	18.2	13.76	17.98	17.25	17.16
Subject 3	17.85	16.83	15.93	17.69	17.57
Subject 4	17.91	16.09	17.2	18.58	17.32
Subject 5	17.52	16.26	16.28	16.21	18.34
Subject 6	17.66	16.55	19.76		
Mean	17.97167	15.825	17.125	17.216	18.036
Median	17.88	16.175	16.74	17.25	17.57
Standard Deviation (Absolute)	0.421398	1.1128836	1.55868855	0.98085677	1.0800602
Standard Deviation (%)	2.344793	7.03244	9.10183096	5.69735576	5.9883576

Table A7.5: Mass of murine test subjects after Day 5 of *in vivo* treatment with paclitaxel derivatives

Day 6	Treatment Groups for *In Vivo* Studies of Murine Subjects				
	Paclitaxel	**Abraxane**	**Compound 9**	**Compound 10**	**PBS (Control)**
Subject 1	16.8	14.8	17.36	16.55	16.98
Subject 2	17.34	15.63	15.88	16.69	19.06
Subject 3	17.58	14.78	14.59	16.35	17.26
Subject 4	17.54	12.94	19.13	16.55	16.13
Subject 5	18.19	14.85	15.44	17.53	17.06
Subject 6	17.45	15.98	17.18		
Mean	17.48333	14.83	16.5966667	16.734	17.298
Median	17.495	14.825	16.53	16.55	17.06
Standard Deviation (Absolute)	0.447333	1.052464	1.62597253	0.46117242	1.0756486
Standard Deviation (%)	2.558624	7.096856	9.7969825	2.75590067	6.2183411

Table A7.6: Mass of murine test subjects after Day 6 of *in vivo* treatment with paclitaxel derivatives

Day 7	Treatment Groups for *In Vivo* Studies of Murine Subjects				
	Paclitaxel	**Abraxane**	**Compound 9**	**Compound 10**	**PBS (Control)**
Subject 1	16.67	12.3	14.98	16.71	15.41
Subject 2	17.36	14.54	15.85	16.27	19.66
Subject 3	17.11	15.74	17.93	16.39	16.92
Subject 4	17.18	14.22	19.15	16.68	17.68
Subject 5	17.15	15.55	15.85	17.41	
Subject 6	18.29	14.21	16.55		
Mean	17.293333	14.42667	16.7183333	16.692	17.4175
Median	17.165	14.38	16.2	16.68	17.3
Standard Deviation (Absolute)	0.5391351	1.23385	1.54526912	0.44308013	10.149521
Standard Deviation (%)	3.1175893	8.552567	9.24296157	2.65444601	1.7677929

Table A7.7: Mass of murine test subjects after Day 7 of *in vivo* treatment with paclitaxel derivatives

Day 8	Treatment Groups for *In Vivo* Studies of Murine Subjects				
	Paclitaxel	**Abraxane**	**Compound 9**	**Compound 10**	**PBS (Control)**
Subject 1	16.65	13.88	16.29	16.51	14.78
Subject 2	17.47	15.7	18.3	16.87	17.23
Subject 3	17.15	14.28	15.14	15.75	18.36
Subject 4	17.16	14.36	16.4	17.52	19.62
Subject 5	18.27	15.61	17.15	17.13	
Subject 6	17.2	12.56	19.66		
Mean	17.31667	14.39833	17.1566667	16.756	17.4975
Median	17.18	14.32	16.775	16.87	17.795
Standard Deviation (Absolute)	0.537165	1.168425	1.6102505	0.67251766	2.0579338
Standard Deviation (%)	3.102014	8.115001	9.38556731	4.01359309	11.761302

Table A7.8: Mass of murine test subjects after Day 8 of *in vivo* treatment with paclitaxel derivatives

Day 9	Treatment Groups for *In Vivo* Studies of Murine Subjects				
	Paclitaxel	**Abraxane**	**Compound 9**	**Compound 10**	**PBS (Control)**
Subject 1	18.32	14.32	18.73	18.18	15.26
Subject 2	18.63	15.22	16.45	18.32	20.54
Subject 3	20.05	15.92	17.52	19.3	20.18
Subject 4	20.04	13.59	15.74	16.78	17.9
Subject 5	17.68	16.23	17.97	16.51	
Subject 6	19.07	14.47	15.55		
Mean	18.965	14.95833	16.9933333	17.818	18.47
Median	18.85	14.845	16.985	18.18	19.04
Standard Deviation (Absolute)	0.9511414	1.012787	1.28035412	1.15841271	2.4384421
Standard Deviation (%)	5.015246	6.770718	7.5344495	6.50136215	13.202177

Table A7.9: Mass of murine test subjects after Day 9 of *in vivo* treatment with paclitaxel derivatives

Appendix A8: Chemicals and their related information used in Section **2.4**

Reagent/Equipment	**Commercial Source**
Dulbecco's Modified Eagle Medium (DMEM), High Glucose	Life Technologies, Carlsbad, California
10% Fetal Bovine Serum	Atlanta Biologicals, Lawrenceville, Georgia
Minimum Essential Medium (MEM), Non-Essential Amino Acids (1×)	Life Technologies, Carlsbad, California
Minimum Essential Medium (MEM),Vitamin Solution (1×)	Life Technologies, Carlsbad, California
Sodium Pyruvate (1×)	Life Technologies, Carlsbad, California
96-Well Flat-Bottom Sterile Plates	Becton, Dickinson and Co., Franklin Lakes, New Jersey
Dulbecco’s Phosphate Buffered Saline (PBS)	Life Technologies, Carlsbad, California